UNIVERSITY OF ŽILINA

FACULTY OF MANAGEMENT SCIENCE AND INFORMATICS

Assessment of Innovative Solutions for the European Electricity Market

DISSERTATION THESIS

28360020223008

Study Program:	Intelligent Information Systems
Field of Study:	Informatics
Workplaces:	Department of Mathematical Methods and Operations Research, Faculty of Management Science and Informatics, University of Žilina, Slovakia
	Unit C.03 – Energy Security, Distribution and Markets, Joint Research Centre, Ispra, Italy
Supervisors:	Prof. Ľuboš Buzna, Ph.D. Prof. Peter Braciník, Ph.D. Gianluca Fulli, Ph.D.
Reviewers:	Prof. Ettore Bompard, Ph.D. Georgios Antonopoulos, Ph.D.

Žilina, 30.06.2022 **Luca Lena Jansen, MSc.**

Declaration

I sincerely declare that this thesis named *Assessment of Innovative Solutions for the European Electricity Market* has been composed solely by myself and that it has not been submitted, in whole or in part, in any previous application for a degree. Except for the cases where stated otherwise, either by reference or an acknowledgment, the work presented is entirely my own created under the guidance of the aforementioned supervisors.

Author signature: .....

Acknowledgements

This thesis is the result of three years of research in the context of the Collaborative Doctoral Program (CDP) between the Department of Mathematical Methods and Operations Research of the Faculty of Management Science and Informatics of the University of Žilina and the Unit C3-Energy Security, Distribution and Markets of the European Commission's Joint Research Centre in Ispra.

I would like to thank both institutions for granting me this opportunity and funding my research. I am grateful for my supervisors Gianluca Fulli and Peter Braciník, who provided useful guidance. Further, I would like to express my appreciation for Silvia Vitiello, for her availability and support throughout my time at the JRC. A big thank you to Georgios Antonopoulos, who provided me with so much useful feedback and guidance and was always available for interesting and insightful discussions. Vielen Dank an Georg Thomaßon, für die hilfreichen Diskussionen und Tipps. I would like to extend my gratitude to the entire Unit C3 and especially to Gianluca, Marta, Giuseppe, Stamatis, and David. I wished it would have been more normal times, then we could have had even more fruitful exchanges and shared coffee breaks.

I would like to congratulate every future Ph.D. student, who will be lucky enough to have Ľuboš Buzna as their supervisor. I could have not asked for a more dedicated and helpful mentor throughout these three years. Thank you a lot.

I would like to thank all the Milans for all their help and company during my time in Žilina.

Lastly, I would like to thank my family and friends for their support and understanding in the past years and most of all my partner Jurgena, who is always my greatest support.

Abstract

This dissertation thesis assesses different design options for a model of the European electricity market to investigate nodal pricing. Concretely, technical aspects such as the choice of power flow model, network representation, intertemporal constraints and economic aspects such as demand elasticity were investigated. In a preliminary analysis, two formulations of the power flow model AC-OPF and DC-OPF were compared against each other in terms of obtaining nodal prices. While AC-OPF leads to a higher accuracy, which can be significant for operational purposes. For a model with a stronger focus on electricity markets and pricing mechanisms, DC-OPF is preferred, especially considering the computational benefits. A study that implements demand elasticity into the making of prices in a European context was conducted. It showed consumers' price elasticity impact on dispatching and the costs to generate power. The presented case study investigated these effects in the context of switching from a lower to a higher resolution of networks, which emphasizes the role demand elasticity could play in a system with a higher number of zones and ultimately under a nodal pricing regime. The main contribution of this Ph.D. thesis represents the development of a heuristic algorithm to model hydro storages in large-scale nodal pricing models. It allows overcoming the lack of data on hydro state of charge time series and issues with intertemporal constraints, when simulating large-scale models in sequences and displays the seasonality of hydro reservoir filling. Thereby, a nodal model of the European electricity market was developed that is capable of assessing nodal against the existing zonal pricing scheme through the incorporation of redispatching in the zonal modeling approach. A study of the costs of redispatching proves the applicability of the model and indicates the potential cost savings for congestion management that nodal pricing can signify.

Keywords: nodal pricing, electricity market model, internal European market, optimal power flow, optimization, heuristic

Abstrakt

Dizertačná práca analyzuje rôzne možnosti návrhu modelu európskeho trhu s elektrinou pre preskúmanie uzlových cien. Konkrétnejšie boli skúmané technické aspekty, ako voľba modelu pre tok výkonu, sieťová reprezentácia a podmienky zabezpečujúce časovú nadväznosť, ako aj ekonomické aspekty ako elasticita dopytu. V prvotnej analýze boli navzájom porovnané dve formulácie pre model toku výkonu, konkrétne AC-OPF a DC-OPF podľa uzlových cien. AC-OPF vedie k vyššej presnosti, ktorá môže byť signifikantná pre operačné dôvody. Pre model so väčším zameraním na elektrické trhy a cenové mechanizmy, sa preferuje DC-OPF, berúc do úvahy najmä menšiu výpočtovú náročnosť. Takisto bola vykonaná štúdia, ktorá implementuje elasticitu dopytu do tvorby cien v európskom kontexte. Výpočtové experimenty dokumentujú vplyv cenovej elasticity odberateľov na aktualizované objemy generovania energie jednotlivými zdrojmi a výrobné náklady. Prezentovaná prípadová štúdia skúmala tieto efekty v kontexte zmien z nižších na vyššie rozlíšenia sietí, ktoré zdôrazňujú úlohu dopytovej elasticity v systéme s vyšším počtom zón a v konečnom dôsledku pod režimom uzlových cien. Hlavný prínos tejto dizertačnej práce prezentuje vývoj heuristického algoritmu pre modelovanie vodných nádrží vo vysoko škálových modeloch uzlových cien. Práca napomáha prekonať nedostatok dát o časových radoch stavov vodných nádrží, problémy s podmienkami zabezpečujúcimi časovú nadväznosť pri rozsiahlych simulačných modeloch v sekvenciách a zobrazovaní sezónnosti naplnenia vodných nádrží. Z týchto dôvodov bol vyvinutý uzlový model európskeho trhu s elektrinou, ktorý aplikuje uzlový prístup oproti existujúcej zónovej cenovej schéme pomocou zahrnutia redispečovania zónového modelovacieho prístupu. Štúdia cien redispečovania dokazuje aplikovateľnosť modelu a indikuje potenciálne šetrenie nákladov pre manažment preťaženia spôsobeného uzlovými cenami.

Kľúčové slová: uzlová cenotvorba, model elektrického trhu, vnútorný európsky trh, optimálny tok výkonu, optimalizácia, heuristiky

Contents

List of Figures

List of Tables

List of Abbreviations

AC	Alternating Current
ACER	Agency for the Cooperation of Energy Regulators
ATC	Available Transfer Capacity
COP	Conference of the Parties
DAM	Day-Ahead Market
DC	Direct Current
DF	Delivery Factor
EUPHEMIA	Pan-European Hybrid Electricity Market Integration Algorithm
FND	Ficticious Node Demand
ISO	Independent System Operator
JRC	Joint Research Centre
KKT	Karush-Kuhn-Tucker
LMP	Locational Marginal Price
LP	Linear Program
MILP	Mixed-Integer Linear Program
OPF	Optimal Power Flow

OSM	Open Street Map
p.u.	Power Unit
PCR	Price Coupling of Regions
RAM	Remaining Available Margin
RTO	Regional Transmission Organization
SCOPF	Security-Constraint Optimal Power Flow
SO_2	Sulfur Dioxide
TSO	Transmission System Operator
UC	Unit Commitment

Nomenclature

$\mathcal{D}$	Set of Consuming Nodes
$\mathcal{E}$	Set of Edges
a	Demand Intercept
B	Susceptance
b	Demand Slope
d	Demand
F	Power Flow
f	Objective Function
G	Conductance
g	Power Generation

I	Current
N	Set of Nodes
$N(i)$	Set of Nodes Adjacent to Node i
P	Active Power
p	Price
Q	Reactive Power
q	Quantity of Power (Supply or Demand)
S	Apparent Power
V	Voltage
v	Voltage Amplitude
Y	Admittance
ϵ	Demand Elasticity
$\mathcal{G}$	Set of Generating Nodes
θ	Voltage Angle
I_d	Set of Demand Bids

Chapter 1

Introduction

Humankind is facing one of the most challenging tasks in its history, which is the proceeding climate change. The increasing amount of carbon dioxide released into the atmosphere since the industrial revolution is becoming an obvious issue that needs to be addressed with joint efforts. In the aftermath of COP21 in 2015 in Paris, countries have committed to contribute to this major change in various aspects of human life, but most prominently within the energy sector (UNFCCC, 2015). How energy is produced, distributed, and consumed contributes largely to global emissions. Hence, the need for a transition of the whole energy system is commonly agreed upon and pursued with joint efforts within the EU (Agora Energiewende and Sandbag, 2018).

Different strategies and regulations have been put forward to enable the transition of the energy system from a fossil fuel-based one to a system relying predominantly on renewable energies. In the context of the "Clean Energy for all Europeans", the European Commission has proposed a set of regulations in 2016, and the Council and the Parliament have approved these in 2018 and 2019, respectively (European Commission, 2016a). As a part of this, the European Commission aims to push for the so-called Energy Union, which among others, aims at redesigning and integrating the European electricity market. This will allow electricity to flow freely across borders, not being held back by physical or regulatory constraints. Integrating the electricity market is expected to allow for a broader competition between energy utilities and ultimately reduce overall system costs (Newbery et al., 2016).

Therefore, it is a task of high political interest to investigate possible future designs for the European electricity market that can facilitate the formation of the Energy Union and

enable the integration of an increased amount of renewable generation into the electricity mix.

Currently, the European market is based on zonal pricing. A uniform electricity price is determined for bidding zones, which predominantly follow country borders. Thereby, the physical limitations within the zones to the flow of electricity are disregarded. This calls for congestion management, as intra-zonal capacity limits of the electricity network are ignored in the price formation process, and flows that exceed these limitations represent a danger to the system's stability. One of the possible remedies to mitigate this problem that is increasingly gaining interest since its development is the concept of nodal pricing (Schweppe et al., 1988). In the process of determining nodal prices, the physical capacity limits of the network are being taken into account, which can thus reduce the need for redispatching and sending correct price signals to market participants (Hogan, 1999).

To assess nodal pricing or any market design for that matter, it is vital to rely on sound modeling of the electricity system. Mende et al. (2018) point out that combining grid and market models is vital to assess the electricity system properly. Market clearing models of the day-ahead electricity market are formulated as optimization problems, where either system operation costs are minimized, or social welfare is maximized (Purvins et al., 2018; Brancucci Martínez-Anido et al., 2013b). These problems are referred to as economic dispatch models, as the employment or dispatch of generation units is the outcome of the optimization that is to be determined. Now, in order to assess the zonal market design, it is necessary to combine a day-ahead market model, with a redispatching model that ensures that power flows are feasible throughout the entire network (Kunz et al., 2016; Poplavskaya et al., 2020). The result of such a combined model can then be compared against a nodal model, where the grid is already depicted in full detail. Therefore, one has to solve large-scale so-called optimal power flow problems, which is the aforementioned economic dispatch problem, including capacity limits for line flows that result from the dispatch of generators (Felling et al., 2019; Leuthold et al., 2012; Bjørndal et al., 2014). The assessment of design options for large-scale electricity market models for nodal pricing lies in the focus of this work. Further, the solution to these problems, given the complexity of such large-scale optimization problems, is an aspect addressed in this thesis.

Chapter 2

Research Question

The energy system is undergoing significant changes in the face of decarbonization and the incorporation of increasing renewable energy sources into the electricity mix. In order to facilitate this system integration, the European Commission aims to push for the so-called Energy Union (European Commission, 2016a). The aim is to create a fully-integrated internal energy market across Europe as one of the pillars of the European Commission's roadmap for the Energy Union. Thus, it is a topic of political relevance to advance this integration process and given the challenges the electricity system is facing, to also investigate possible future pathways to redesign the current system. One design option for the future electricity market that has received increasing interest by policymakers and researchers alike is nodal pricing, which represents an alternative to the currently-in-place zonal pricing-based market design. In order to evaluate the impacts of a switch to nodal pricing or any other market design for that matter, it is important to rely on sound electricity market modeling.

The electricity market is a complex and interconnected system with many stakeholders. Thus, alternations in its functioning and the making of prices need to be carefully assessed prior to implementation. Electricity market models are a key enabler to sound decision-making in such a complex environment. There are different design options when building a model of the European electricity market. Section 4 gives background information and sums up approaches to model electricity markets, with a special focus on incorporating nodal pricing. Each model features its individual focus and level of detail on different modeling options. In the context of nodal pricing, it will be of particular interest to incorporate a sound representation of transmission capacities along with modeling of

power flows.

Besides this, there are other aspects that can be of interest, e.g., time interdependencies between optimization problems, when executing simulations in sequence due to the size of a model with a long timescale; multiple criteria optimization taking into consideration several objectives as environmental aspects besides economic objectives; fair optimization to investigate the distribution of welfare among market participants; the exercise of market power; or other market sessions as real-time or balancing markets as well as congestion management.

Their importance will be evaluated on case studies, which will allow a comparison of nodal and other market designs and ultimately assess the relevance of different modeling aspects in terms of such a comparative study. Concretely, the overall research goal of this thesis is:

The design of an extended electricity market model capable to investigate market designs based on alternative pricing mechanisms with a special focus on nodal pricing.

The particular modeling design aspects that shall be investigated with respect to their relevance when moving from a zonal to a nodal market design can be subdivided into two main groups:

- Technical aspects concerning the modeling of the physical grid, e.g. transmission capacity representation and utilization, the impact of AC-OPF and DC-OPF, or intertemporal dependencies.
- Economic aspects of modeling electricity markets, e.g. demand elasticity, or distribution of economic welfare.

The relevance of these modeling aspects will be quantified with regard to their impact on system performance, in particular under a nodal market design. The expected outcomes are twofold, on the one hand, this research will employ improved modeling tools to assess the performance of electricity markets employing nodal pricing and enhance the understanding of the impacts of different modeling aspects on electricity market outcomes. On the other hand, this work will conclude with recommendations regarding the relevance of each individual modeling aspect, weighing benefits and accuracy against additional data

dependency, complexity, and computational expense.

Therefore, the remainder of this document is organized in the following fashion to address the questions introduced above. Section 3 introduces the theory behind the modeling of electricity markets by discussing optimal power flow and relevant economic concepts. Further, the evolution of electricity markets and their current functioning are laid out. In Section 4, the fundamental literature on nodal pricing is introduced. Further, the state of the art of modeling of nodal and zonal prices will be in the focus of this section, by discussing developed models and their applications. Selected relevant modeling aspects will be investigated in greater detail, which lays the ground for the studies conducted in the context of the PhD studies. Lastly, the issue of data and tool accessibility will be discussed, and different open-source models will be introduced. The main outcomes of the PhD project are in the center of Section 5. The main findings have been published in international conference proceedings and peer-reviewed journals. These papers serve as guidance for this section. Section 6 concludes this work and provides a critical view on shortcomings of the conducted studies, and formulates recommendations for future research.

Chapter 3

Electricity Markets: Theory and Background

3.1 Theoretical Background

This section will give an overview of relevant concepts from power flow modeling and economics that are essential to understanding electricity markets, which will be the focus of the second part of this section. The European electricity market and its functioning will be explained, and a short introduction to the US electricity system will be given as an example of a successful introduction of nodal pricing.

3.1.1 Power Flow and Optimal Power Flow

In power flow analysis, we can consider the electricity grid a graph, which consists of a set of nodes or buses N connected through a set of lines or edges $\mathcal{E}$ [1]. With each node i a number of variables are associated: voltage amplitude v_i, voltage angle θ_i, net active power P_i and net reactive power Q_i. There are different node types defined according to the variables known at that particular node: PQ nodes, P_i and Q_i are known, and v_i and θ_i need to be calculated; and PV nodes, where P_i and v_i are known and Q_i and θ_i need to be determined. The former ones are usually associated with loads without voltage control, while the latter represents generating nodes that do have voltage control. Additionally, there are so-called slack nodes or reference nodes $V\theta$, where v_i and θ_i are known and P_i and Q_i need to be calculated. As the name suggests, a reference node serves as a

[1] Much of this chapter is drawn from Andersson (2012).

point of reference for the voltage angle, because this variable is determined with respect to a reference angle. Furthermore, $V\theta$ nodes are needed to balance generation, loads, and losses, due to the initially unknown active power losses. The physical properties of lines connecting node i with node k are described through the conductance G_{ik} and the susceptance B_{ik}.

The equations describing the network flow can be derived from Kirchhoff's Law[2]. Active and reactive power injected at node i are expressed through:

$$P_i = v_i \sum_{k \in N(i)} v_k (G_{ik} cos(\theta_i - \theta_k) + B_{ik} sin(\theta_i - \theta_k)), \tag{3.1}$$

$$Q_i = v_i \sum_{k \in N(i)} v_k (G_{ik} sin(\theta_i - \theta_k) - B_{ik} cos(\theta_i - \theta_k)), \tag{3.2}$$

where $N(i)$ is the set of nodes connected to node i. These nodal power equations describe the main power flow problem, which is represented by a set of nonlinear equations. Depending on the node type, either P_i and Q_i or P_i and v_i are known, and the other variables need to be determined. This problem is usually formulated as a root problem and solved by using for example Newton-Raphson method.

Optimal Power Flow (OPF) is an optimization problem that seeks to minimize costs, with respect to constraints, which reflect physical limitations of the electricity grid as well as those of generators and loads. It is an essential tool that finds application in power system operation and planning. There are different formulations of OPF, while they can be very precise e.g. in taking into account various aspects of power plant operational constraints, we will introduce the general formulation of the AC-OPF and the linearized approximation referred to as DC-OPF.
In the following, $\mathcal{G} \subset N$ is the set of power-generating nodes and $\mathcal{D} \subset N$ is the set of power-consuming nodes. The objective function f of the minimization is usually considering generation costs, while the choice of cost functions varies predominantly between linear,

[2]For a more detailed explanation, see Appendix A.1.2

quadratic, and piece-wise linear. In the AC formulation, the OPF reads:

$$\underset{P,Q,\theta,v}{\text{minimize}} \sum_{i\in\mathcal{G}} f(P_i) \tag{3.3}$$

subject to

$$P_i = \sum_{k\in N(i)} P_{ik} = \sum_{k\in N(i)} v_i v_k (G_{ik} cos(\theta_i - \theta_k) + B_{ik} sin(\theta_i - \theta_k)), \quad i \in N \tag{3.4}$$

$$Q_i = \sum_{k\in N(i)} Q_{ik} = \sum_{k\in N(i)} v_i v_k (G_{ik} sin(\theta_i - \theta_k) - B_{ik} cos(\theta_i - \theta_k)), \quad i \in N \tag{3.5}$$

$$P_{ik}^2 + Q_{ik}^2 \leq F_{ik}^2, \qquad i \in N, \quad k \in N(i) \tag{3.6}$$

$$\underline{P}_i \leq P_i \leq \bar{P}_i, \qquad i \in \mathcal{G} \cup \mathcal{D} \tag{3.7}$$

$$\underline{Q}_i \leq Q_i \leq \bar{Q}_i, \qquad i \in \mathcal{G} \cup \mathcal{D} \tag{3.8}$$

$$\underline{v}_i \leq v_i \leq \bar{v}_i, \qquad i \in N, \tag{3.9}$$

where one seeks to minimize (3.3), subject to the following constraints: relation between power and voltage through admittance or the power flow constraints for active and reactive power (3.4)&(3.5), apparent power flow limits of the lines (3.6), operational power limit for generation and load (lower active and reactive power limits $\underline{P}_i$ and $\underline{Q}_i$ and upper active and reactive power limits $\bar{P}_i$ and $\bar{Q}_i$) (3.7)&(3.8) and voltage magnitude limits (lower $\underline{v}_i$ and upper $\bar{v}_i$) (3.9) (Andersson, 2012; Taylor, 2015).

AC-OPF is a quadratically constrained (3.6) non-convex optimization problem, because of the power flow constraints (3.4)&(3.5). DC-OPF presents an approximation of this problem, which is achieved through a number of assumptions that lead to a simplification of the OPF: voltage magnitudes v_i are close to 1 p.u. (power unit); reactive power flows are neglected; conductances G_{ik} are negligible relative to susceptances B_{ik}; voltage angle differences are (in stable operation mode of the grid) small, so that $sin(\theta_i - \theta_k) \approx \theta_i - \theta_k$. This leads to the DC-OPF, which reads:

$$\underset{P,\theta}{\text{minimize}} \sum_{i \in \mathcal{G}} f(P_i) \tag{3.10}$$

subject to

$$P_i = \sum_{k \in N(i)} P_{ik} = \sum_{k \in N(i)} B_{ik}(\theta_i - \theta_k), \quad i \in N \tag{3.11}$$

$$-F_{ik} \leq P_{ik} \leq F_{ik}, \qquad i \in N, \quad k \in N(i) \tag{3.12}$$

$$\underline{P}_i \leq P_i \leq \bar{P}_i, \qquad i \in \mathcal{G} \cup \mathcal{D}. \tag{3.13}$$

The following section will provide the economic motivation behind the OPF problem formulation, and eventually will explain how one can derive nodal prices from these optimization problems.

3.1.2 Electricity Pricing, Economic Dispatch and Unit Commitment

In electricity markets, the market clearing problem is usually formulated as an economic welfare maximization problem (for more details, see Appendix A.1.3.1). When the elasticity of demand is set to zero, i.e. the demand is a constant quantity d, then instead of welfare maximization, one can formulate the problem as the minimization of generation costs. In the simplest formulation of the so-called economic dispatch, the optimization problem can be formulated in this way:

$$\underset{g_i}{\text{minimize}} \; f(g) \tag{3.14}$$

subject to

$$\sum_{i \in \mathcal{G}} g_i - d = 0. \tag{3.15}$$

Where the costs function f to generate power g is minimized, subject to the real power balance in the system, i.e. the sum of all power generated g_i from generators $\mathcal{G}$ needs to equal the overall demand d. This is the simplest approximation of power flow (see Section 3.1.1) (Taylor, 2015). The market-clearing price should reflect the costs of producing (or consuming) one additional MWh of electricity. In the context of duality,

this is represented by the dual variables λ of the power balance constraint (3.15)[3]. Usually, the economic dispatch problem includes constraints reflecting the operational limitations of generation units. Further, when also flow limits are included represented by the power grid, one speaks of OPF (see Section 3.1.1). In the DC-OPF formulation, the optimization problem takes the form as it has been stated in Equations (3.10)-(3.13).

In a zonal representation, which is currently in place in Europe, for every pricing zone, one power balance is enforced as well as flow limits between the zones. The dual variables associated with each power balance constraint will render the zonal market-clearing price. Moving towards a more detailed representation of the electricity network, further energy balances can be introduced, in which case one would speak of a nodal representation and the dual variables of these constraints will render the nodal prices or locational marginal prices (LMP).

In the above formulation of the economic-dispatch problem, power could be drawn continuously. However, in reality, it will be delivered by a discrete number of power plants (units) that are committed to delivering. Therefore, the problem formulation needs to include binary variables, which leads to Unit Commitment (UC).

3.2 Evolution of Electricity Markets

Electricity markets worldwide were undergoing some evolution in the 1990s. Before, electricity systems were vertically integrated and in their entirety highly regulated. Often a single utility controlled generation, transmission i.e. electricity networks and their operation and distribution, they thus held a monopoly on electricity and had to be overseen by regulatory authorities to ensure fair pricing for consumers. Then there was a push for deregulation in many countries, which led to the unbundling of the energy value chain and allowed more players to enter into the market, giving room for competition. The EU initiated the process of liberalizing electricity markets in 1996 within the First Energy Package (European Union, 1996). With the Third Energy Package in 2009, ownership unbundling became mandatory and in this context, ACER was founded to further facilitate the cooperation across countries (European Union, 2009). However, the operation and maintenance of the power grid remain the task of regulated entities, as it

[3]The concept of Lagrangian duality and the Karush-Kuhn-Tucker conditions are presented in Appendix A.1.1

represents a natural monopoly on distribution. With the deregulation of the energy sector, energy utilities had to sell their generation units, allowing others to enter the market. As a result of more market participants, wholesale electricity markets were created.

3.2.1 The European Electricity Market

The liberalized European electricity market can be subdivided into three sequences, as indicated in Figure 3.1.[4] On the forward market, long-term agreements are made for months and years before the physical delivery of electricity. Moving closer to real time, the day-ahead market (DAM) plays a central role and can be viewed as the reference market. DAM auctions open at 10 CET and close at 12 CET the day before the delivery of the good. Electricity is traded with an hourly granularity for all the 24 hours of the following day. Within a bidding zone, electricity offers and demand bids are collected, and the market is cleared at a uniform market clearing price for an entire zone. A bidding zone is predominantly equal to a country within Europe, while inter-zonal trading is possible. Between zones, a difference in prices can exist, as for inter-zonal trading the capacities of transmission lines are taken into consideration through available transfer capacities (ATC). A consideration of line capacities of the grid is not implemented within zones, which can be understood as viewing a zone as a copperplate. This may lead to congestions of lines when their capacity is exceeded and calls for measures to be taken to ensure a secure operation of the grid. These measures are referred to as congestion management (including re-dispatching, counter trading) and are taken by the transmission system operators (TSO) responsible for the respective zone (Holmberg and Lazarczyk, 2015). On the last sequence of the market the real-time or balancing market, balancing service providers can offer their services in terms of reserves (i.e. capacities to increase or decrease generation or demand) to TSOs, in order to allow them to perform congestion management as well as ensure the overall balance of supply and demand in the system.

Following the zonal design of the market sequence, it is interesting to consider where nodal pricing should be implemented within the existing scheme. The possible introduction of nodal pricing in the DAM and the real-time market is the subject of various research. Therefore, the next chapter shines light on the current functioning of

[4] A number of regulations of the European Commission lay out the rules for the operation of the transmission system and electricity markets, which are commonly referred to as Network Codes (European Commission, 2017a, 2015, 2017b, 2016b).

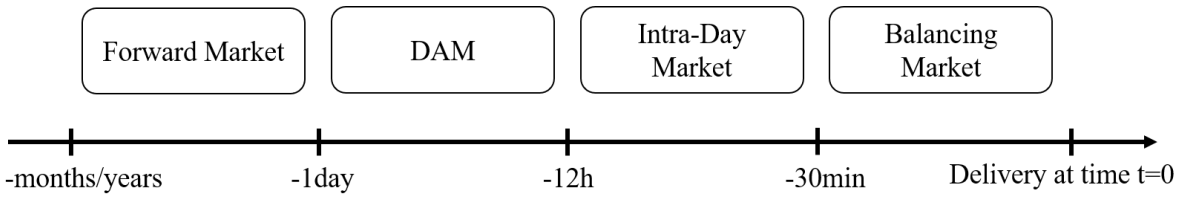

Figure 3.1: Market sequence in Europe consisting of forward market, DAM, intra-day market, and real-time balancing market (Schittekatte et al., 2019).

the European DAM.

3.2.2 The US Electricity Market

The unbundling of electricity markets has also happened in the US in the late 1990s and their system is in general comparable to the European model, though with some important differences, which will be outlined in this section. The transmission grid is owned and operated by so-called Regional Transmission Organizations (RTO) and Independent System Operators (ISO), which are similar to each other and comparable to European TSOs. RTOs carry out their duties on a larger geographic scale than ISOs, differently than TSOs they usually also operate electricity markets.

The structure of markets varies across the country, but in general, the sequence of markets is DAM, intra-day market, capacity market, and ancillary service market. Capacity markets are used to ensure that a reserve margin of electricity generation is available in order to maintain grid reliability. Ancillary service markets are used to reward other services provided by utilities that are used, e.g. for frequency control. Even though the US has a similar market structure in place to Europe, in order to provide RTOs/ISOs with the tools to ensure grid stability, additionally and most importantly, some US markets have implemented locational marginal pricing (PJM 1998, New York 1998, New England 2003) (Dietrich et al., 2005). Through prices that vary across regions, congestions in the transmission grid are reflected, and this is the first countermeasure to manage these congestions. LMPs are determined at the DAM and intra-day stage.

3.3 Nodal Pricing in the European Electricity Market

While the current design of the European electricity market is based on zonal pricing, in the phase of the challenges that the electricity system is facing, several changes to the functioning of markets are being under consideration. The European Commission (2016c) in their impact assessment have investigated four possibilities for improving local price signals to improve dispatch decisions and investments in the EU wholesale market (Antonopoulos et al., 2020). It is stated that a switch from zonal to nodal pricing would incorporate the value of available transmission capacity across market regions, which would utilize available resources more efficiently. The impact assessment further points out that for electricity markets and networks, nodal pricing is theoretically the most optimal pricing system and would render remedial actions by TSO to alleviate congestions unnecessarily. However, implementing nodal pricing in the European internal electricity market would imply a fundamental change to the structure of markets, the management of the grid, and trading mechanisms and was deemed disproportionate. Further, stakeholders expressed concerns about creating a single EU Independent System Operator, instead, a step-wise regional integration of system operation is preferred. Thus, currently, there are some regulatory barriers to implementing nodal pricing in the European electricity system, as well as some opposition by stakeholders, that would need to be overcome.

Chapter 4

Electricity Market Modeling: State of the Art

4.1 Nodal Pricing in a Broader Context

A potential transformation of the European electricity market towards nodal pricing is subject of various discussions in research as well as in a policy context (Antonopoulos et al., 2020) since it was proposed by Schweppe et al. (1988). The market design currently in place in Europe is based on zonal pricing as mentioned above. One of the arguments to maintain this is as opposed to moving to a nodal pricing-based market design is the level of complexity that would arise when switching market design. However, this has been questioned to be a valid argument as experiences made in the USA suggest (Neuhoff and Boyd, 2011). In the following, some concrete advantages and challenges linked to the introduction of nodal pricing will be highlighted, as they are being discussed in literature. One of the main cases made in favor of nodal pricing is "getting the price right" (Hogan, 1999). This means that several prices are needed to sufficiently display the economic and physical reality of a transmission grid. Conversely, a single price i.e. a zonal price will not reflect the physical constraints within a zone appropriately. Capacity limits of the grid do not allow for a free flux within a zone, as a homogeneous price suggests. This fact is giving rise to readjustments as counter-trading and re-dispatching done by TSOs in order to ensure system stability. This is because the reality i.e. the bottlenecks of the grid are not displayed in electricity prices. These issues can be addressed through the introduction of nodal pricing (Schweppe et al., 1988). Furthermore, nodal prices can

facilitate the integration of day-ahead and balancing markets. As has been mentioned above, in the zonal design of the market, as it is in place in Europe as of today, firstly, the DAM is cleared. In a subsequent step, real-time trading is needed, in order to provide for balancing of the system by TSOs through managing reserve capacity. In this context nodal pricing can make this step of re-dispatching obsolete or less important, which is mostly necessary because the physical grid constraints are being disregarded in the zonal approach (Hogan, 1992).

In every node, the particular price will display the physical reality and thus send the correct economic signals. By sending the right price incentives, nodal pricing can also contribute to avoiding boom and bust cycles as they tend to appear within investments in generation units (Schubert et al., 2006). Boom and bust cycles refer to the phenomenon that in times of low electricity prices investments in electricity generation units decrease (Ford, 2002). They do so up to a point, when there are fewer and fewer units in the market, which will eventually cause an increase in electricity prices, which will in return increase investments in generation units again. However, this is not a cost-effective investment scheme for the overall system, and the potential to mitigate it through nodal pricing an opportunity worth mentioning. A prominent argument made against nodal pricing is the increased presence of market power. Market power is exercised when a market participant is able to dominate the market due to its strong position in the same and abuse this power. A larger bidding zone does not only offer a higher liquidity, but as there is a large number of participants, their individual capabilities to gain and exercise market power is mitigated. Based on technical considerations and experiences gained from the implementation of several zones in the Californian market, Harvey and Hogan (2000) arrive at opposite conclusions. While a node represents a smaller area than a zone, the optimization and clearing of market prices is done considering a much larger area. Thus, at the same time, in the face of smaller bidding areas on a nodal level, market surveillance can become simpler.

Hu et al. (2018) perform a literature review of market designs favoring increased RES in the system. Their findings are that there are many barriers in the way of RES integration, one of them being the integration costs. As a remedy, they identified among other locational marginal pricing, as it reduces grid costs. Therefore, they suggest further

work to focus on model based cost-benefit analysis of suggested LMP based markets.

In a technical report of the JRC, Antonopoulos et al. (2020) conduct an analysis of the effects and possibility to implement nodal pricing in the European internal electricity market. While they point out the possible benefits, they identify a couple of challenges as the practical transitioning, which would be cumbersome in the face of several technical and regulatory challenges. Further, a shift in the reference market would be required, i.e. balancing market would be the reference market while DAM and intra-day market would be considered forward markets. Thus, further harmonization of European balancing markets is a prerequisite. Lastly, Antonopoulos et al. (2020) also stress the question of the roles of TSOs and DSOs and their interactions in the face of increased decarbonization and decentralization of the electricity system. As opportunities for future research, they identify the investigation of zonal-nodal hybrid systems, as well as the possible benefits of a pan-European nodal system.

Weibelzahl (2017) survey nodal, zonal, and uniform pricing mechanisms in the context of congestion management. The main advantages of nodal pricing are identified to be welfare maximization and efficient pricing; and perfect integration of generation and transmission. Disadvantages, on the other hand, are a large number of prices, low liquidity, and a small number of traders and resulting low competition as well as the complex coordination of submarkets. The author concludes that nodal pricing yields the first best outcomes, as congestion is reflected in LMPs. Though many countries still maintain a uniform or zonal pricing scheme due to the discussed disadvantages of a full nodal pricing mechanism. This in consequence leads to welfare losses, thus, studies need to carefully assess and quantify the advantages and disadvantages. Thereby, one is faced with a trade-off between the detailed technical depiction of nodal systems and computational solvability. While there may be some difficulties in the joint implementation of nodal pricing in Europe, it is worth investigating the feasibility given the advantages nodal prices could provide.

4.2 Models of Zonal and Nodal Markets

The algorithm utilized to clear the European area covered under the price coupling of regions (PCR) is EUPHEMIA (Pan-European Hybrid Electricity Market Integration Algorithm). EUPHEMIA is an algorithm focused on the economics of the electricity system that includes great detail in terms of possible bid types that market participants can utilize. Though, the algorithm does not include the actual technical constraints that the participating units and the grid actually encompass. Due to the large variety of bid types and the corresponding complexity, most market models presented in literature do not try to realistically emulate EUPHEMIA, but rather rely on unit commitment or economic dispatch, which include technical constraints and merge them with an economic perspective.

In the following various studies that rely on zonal, nodal or a combination of both are presented and applications of these models are discussed.

4.2.1 Zonal Models

The Joint Research Centre (JRC) of the European Commission has developed a pan-European economic dispatch model (Purvins et al., 2018; Zalzar et al., 2020). The optimization problem is formulated as a generation cost minimization problem. Costs are minimized for a period of 24 hours, while constraints are enforced for every hour of a day. The typical simulation horizon is one year. The commercial energy modeling software PLEXOS is used to implement the described model (`energyexemplar.com`). The model includes 33 countries, which are modeled through 55 nodes. Purvins et al. (2018) applied the economic dispatch model to perform a techno-economic cost-benefit analysis of a submarine cable linking North America's and Europe's electricity systems. For this purpose consumer, producer, and merchant surplus were determined. Following basic economic theory, consumer surplus cannot be obtained when demand is a fixed input, which corresponds to a vertical demand function leading to infinite consumer surplus. Thus, Purvins et al. (2018) apply linear demand functions determined through a short-run demand elasticity value applied to all the nodes for the entire year of the simulation horizon. More detailed modeling of flexible demand has been identified as a shortcoming of the thus far conducted work and was picked up already as a starting point for improving

the present model (see Section 5.2).

Bakirtzis et al. (2018) of the Aristotle University of Thessaloniki developed *PHOEBE* a European market model. PHOEBE is implemented using GAMS, MATLAB and MS Excel. At the core of the bottom-up model lies the 3-level unit commitment optimization model. The optimal scheduling of power plant electricity generation is done in three successive steps that clear the different markets: day-ahead market, intra-day market, and balancing market. The model resolution features the hourly operation of the system for a yearly horizon. The main application of their model is the assessment of different demand response schemes and the impact of system adequacy and flexibility. The employed market model is a unit commitment model formulated as a mixed-integer linear program (MILP), which is executed in GAMS. The objective is to minimize the overall costs over all hours of the scheduling horizon, which is usually 24 hours. The results are assessed based on factors quantifying the adequacy and flexibility of the system. The main features of this model are the holistic view of 21 European countries, the great technical detail in modeling the power plants and their operation, and the coupling of a 3-level market optimization model with probabilistic considerations based on Monte Carlo simulations that can assess different scenarios based on climatic variations. Possible extensions to PHOEBE can be a higher time resolution going from hourly to quarter-hourly operation as well as the extension to include more countries. Especially, a more detailed representation of the transmission grid can be a useful extension to the model.

Ringler et al. (2017) analyze the potential benefits of creating an integrated European electricity market through an agent-based model. They give special attention to design aspects such as cross-border congestion management and capacity mechanisms. These are investigated with respect to their impact on two system performance measures, i.e. market-wide welfare and adequacy. In a case study considering Central Western Europe, they confirm the benefits entailed by cross-border market coupling and the furthering of market harmonization across Europe.

4.2.2 Nodal Models

Leuthold et al. (2012) developed ELMOD a model of the European electricity market, building up on the work of Dietrich et al. (2005). The model is formulated as a welfare maximization problem, where the cost of generation is represented by a step-wise supply

function, while the demand is modeled through a linear function. Furthermore, the model includes start-up costs and hydro storage. Simulations are conducted at increments of one hour and social welfare is maximized considering the entire time horizon, which in the foreseen application of this model is 24 hours. Another simplification is fixing the demand levels, which allows formulating the objective as a generation cost minimization problem and making it a linear program (LP). Extending this problem again to include unit commitment makes it a MILP. The model is implemented in GAMS.
Leuthold et al. (2012) model the European grid considering more than 4,000 nodes and more than 2,000 lines. Janda et al. (2017) utilize ELMOD for a study on the impacts of renewable energy sources on transmission networks in Central Europe. In particular, they assess the implication of the German Energiewende through different scenarios for 2050 for the transmission system and cross-border flows. They find that increased wind and solar power increase the flows between zones and their volatility. Due to a lack of capacity especially in the German system, higher in-feed of wind is identified as the main contributor to loop-flows through neighboring countries. Interestingly, they further find that the nuclear phase-out does not contribute significantly to this increased volatilities and stress to the system.

Quelhas et al. (2007) consider the US energy system and model the flows of energy through a generalized minimum cost flow problem. What differentiates their model from the previously introduced one is that next to physical and economic aspects, they also include environmental factors. Though their general problem formulation is similar to previous models, they use a slightly different approach of a standard network flow model. They perform a transformation, in which node-like facilities are represented through a pair of nodes connected by an arc and consequently the arc parameters represent the facility's properties that restrict the flow through it. Generation costs are a convex function of the flow and are being approximated with a piece-wise linear function, which is comparable to the previously discussed generation bids making up the supply curve in the actual DAM. Now, additionally they propose another side constraint that ensures that the overall nationwide Sulfur dioxide (SO_2) emission target will be respected:

$$\sum_{i \in \mathcal{G}} \sum_{j \in N(i)} \left(SO_{2i} \cdot (1 - \eta_i) \cdot \sum_{l \in I_g} F_{ijl} \right) \leq NSO_2, \tag{4.1}$$

where SO_{2i} is the Sulfur dioxide emission rate of generation unit i, η_i is the SO_2 efficiency rate of the emission removal equipment installed at unit i, NSO_2 is the national SO_2 limit.

Horsch and Brown (2017) study the role of spatial scale on the optimization of transmission and generation capacity for a European system with 95% reduction in CO_2. In order to identify locations for solar, on- and offshore wind, and grid expansions a sufficient spatial resolution is necessary, to determine the hotspots and benefits of such expansions. From their case study, they find that a scenario with no grid expansion is only 20% more costly than the system with optimal grid expansion. By focusing investments on expansions of existing lines, the issue of public acceptance of newly build transmission lines can largely be avoided. The authors stress that their results rely on the assumption of a fully-integrated European system relying on nodal pricing.

4.2.3 Nodal vs. Zonal Models: Case Studies and Applications

Dietrich et al. (2005) investigate nodal and zonal pricing in the German electricity system through a welfare economic analysis. The electricity system model ELMOD is used for the assessment of increased integration of wind power into the electricity system, with a focus on Germany. They identify potential for savings in cost for congestion management in the nodal system but conclude that there is a need for extension of grid representation in such case studies.

Egerer et al. (2016) employ ELMOD in order to assess a splitting of the single German bidding area into two. This is a topic of interest given the heterogeneous distribution of demand and supply in Germany, which is only expected to become more pronounced with the increasing installation of on- and offshore wind in the North. In their case study, Egerer et al. (2016) find that there is a modest decrease in cross-border re-dispatching levels. However, the need for congestion management remains high even under a splitting of bidding zones. Further, results are very sensitive to more than two bidding zones. Future work can include a geographical extension to investigate the effects on exports, especially to Southern Europe.

Bjørndal et al. (2014) develop an electricity pricing model, which investigates a hybrid pricing scheme consisting of areas with zonal and areas with nodal pricing in the Nordic electricity market and the impacts on congestion management. The model is applied to

a 13-node system emulating the Norwegian and Swedish power systems. The authors pay special attention to a high-demand scenario, in which they conduct simulations for a single hour of peak demand. Results for the three pricing schemes are compared in terms of prices, line loading and utilization, social surplus, and total production and generation. Bjørndal et al. (2018) apply their hybrid zonal-nodal pricing model to a case study including the Czech Republic, Germany, Poland, and Slovakia. In their scenario, Poland adopts a nodal pricing scheme, and they investigate a case of business as usual and one of high wind penetration. They find that Poland can benefit from a shift to a nodal pricing scheme, as it helps them manage impacts on their grid caused by their vicinity to wind power generation units. Poland is able to reduce their needs for redispatching. At the same time, Bjørndal et al. (2018) find that a country like Germany with a diverse supply and demand structure can benefit from keeping a zonal pricing scheme, as it helps them maintain a relatively low electricity price level throughout the entire country.

Felling et al. (2019) investigate the existing price zone configuration in central Western Europe and propose different configurations based on the results obtained from employing a large-scale modeling framework. Their model is based on flow-based market coupling. The comparison performed by Felling et al. (2019) comprises technical and socio-economic impacts of the different configurations.

Their modeling efforts can be best described in a step-wise scheme. In the first step, an OPF model is employed to calculate LMPs for all nodes. Their OPF is based on the DC-lossless approximation, for which they use MATPOWER (Zimmerman et al., 2011).

In the consecutive step, an algorithm is used in order to cluster nodes into zones. The hierarchical process firstly assigns one node to one zone and continues until all nodes are part of a single zone. Nodes are assembled based on the smallest difference in LMPs between the different nodes, i.e. the merging criterion is for the variation in prices within a zone to be as small as possible (see (Felling and Weber, 2018)).

At the D-2 stage (two days before delivery), the allocation of capacity is determined, which is in reality a task of the TSOs (see also Figure 4.1 for a comparison between real-world mechanisms and the modeling approach of the same suggested by Felten et al. (2019a)). These capacities are the remaining available margins (RAM) resulting from the zonal power transfer distribution factors.

At the D-1 stage (day-ahead stage), the WILMAR Joint Market Model (JMM) is

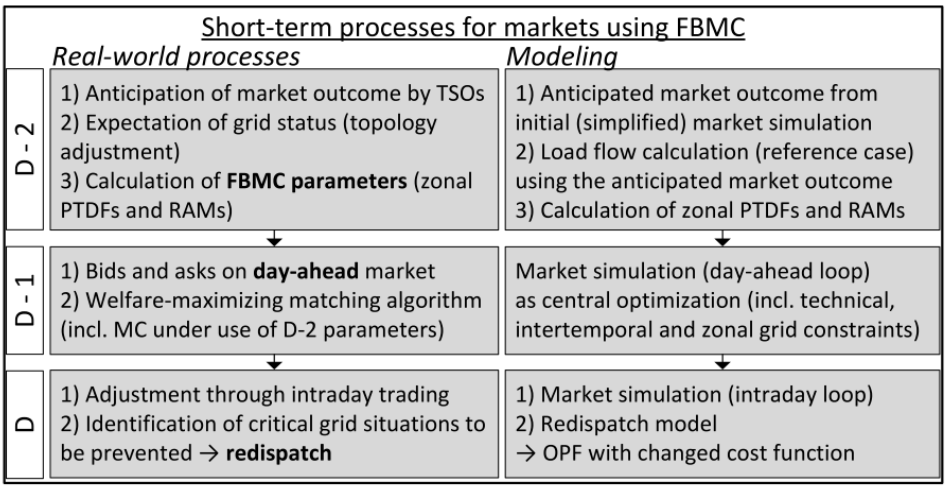

Figure 4.1: Illustration of real-world processes and the corresponding modeling (Felten et al., 2019b).

employed to clear the market (Tuohy et al., 2009; Meibom et al., 2011). This scheduling model depicts almost the complete European electricity market and hence they merely employ the linear deterministic program version in order to keep calculation times manageable. This assumes that plant operators have perfect knowledge of their generation at the day-ahead stage, even for a renewable-based generation. Furthermore, generation units are grouped in units of similar age and capacities within a single pricing zone. The level of knowledge results in very similar prices reached at the day-ahead and intra-day stage of the market, yet this feature is only present in the market model. In general, the JMM solves a cost minimization objective subject to inter-zonal capacity limits (RAMs), zonal power balance, and generator operation constraints. However, in its actual implementation, JMM has more than 40 constraints that are being enforced and are thus not all depicted here in detail. At the D stage, the real-time stage, or redispatching stage, the TSO needs to adjust the dispatching of power. After the scheduling of plants is determined from the market-clearing stage, TSOs calculate the corresponding line loadings and in case of overloadings redispatch power plants. The redispatching model is formulated as an OPF with the objective of minimizing redispatching costs, i.e. those for ramping up or down generators. The constraints enforce nodal flow capacity limits, energy balance, and various limitations to redispatching capacities.

Felling et al. (2019) apply their model to assess alternative bidding zone configurations for Central Western Europe and neighboring countries. Bidding areas are clustered based on LMPs using a novel hierarchical clustering algorithm (Felling and Weber, 2018). Felling

and Weber (2018) conclude that welfare gain can be generated through a switch in configuration. The benefits originate mostly from reduced costs for redispatching due to avoided intra-zonal line congestions.

Mende et al. (2018) stress the need to combine market and grid models in order to perform studies that can assess the increased integration of RES into the electricity system. When exploring future scenarios for the power system, the market perspective can only be a starting point, as especially grid extension and operational issues will play a key role in the future evolution of the system. Thus, they propose a soft-linked combined market and grid model. They apply their model to a case study on the German system and study the level of congestion due to a zonal dispatch of generators. They conclude that, especially given the spatial distribution of RES, a detailed representation of the grid and all power systems components is vital for a sound contingency analysis of future power systems.

Poplavskaya et al. (2020) develop a novel market design that integrated redispatching into a zonal market with flow-based market coupling. They compare their outcomes against a full nodal model and a zonal model without integrated redispatching. They find that their approach can reduce the need for ex-post redispatching and increase cross-border capacity utilization.

Kunz et al. (2016) compare nodal to zonal pricing through two models. The zonal model minimizes generation costs subject to zonal balance and generation constraints. In a subsequent step, congestion management is modeled through another cost minimization problem, where line capacity limits are enforced as constraints. The nodal model combines this two-step approach in a single optimization. Kunz et al. (2016) investigate distributional impacts of a switch from zonal to nodal pricing in Germany. Through the allocation of financial transmission rights (FTR), the impacts of price changes on individual actors can be mitigated. In their case study, they find that the distributional effects on the demand side and also largely on the conventional generation can be successfully mitigated with the right allocational design of FTR. However, they identified more challenges with regards to intermittent renewable generation, where more sophisticated FTR design is needed to facilitate an effective switch from zonal to nodal pricing.

It can be seen from various of the previously discussed studies that for a comparative

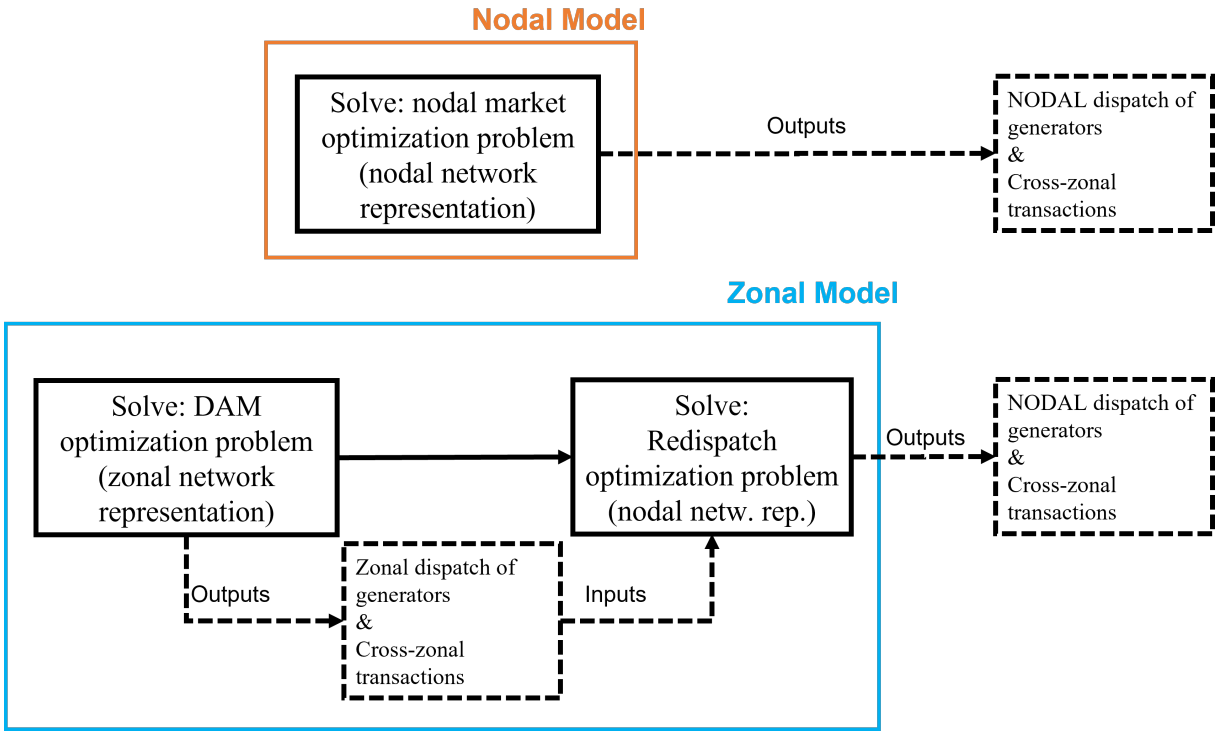

Figure 4.2: Schematic depiction of nodal model and zonal model, including redispatching.

assessment of the performance of a nodal market design against a zonal market design, it is necessary to include redispatching into the consideration. This is because a model that determines zonal prices and employs a zonal network representation, disregards intra-zonal congestions that occur. While a model with nodal network representation that determines nodal prices will regard the physical limitations of the grid. Therefore, it is necessary to combine a zonal model with a redispatching model to have a comparable picture of the final results. This higher level rational is depicted in Figure 4.2. It can be seen that a nodal model can arrive at a dispatch of generators that is feasible, in the sense that grid constraints are respected. On the other hand, the generator dispatch of a zonal model needs to be readjusted by a redispatching model to ensure feasibility. According to Schittekatte et al. (2019), redispatching actions are firstly applied within a zone, and only if this is not sufficient to relieve all congestions, also cross-zonal redispatching is employed.

In the literature, different formulations of the redispatching problem have been proposed. In general, the objective is to avoid line overloadings (Felling et al., 2019). Concretely, this objective is either formulated as cost-based or technical-based (also referred to as volume-based) redispatching. The former is more common, where the costs

of redispatching are minimized. It is employed in several studies and regarded to be the approach closer to reality (Spieker et al., 2016; Grimm et al., 2018; Van Den Bergh et al., 2015; Chychykina, 2019). Usually, upward redispatching makes a positive contribution to the objective function, and downward redispatching a negative distribution. Felling et al. (2019) suggest to price upward redispatching at the marginal costs of the respective generator and downward redispatching at a positive cost that is determined by an inverse merit order. This means that the generator with the highest marginal costs is the cheapest to be utilized for downward redispatching and conversely the generator with the lowest marginal costs is the most expensive to be downregulated. Thereby, they avoid arriving at the same dispatch of generators with the redispatching model as they do with the nodal model.

In the volume-based approach, the intervention in the dispatch of generators is minimized. This means that the minimization of redispatched power is the objective, regardless of the type of generator and the connected costs. Poplavskaya et al. (2020) suggest a parametrized objective that puts weights on minimizing either the volume or the cost of redispatching. Similarly, also Mende et al. (2016) introduce a multiobjective optimization that considers a trade-off between the volume- and the cost-based redispatching approach.

4.2.4 Overview and Summary

The previous section presented a literature review on different nodal and zonal models as well as their applications. To conclude this overview, a closer look will be taken at the different modeling aspects that are included in the previously mentioned papers. Further, the applications of various models will be summarized by considering what case studies were performed and what were major outcomes and shortcomings of these studies.

In order to build a model of the electricity market, one is faced with different design choices. However, there are some set building blocks that are virtually always present in such models. An overview of these modeling aspects and examples of choices presented in the literature are summed up in Table 4.1. The market-clearing model is formulated as an optimization problem subject to a number of constraints. The objective can be formulated as cost minimization or welfare maximization. Closely related to this is the way costs of supply and surplus of demand are depicted. Supply functions are often

approximated as linear, piece-wise linear, step or quadratic functions. If the objective is to minimize costs, then the demand is modeled to be inelastic. While in the case of welfare maximization, demands are depicted as functions in the model. Related to the level of technical detail of power plant operations is the formulation of the problem as economic dispatch or unit commitment. The former considers plant operation to be continuous, while the latter takes into account that there is a minimum operational point, which calls for binary decisions of plants to be either on or off. Thus, the unit commitment would render the optimization problem a mixed-integer problem. The operation of power plants is virtually always at least modeled through setting an upper limit for the power of the respective generation unit. Other aspects of modeling power plant operations can be the following. Start-up and -down costs that add additional terms to the objective function. Ramping constraints take into account that in order to start or stop a power plant, it takes time (and fuel/costs) to arrive at the minimum operation power level. Minimum up- and down-times to avoid unrealistic shutting on and off of power plants from one hour to the next. Lastly, the choice of power flow model is being considered. The most accurate model of displaying power flows is the AC-OPF, which considers all physical properties of lines, and flows are calculated accordingly. The DC-approximation represents a common simplification of the full flow model, which is also referred to as linear approximation. The simplest approximation to display electricity flows in power lines is the transport model, which is ensuring flow conservation.

From the overview in Table 4.1 one can see that both types of objectives cost minimization and welfare maximization are being employed in the literature. Regarding the formulation of the supply function, linear functions are common, while also piece-wise linear or step-wise functions are being used. For the models that do consider elastic demand, linear demand functions are used exclusively. When it comes to the detail of generation unit operation, economic dispatch is prevalent, while also unit commitment receives due attention. Also, the consideration of start-up and down, and on- and offline constraints, as well as reserves is sometimes included in the models, but not imperative in the surveyed studies. Last, the choice of power flow model is rather dominated by DC-OPF. Only dedicated studies explore more detailed formulations of the power flow equations. Transport models are sometimes used, which is predominantly the case in zonal models.

Table 4.1: Modeling choices for electricity market models; objective function formulation, supply and demand function, economic dispatch or unit commitment, intertemporal constraints or reserves, and power flow model. Shown are references that present electricity market models and the choices made for the respective models.

Reference	Objective Function	Supply function	Demand function	Economic Dispatch (ED) / Unit Commitment (UC)	Further operational constraints & reserves	Power Flow Model
Felling, et al., (2019)	min cost	piece-wise linear	none	ED	start-up & -down, on- & offline constraints	DC
Grimm, et al. (2018)	max welfare	linear	linear	ED	none	DC
Bakirtzis, et al. (2018)	min cost	linear	none	EDUC	start-up & -down, on- & offline constraints, reserves	DC
ENTSO-e. (2018)	min costs	N/A	N/A	ED	none	DC
Leuthold, et al. (2012)	max welfare	step-wise	linear	UC	on- & offline constraints	DC
Bjørndal, et al. (2014)	max welfare	piece-wise linear	linear	N/A	N/A	DC
Baghayipour, et al. (2012)	N/A	quadratic	none	ED	none	DC, improved DC and AC
Breuer, et al. (2013)	min cost	linear	none	ED	none	DC
Purvins, et al. (2018)	min cost	piece-wise linear	optional (linear)	ED (UC optional)	reserves	transport
Quelhas, et al. (2007)	min cost	piece-wise linear	none	ED	none	DC
Kunz et al. (2016)	min cost	linear	none	ED	none	DC

4.3 Selected Modeling Topics

From the literature on various market models, one can understand that depending on the focus and the aim of the modeling exercises and case studies, there are different design options to build a model of the European electricity market. In the following, a more detailed view of some design options of models is given.

Firstly, the choice of flow models will be investigated. In OPFs, the representation of flows in the network is a central choice. In the simplest way, network flows can be represented by a so-called transport or network flow model, where only the conservation of flows needs to be ensured. However, in order to account for physical flows, one needs to either choose a DC-OPF or AC-OPF. Even though it is rather common to account for power flows through a DC-approximation, there is increasing interest also in employing the full AC-OPF or improved approximations thereof. The state of the art in research in this area will be detailed in Section 4.3.1.

For comparative studies of zonal and nodal pricing-based electricity systems, the representation of networks is essential. Models of these two pricing systems need to rely on different spatial representations of the same network. Research in this area will be laid out in Section 4.3.2.

In the context of the restructuring of the electricity system also the role of the different players and stakeholders in the market will change. In order to increase the resilience of the grid and incorporate a high share of RES into the grid, more flexibility is needed. Thus, the flexibility of consumers and their reaction to price signals can play an increasingly important role in future market designs. Therefore, the modeling of demand elasticity, the sensitivity of consumers to price signals, is a topic that is receiving increasing interest and should be considered carefully when designing models to assess future market designs. Section 4.3.3 gives an overview of modeling methodologies for demand elasticity.

When it comes to medium-term electricity system models that investigate the dispatch and price evolution throughout a year, it is vital to consider seasonal patterns of hydro storages to model their role in the system accurately. Thus, a review of the literature on hydro storage modeling is reviewed and presented in Section 4.3.4.

4.3.1 Power Flow Models: DC-OPF vs. AC-OPF in the Context of Nodal Pricing

Optimal power flow is a central tool in power system operation and planning, as the optimization problem takes the physical limitations of the power grid into account and renders optimal flows that minimize the overall costs of the system. The question of whether one should employ the full AC formulation, or the approximate DC formulation is sufficient in some contexts, is the subject of continuous research efforts.

Overbye et al. (2004) perform a comparative study between the AC and the DC formulation of the OPF in the context of LMP. They do not employ the conventional formulation of OPF but an extended one that allows considering contingency constraints, commonly known as security-constrained OPF (SCOPF). Without going into detail, this extension includes additional constraints to the OPF that account for a more robust system, which is more resilient against unforeseen line outages, sudden demand increases, and alike. Two case studies are conducted.

The first case considers a 37 node system with 58 branches. Beginning with a base case scenario with an initial overall system demand of 750 MW (the load at which line congestions start to appear), 126 demand cases are considered, where the load is increased up to 1000 MW in increments of 2 MW. Each demand case was run for a set of contingencies, which consisted of 58 single line outages. For each of the 126 cases, AC-OPF and DC-OPF simulations are performed and the following observations are recorded. The congested lines and the number of demand cases for which they represent a constraint. Furthermore, the average LMPs for each node over all the 126 demand cases are reported. The found results are the following. The AC-OPF identified 6 congested lines that summed up to an overall number of constraints of 330 (i.e. congested lines in the 126 demand cases). The DC-OPF managed to identify 5 of those lines and 77% of the 330 overall congestions. According to Overbye et al. (2004), average node LMP obtained by AC-OPF and DC-OPF respectively showed a good general agreement with some deviations. They also present tabular contour plots to report the LMP at each node for all the 126 demand cases. One can optically confirm an overall agreement in patterns with some variations, a detailed quantitative analysis is not possible based on the presentation of results.

The larger case study considers a system of 12,925 nodes (of which 1,790 generators) and 17,647 branches. Again, the system load was increased from the initial 171.48 GW, yet it is not specified by what increment and up to what load. Further, the case studies were performed under 1,360 different contingency scenarios of outages or load moves. Initially, the average line flows were compared for the DC and the AC solution and found to differ by only 4.12 MW/MVA (as a difference in LMP only arises from reaching the flow limits in lines, this is a reasonable predictor for the to be expected difference in LMP). [1] Large errors in the flows originated from reactive power flows. They again recorded in what cases the DC-OPF was able to identify the binding constraints. Almost half of the constraints were missed by the DC-OPF . They performed a further analysis as to how much the line loading was in the particular missed cases and they report that most of the unidentified constraints were only missed by a few percent (as only actually hitting a constraint matters). In this larger case study Overbye et al. (2004) report the average overall LMP, which are 38.56 \$/MWh and 36.13 \$/MWh for AC-OPF and DC-OPF respectively. The way that more detailed results are presented allows, for now, accurate evaluation of the numerical values. Computation times, in this case, were 95 seconds for the DC-OPF and 95 min for AC. They conclude that the DC approach generates fairly good results with the clear advantage of having significantly lower running times. They suggest investigating to improve the DC-OPF in future work. Specifically, they point to a technique introduced by Grijalva et al. (2003) that allows accounting for reactive power flows in the DC approximation of OPF.

Li and Bo (2007) develop an improved DC-OPF algorithm that is able to account for losses, which presents an improvement of the commonly used lossless DC approximation of the OPF problem. In their previous work, they introduce the concept of Loss Factor LF of a node i as the change in overall power loss in the system with respect to a 1 MW increase in injection at that node i; and Delivery Factor DF, as $DF = 1 - LF$ (Li et al., 2006). LF and DF can only be calculated once the DC-OPF ran once, therefore their proposed model in an iterative one. Relying on LF the loss is overestimated, prompting an improvement to their model by introducing fictitious node demand (FND) (Li and

[1] LMP differences within a system will only arise when the flow limits are exceeded. What Overbye et al. (2004) explain is that in any case, the results obtained from the AC approach will be higher as they consider the overall total power flow of active P (in MW) and reactive power Q (in MVA) as opposed to the DC one, which only considers active power flows and is hence always lower. Flow limits in AC considerations are given in terms of apparent power S and $S^2 = P^2 + Q^2$.

Bo, 2007). Thereby, they allocate the overall loss to the respective lines or rather the adjacent nodes of each line. The LMPs for their DC-OPF are the sum of the following three factors. The LMP^{energy} for energy is identified to be the Lagrangian multiplier for the flow constraint of their OPF, LMP^{cong} considering the congestion costs are calculated based on GSKs and Lagrangian multipliers for the transmission constraints, and the LMP^{loss} is calculated based on the Lagrangian multiplier of the flow constraint and the DF.

This iterative FND DC-OPF is compared to AC-OPF and the lossless formulation of the DC-OPF using two cases, a 5 node system (PJM) and the IEEE 30 node system. The design of the experiments features an increase of the load level from the initial base case (900 MWh) from 1 to 1.3 per unit of the base case in 0.0025 p.u. increments. The power factor at all loads is assumed to be 0.95 and thus reactive power is thought not to be a limiting factor in their experiments. As results, the maximum difference in LMP and the average difference in LMP of the lossless DC-OPF and the iterative FND DC-OPF each with respect to the AC-OPF is plotted. The lossless DC-OPF matches the AC-OPF in 82% of the load levels, while the iterative FND DC-OPF outperforms the lossless DC-OPF and only shows mismatches at 2 load levels (4%). It needs to be noted that these mismatches are however more significant in amplitude than those of the lossless DC-OPF . Results from the 30-node case are not reported but claimed to be similar [2].
Li and Bo (2007) discuss the origin of the significant differences in LMP obtained by different models. Evidently, differences originate from the approximations made in the DC models. Especially, the dispatching of generation and thus the set of marginal units is identified to have the largest impact on the difference, as marginal units determine the prices. The authors come to the conclusion that their proposed iterative FND DC-OPF produces results close to that of the AC-OPF. They suggest testing their algorithm on other test cases. Running times were not reported.

Baghayipour and Foroud (2012) introduce a method to allocate transmission losses in lines to adjacent nodes, thereby developing an improved DC-OPF model. They compare their approach to the conventional lossless DC-OPF and accurate AC-OPF in three case studies: IEEE 30 and 118 node systems and the Iranian transmission network (648 nodes). In particular, they compare the obtained generation levels, voltage angles and middle line

[2]Results from the IEEE 30-node case are subject of a consecutive paper, see Bo and Li (2008).

flows, and computation time. Their improved DC representation obtains rather accurate results with respect to those of the AC model and has significantly lower running times. The cost functions employed are quadratic polynomials. The two IEEE node test cases are freely available, and they account for their underlying assumptions regarding generation cost coefficients.

Abdel-Karim and Abdel-Ghaffar (2010) investigate the impact of increased wind power injection on the Northeast Power Coordination Council (NPCC) US power system in terms of system operation and costs. They utilize a simplified 36-node representative system as a test case. Different scenarios and levels of wind generation are considered and the impact is measured in terms of: generation outputs and costs, generation dispatch, and in terms of the sensitivity of LMPs to the different injection scenarios. LMPs were calculated through different approaches, i.e. AC-OPF and DC-OPF that considers line losses through loss factors and delivery factors, similar to the approach suggested by Li et al. (2006). The results are compared in terms of differences in LMP, obtained by the two approaches. One of the key findings in terms of the impact of net power injections on the LMP at a particular node is that at nodes with minimum LMP, the values show greater sensitivity to variations in injection. While at nodes with high LMP and expensive generation, the sensitivity of LMP to a change in power injection is low. The nodes with LMPs that showed greater sensitivity to power injection, were also the ones with the largest convergence discrepancies between AC-OPF and DC-OPF. The reasoning behind this is the fact that at nodes with low prices and high injections more constraints are limiting and these are the circumstances under which DC-OPF and AC-OPF tend to diverge the most.

Sharma et al. (2017) compare a DC-OPF model with distributed losses, the conventional lossless DC-OPF and the accurate AC-OPF. A case study is performed on the IEEE 30-node system and different load level scenarios are considered. The results are presented in terms of maximum and average difference in LMP obtained by the three models for the different load scenarios. Lossless DC-OPF shows a decreasing tendency in average difference from AC-OPF as load levels increase. The DC-OPF taking into account distributed losses is outperforming the lossless model consistently throughout the scenarios, reaching average LMP differences in comparison with AC-OPF as low as 2%. Sharma et al. (2017) also report LMPs for the load base case obtained by the three models

per individual node. It is noticeable that AC LMPs vary on each node, while neither the lossless nor the distributed loss DC-OPF deliver significantly varying prices for the base case (with only minor exceptions on 4 nodes). Reasons for the difference in LMP lie in the approximations of the DC-OPF. In the case of no congestions in the system, the only difference in LMP originates from losses, which are not accounted for the DC model. However, the reported results of the loss distribution model are curious in the sense that also its performance is rather poor in the absence of congestions.

Liu et al. (2009) point out the central role that LMPs play in many wholesale power markets and criticize the lack of transparency regarding the derivation of prices from OPFs. They provide a detailed derivation of LMPs from AC-OPF and DC-OPF and thereby tackle this non-transparency regarding market operations. Yang et al. (2018) propose a linear OPF that includes reactive power and voltage magnitudes to improve the commonly applied DC-OPF and obtain results closer to the full AC-OPF. The motivation lies in the improved accuracy, while They iterate that DC-OPF is the method commonly used by system operators even though it can increase operational costs, jeopardize security and threaten market inefficiency, this is because of the robustness and guarantee of convergence as well as the transparency of the solution of linear OPF. Gross and Bompard (2004) investigate the application of the optimal power flow problem (AC-OPF) to obtain nodal prices in competitive markets. They find that there are several issues with using AC-OPF to clear the market. Firstly, this is because of the flatness of the optimal solution and the resulting continuum of "optimal" solutions. Secondly, they identify issues with the level of capability that lie with the central decision-making authority that can execute their powers arbitrarily and discriminate against market participants without greatly affecting market efficiency. According to Gross and Bompard (2004), there is considerable arbitrariness involved in the entire chain of utilizing OPF, i.e. from model formulation, level of detail in network representation, and solution methodology.

4.3.2 Network Representation: Role in Nodal vs. Zonal Based Electricity Market Models

In the process of determining nodal prices, the physical capacity limits of the network are being taken into account, which can thus reduce the need for redispatching and send correct price signals to the market Hogan (1999). Therefore, there is a need for sound

modeling of the electricity system that takes the physical network into account in great detail. There are some challenges to modeling electricity systems based on nodal pricing coming from zonal pricing-based approaches.

While there are numerous modeling design options, there is a common difference between the presented nodal models, when they are contrasted to zonal models, which is the detail of network representation employed. Nodal pricing can only be applied or investigated, for that matter, based on an electricity grid that features a high enough granularity in terms of nodes and lines accounted for. In this context, it is rather important to have network representations to compare the two market designs, which are mostly differentiated by their level of detail in terms of grid representation incorporated. Several studies have explored different methodologies to aggregate networks. Klein et al. (2016) develops a methodology to aggregate large-scale transmission networks based on an optimization algorithm that minimizes flow errors. They apply their clustering methodology to the IEEE 118 node case and aggregate it to a 12-node network. The aim of their study is the reduction of complexity for applications such as network extension studies. They achieve improved results in terms of flow errors in comparison to Shi and Tylavsky (2015), who apply a method based on equivalent transmission lines. Felling and Weber (2018) applies a hierarchical cluster algorithm as an extension to Ward's method Gupta et al. (2018) to create clusters out of nodes with similar nodal prices. By applying their methodology to the European grid, they create zones, which differ significantly from the currently existing bidding zone configuration. They report the benefits of their proposed configurations to be a similar size to the different price zones limiting market power and reduced intra-zonal price fluctuations. Gupta et al. (2018) reports on different aggregation methodologies as well as challenges accompanying these studies. Their findings indicate that the choice of aggregation method should be problem dependent and that the operation point of a system plays a major role when it comes to the accuracy of the aggregated system. Zonal representations of a network can always only be an approximation, as power flows within lines or branches that lie within a zone are disregarded, impacting the flows in interconnecting branches, which will consequently also lose accuracy. What gives rise to nodal prices are congestions in branches, thus an approximation of these flows will affect price outcomes, nodal as well as zonal prices.

4.3.3 Demand Elasticity Modeling

Consumers' sensitivity to electricity prices is a subject that is increasingly receiving attention in electricity system planning. While country studies exist, which are investigating the impact of demand elasticity on electricity market modeling (Thimmapuram and Kim, 2013; Kladnik et al., 2012), even under altered bidding zone configurations (Dietrich et al., 2005; Bjørndal et al., 2013), there is a lack of a holistic view at a pan-European level. In addition, pursuant to the recently entered into force EU regulation on the internal electricity market, transmission system operators and regulatory authorities are encouraged to review the current bidding zone configurations, which emphasizes the need for such research (ENTSO-E, 2018b). Typically, models aiming at considering demand elasticity as a variable of the problem often do so through the introduction of linear demand function into the objective function, which seeks to maximize social welfare (Dietrich et al., 2005; Leuthold et al., 2012; Bjørndal et al., 2014, 2018). Modeling demand as a variable is difficult also considering the fact that historic demand data or demand forecasts are often available in terms of time series of absolute demand values, which only allow for considering demand as inelastic; for this reason, a methodology to estimate demand functions is needed. Various studies determine demand function variables through a given demand elasticity and for (a single) fixed reference price and demand throughout the time horizon. Kladnik et al. (2012) propose a three-step approach to estimate elastic demand bids from the results of market equilibrium calculations.

Eskeland and Mideksa (2010) study the relationship between residential electricity demand, temperature, and climate change. They base their estimate on data from 1995 to 2005 from 32 European countries (Austria, Belgium, Bulgaria, Croatia, Cyprus, Czech Republic, Denmark, Estonia, Finland, France, Germany, Greece, Hungary, Iceland, Ireland, Italy, Latvia, Lithuania, Luxembourg, Malta, Netherlands, Norway, Poland, Portugal, Romania, Slovakia, Slovenia, Spain, Sweden, Turkey, United Kingdom). The resulting overall demand elasticity for households is estimated to be -0.2.
Azevedo et al. (2011) investigate electricity consumption in the EU and the US and the impact of rising prices on CO_2 emissions. Their study is based on annual data on electricity prices and consumption, weather, and income per capita for the years 1990-2004, it covers 15 European countries (we will never know which ones, they mention

explicitly 13). By employing a static regression model and estimating its parameters through OLS (ordinary least square) they obtain an electricity price elasticity of -0.2 to -0.21 for European households.

Blázquez et al. (2013) analyze the residential electricity consumption in Spain. Based on data from 47 Spanish provinces from 2000 to 2008 on aggregated electricity consumption, average electricity price, demographic and weather data. A dynamic partial adjustment approach is used to model the data and GMM is used to extract amongst others the demand elasticity. The estimated short-run electricity price elasticity of Spanish households is -0.07 and the long-run elasticity is -0.19.

Madlener et al. (2011) look at the energy consumption of households in eighteen OECD countries and the industrial sector in Germany, of which the latter will be reported on in more detail in the following section based on a dedicated publication regarding this part of the study by Bernstein and Madlener (2015). The study on the demand responsiveness of households is based on time series data from 1978 to 2008 on residential electricity consumption and price and net disposable income. The authors explore several econometric methodologies based on cointegration analysis to evaluate time series and panel data, i.e. maximum likelihood system approach, fully modified OLS (FMOLS), dynamic OLS group-mean panel estimation framework (DOLS) and autoregressive distributed lag bound testing procedure (ARDL). Many of the obtained results for demand elasticity values of residential consumers in the investigated countries were not statistically significant, those that were ranged from -0.11 to -0.21 short-run and from -0.14 to -0.8 long-run.

Bernstein and Madlener (2015) report on the short- and long-run elasticity of several industrial subsectors in Germany, based on the more extensive study conducted by Madlener et al. (2011). The study is based on data on nominal electricity prices, electricity consumption, real value-added, and value-added price index. They employ a cointegrated vector auto-regression (VAR) model and estimate its parameters using maximum likelihood. For short-run price elasticities, they only obtained significant for the non-metallic minerals sector (-0.57) and for the transport equipment sector (-0.31). Significant values for long-run electricity price elasticities were estimated for the following three sectors: non-metallic minerals -0.3; transport equipment -0.3 and pulp and paper -0.52.

Iimi (2010) studies the elasticity of industrial energy demand in 7 Eastern-European countries with respect to electricity prices. The underlying data is drawn from a survey on a sample of about 1,000 enterprises and their output and cost structures throughout the years 1995 to 2005. Short-run elasticities of energy demand were estimated indirectly by considering translog cost functions of firms and the sensitivity to changes in electricity prices, which were determined through seemingly unrelated regression (SUR) and stochastic-frontier analysis(SFA) estimators. Only the former method yielded statistically significant results for all countries, which are: Albania -0.774, Bosnia & Herzegovina -0.26, Bulgaria -0.33, Croatia -0.37, Macedonia -0.76, Romania -0.21 and Serbia -0.372. With the SFA method, Iimi (2010) obtained higher elasticity values for two countries, i.e. -1.01 for Macedonia and -0.896 for Serbia.

4.3.4 Hydro Storage Modeling in Large-Scale Nodal Pricing Models

The significance of sound hydro storage modeling in medium-term electricity market models, as well as different approaches to do so, has been studied in various research. Stoll et al. (2017) give an overview of the different hydropower modeling challenges. One of the major difficulties is linked to the time horizon considered. While for short-term models with potentially a high time resolution operational constraints are the issue at hand whereas the accurate modeling of hydro storage reservoirs is not very relevant. Medium-term hydro optimization is concerned with the seasonality of reservoirs and inflows as well as the storage aspects throughout a year. Long-term models are more oriented towards considering climatic fluctuations and the impacts on the hydrological system. They discuss the application of soft constraints to model hydro storages and the difficulties of choosing penalty costs correctly and balancing well between different objectives. Lastly, run-time requirements are identified as a major challenge and discussed in the context of finding a trade-off between accuracy and computational tractability. Stoll et al. (2017) discuss the use of cost functions to forecast the future value of water stored in hydro reservoirs. This is especially relevant when optimizing a model in sequence over a longer time horizon. This needs to be done through additional constraints to account for the time-dependent factors. The relevance of hydro storages for zonal modeling and

the impact it has on different pricing regimes are explored by Weibelzahl and Märtz (2018). They investigate the challenges hydro storage dispatch pose also in the context of congestion management and different zonal configurations. In EUDispatch a zonal model of the European electricity system, the seasonality of hydro is captured through a preliminary run where a temporal aggregation of the model allows obtaining weekly SOC profiles. These serve as input to simulations with hourly resolutions that are performed in sequences of a week. The weekly SOC profiles provide fixed target values for the beginning and end of each simulation step (Brancucci Martínez-Anido et al., 2013a,b). Sahraoui et al. (2019) study the hydro unit commitment problem formulated as MILP cost maximization and in particular focus on mitigating data errors and infeasibility issues. They suggest providing fixed operational points to hydro facilities, as well as mid-horizon and final target volumes. Through the introduction of marginal corrective slacks into their model, they eliminate infeasibility issues through a two-stage method. They test their methodology on real-world test cases that are comparatively small. Fosso et al. (1999) discuss the standardized bidding procedures for the dispatch of hydro storages in Norway. They describe the use of water values to be utilized as bidding prices in long and medium-term models. While under some circumstances constant bid prices for hydropower can be used (Fosso and Belsnes, 2004), it is rather common to work with dynamic bid prices. These bids are deduced as shadow prices of the hydro storage reservoir continuity constraint (Fernández-Blanco et al., 2017; Braun, 2016; Baslis et al., 2009).

4.4 Open-Source Data, Tools and Models

In power system modeling there are initiatives as Open Energy Modeling (openmod), an initiative of researchers from different universities and research institutes that promote and practice openness in energy models and data (Open Energy Modeling Initiative, 2022). Through an open-source policy in energy system modeling, transparency and reproducibility will be improved, which is vital also when it comes to public acceptance of studies on future scenarios for the electricity system (Wiese et al., 2014). The accuracy of models can be improved through the facilitation of cooperation and joint projects, which help to avoid double work and redundancies. Especially, the necessity of reliable input data for sound energy modeling is an issue raised by the open-source community and

addressed in the open power system data project that developed as part of the openmod initiative (Wiese et al., 2019).

Also, Medjroubi et al. (2017) stress the issue of grid data availability in the context of energy system modeling. They discuss the different types of grid models as *copper plate approach*, where there is only a single node present; *transshipment models*, which feature different nodes or regions. The latter regularly employ a transport model approach, where physical flow principles are neglected. This is addressed in more detail in DC-OPF models and even more sophisticated AC-OPF models, which also account for reactive power flows. Medjroubi et al. (2017) discuss further the data requirements for the different types of models. In the simplest copper plate models, 'merely' data on generation and demand are required. In transshipment models, additional information about NTC is the only physical properties of the grid considered, this, however, already requires additional regional information of generation and demand. DC-OPF additionally calls for additional knowledge on power lines as their thermal capacities, and the susceptance. Additionally, AC-OPF models require the definition of buses as PQ- or PV-bus as well as specifications of generation and demand with regard to reactive power and voltage. Further, line property information also needs to be extended to include conductance and reactive power limits. There exist several issues regarding data accessibility not only with regard to grid data but also renewable energy source locations, load data, power plant locations, and operational properties. ENTSO-E has released a partial dataset on the European grid topology, however, it is not geo-referenced, this can also not be compensated by the fact that some TSOs have released more comprehensive data. Therefore, research on energy system modeling, especially considering the transmission grid, needs to draw from open-source data. There are several research projects building upon publicly available data and Medjroubi et al. (2017) focus in particular on open street map (OSM) and power data in OSM. This data includes geolocations of different components as well as transmission line types, voltage levels, and frequency. It represents the basis for models of the transmission system such as SciGRID, osmTGmod, and GridKit. Comparative studies of these and other models focus largely on the German grid (Heitkoetter et al., 2019; Medjroubi et al., 2017; Medjroubi and Vogt, 2017). Also Syranidou et al. (2022) compare power system and grid models in Germany against each other, these are ELMOD, eTraGo, Europower, ISAaR, MarS/ZKNOT, MILES, PERSEUS, PowerFlex. While several of the

above-mentioned models are open source for single countries or regions, there is a scarce amount of models that cover a larger geographical scope and are freely accessible. A model of the European system that was introduced by Zhou and Bialek (2005) and updated by Hutcheon and Bialek (2013), covers transmission lines, but only includes cross-border capacities. On the other hand, SciGRID and GridKit, which is developed as an extension of SciGRID, cover the entire transmission system. They both rely on OSM data but use different data types to build up the network of lines. Hörsch et al. (2018) developed PyPSA-Eur, which is an open-source energy system model of the European transmission grid. It uses GridKit to extract the grid topology from ENTSO-E's interactive map (ENTSO-E, 2022). Given the fact that this map is a somewhat artistic depiction of the reality, there are admittedly some errors in the dataset, however, in comparison to other approaches, there is merit in reproducibility and accessibility of data. PyPSA-Eur builds up on the topology data and assigns standard line types and properties to transmission lines. Thereby, the transmission system at and above 220 kV voltage level is covered as well as DC lines. The resulting network is depicted in Figure 4.3. Further, load and generation units are collected from open sources and added to the network. Load is allocated to nodes based on a heuristic that is oriented on the population density. Time series for the availability of renewable energy sources are also added, as well as other meteorological data as hydro inflows to storage reservoirs. By design, PyPSA-Eur can analyze future scenarios for capacity extension of grid and generation. The model relies on PyPSA a Python-based power system model, which can build and solve different types of optimization problems such as OPF, PF, and capacity extension (Brown et al., 2018).

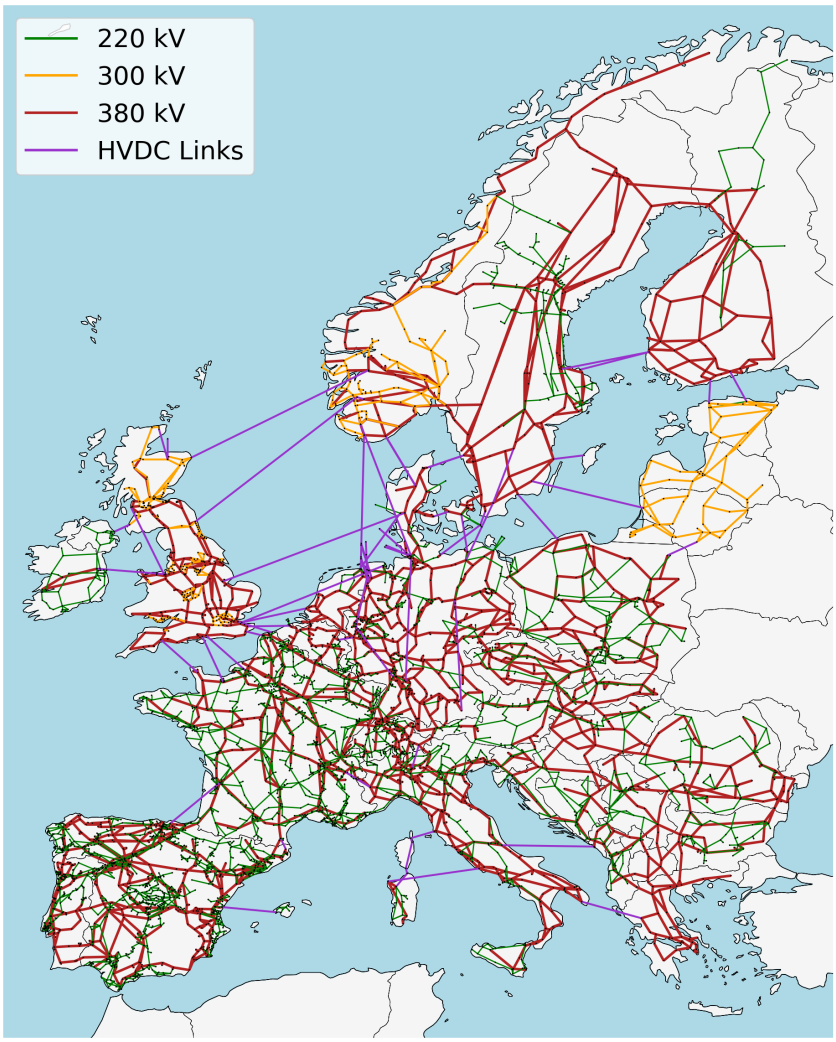

Figure 4.3: European transmission network as extracted from ENTSO-E's grid map by PyPSA-Eur (Hörsch et al., 2018).

Chapter 5

Towards a European Nodal Pricing Model: Results

This chapter presents the main outcomes of the work performed in the context of this PhD studies. Firstly, the choice of power flow model and the role for nodal prices as well as the impact of different network representations are examined in Section 5.1. This part is thus dealing with some more traditional modeling aspects and represents a first approach to performing analyses on the assessment of modeling choices.

Secondly, a study on demand elasticity in a European context is presented in Section 5.2. The commonly used commercial modeling tool Plexos is used to implement demand elasticity. Incorporating consumers' elasticity to prices on a European scale represents a novelty.

Thirdly, the issue of modeling hydro storage state of charge evolutions under myopic foresight is addressed in Section 5.3. This is necessary due to a lack of data and the computational challenge of solving large-scale optimization problems of systems with very high spatial and hourly time resolution. Through the development of a heuristic algorithm, hydro state of charge profiles were obtained that allow for comparative nodal vs. zonal case studies. Lastly, to demonstrate the applicability of this heuristic, a case study on the costs of redispatching is performed. The methodology relies on a full nodal model and a zonal model coupled with a redispatching model.

The following sections are all structured in a similar fashion. An introduction along with the description of the problem initiates the sections. This is followed by outlining the methodology and the formulation of the underlying model used for the respective studies.

The data and case study design is introduced in the subsequent section. Thereafter, the results of the performed numerical experiments are presented and conclusions for each section are presented at the end.

5.1 Study on Power Flow Models and Network Representation

5.1.1 Introduction and Problem Description

The electricity system is evolving with the increasing incorporation of renewable energies, therefore also the transmission system is facing expanding challenges. As a consequence, electricity markets are also evolving. A topic of increasing interest is nodal pricing as an alternative to zonal pricing-based electricity markets in Europe. As nodal prices arise from physical constraints of the electricity grid, accurate modeling of flows in networks through optimal power flow models is a necessity. This section is focusing on two aspects of this modeling endeavor, being the type of optimization problem: DC-OPF, AC-OPF, or unit commitment DC-OPF on the one hand; and the network representation on the other hand. In Sections 4.3.1 & 4.3.2 a literature review on these topics has been presented.

Firstly, the two most widely used formulations for OPFs AC-OPF and DC-OPF and their performance at determining nodal prices are compared, through the consideration of border cases, where larger differences tend to arise. Further, computational costs are assessed in a second case study. Lastly, the impact of different network representations is investigated.

5.1.2 Model Description

The formulation of the optimal power flow problem has already been formally introduced in Section 3.1.1. The full AC formulation was presented in (3.3)-(3.9). The costs to produce power are minimized (3.3), subject to active (3.4) and reactive power flow constraints (3.5), flow constraints for apparent power (3.6), operational limits for active (3.7), reactive power (3.8) and voltage (3.9) (Andersson, 2012; Taylor, 2015).

The linear approximation DC-OPF has been introduced in (3.10)-(3.13). Additionally, unit commitment is considered in this study and therefore the unit commitment

formulation of the DC-OPF is presented here:

$$\underset{p,\theta}{\text{minimize}} \sum_{i \in \mathcal{G}} f_i(P_i) \tag{5.1}$$

subject to

$$P_i = \sum_{k \in N(i)} P_{ik} = \sum_{k \in N(i)} B_{ik}(\theta_i - \theta_k), \quad i \in N \tag{5.2}$$

$$-F_{ik} \leq P_{ik} \leq F_{ik}, \qquad i \in N, \quad k \in N(i) \tag{5.3}$$

$$\alpha_i \underline{P}_i \leq P_i \leq \alpha_i \bar{P}_i, \qquad i \in \mathcal{G} \cup \mathcal{D}. \tag{5.4}$$

The objective function, power flow and flow constraints are the same as for the previously introduced DC-OPF. What renders this formulation different is the introduction of binary decision variables α_i. They indicate whether a generator is in operation or not and render the unit commitment formulation of the OPF a MILP (see also Section 3.1.2).

According to Liu et al. (2009), nodal price or locational marginal price (LMP) is the price to provide an additional increment of power at a node while respecting all network constraints. They can be derived as Lagrange multipliers or dual variables for the active power balance constraints (3.4), (3.11) and (5.2) respectively.

5.1.3 Data & Case Study

The computational experiments were conducted using MATPOWER , a built-in tool of MATLAB designed to perform power flow calculations (Zimmerman et al., 2011). A first case study was conducted on the ACTIVS 500-node test case, for which LMPs were calculated using DC-OPF and AC-OPF. In an effort to identify borderline cases, where differences in DC-OPF and AC-OPF are expected to occur, the system was put under stress by altering its constraints. The second part of the study relies on 41 test cases that are freely available. Cases are chosen, which include cost functions as only they are appropriate to perform OPF calculations. For the first part of the study, all cases are solved using DC-OPF, AC-OPF and unit (de)-commitment. Computational times are recorded and the average run times over 10 runs are reported. DC and AC-OPF are solved using MIPS (Matpower Interior Point Solver) (Wang et al., 2007). MATPOWER does not support the solving of mixed-integer problems, therefore the unit commitment problem is solved as "unit de-commitment" problem. Thus, it is not the MILP presented

in 5.1-(5.4) that is solved. Instead, the heuristic approach of MATPOWER follows two steps. Firstly, the DC-OPF is solved as it is presented in (3.10)-(3.13). In this step, *all* generation units are dispatched, at least with their minimum capacity as imposed by (3.13). In a consecutive step, a heuristic algorithm is applied that shuts down generation units until no further improvement can be achieved. However, the solution found through this approach is not guaranteed to be optimal.

The third part of the experiments takes a closer look at one example case, the IEEE 118 node case. A special focus lies on an approximation of this case. Klein et al. (2016) proposes a methodology to aggregate large-scale networks into smaller representative networks. Their methodology is applied to the 118-node test case in order to reduce it to a 12-node case. The original nodes are aggregated into clusters, which consist of 2 to 20 nodes. Clusters are found by solving an optimization problem, which seeks to minimize the error between line flows calculated from the original 118-node case and the aggregated case. The authors find that 12 clusters lead to a minimization in flow errors as opposed to other numbers of clusters. Besides the clustering of nodes, they also report the parameters of the lines connecting clusters. However, these parameters do not feature limits on line flow capacities, as imposed by (3.6), (3.12) and (5.3) respectively. Thus, capacity limits are introduced to the 118-node case, which are oriented according to the outcomes of a power flow calculation for the base case, consequently, capacity limits are introduced that allow an unconstrained flow in the base case. The results of line flows are used, and 1 MW is added to all line capacities in order to ensure uncongested flows. For the aggregated 12-node case, capacity limits are not derived from flow calculations, but capacity limits stem from the aggregations of the 118-node case's lines and the previously imposed new capacity limits. For the comparative study of several cases, the load factor is increased within the entire system in steps of 0.02 from 1 to 1.018, which is the highest value for which the optimization problem remains feasible. This is an artifact of the way capacity limits are introduced to the system, which makes it not very flexible to accommodate higher load levels. However, this experiment gives us the chance to study the system in 10 different states in a comparative fashion.

It needs to be noted that the IEEE 118 node test case and the aggregated 12 node case of the former do not directly emulate the difference in a nodal vs. a zonal network representation. However, the rationale is that also the transmission network's nodes

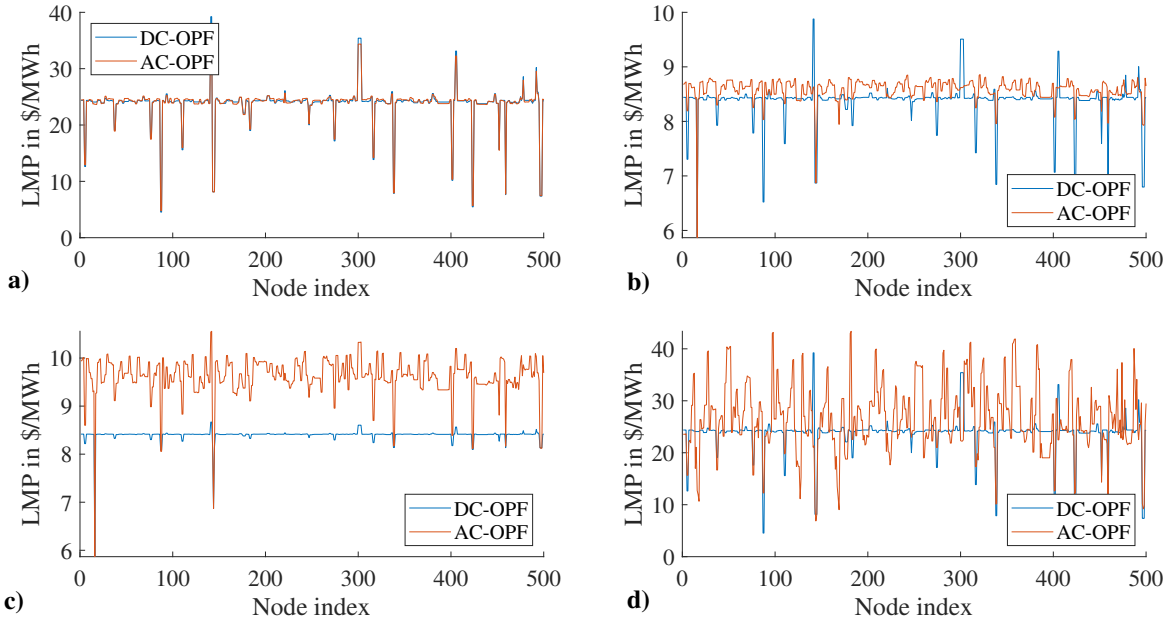

Figure 5.1: Locational Marginal Prices (in $/MWh) obtained through performing a DC-OPF and an AC-OPF for four case studies on the ACTIVS 500-node test case system. a) Base case. b) Increased upper limit for active power generation. c) Increased ranges for active and reactive power generation (increased upper and decreased lower limits). d) Increased reactive demand (1.83 p.u. wrt the base case).

are clustered into zones, while the zone borders follow predominantly country borders. Therefore, the presented test case represents a somewhat ideal case of a clustering that follows an optimization strategy rather than geographical clustering.

5.1.4 Numerical Experiments

A. LMPs from AC-OPF and DC-OPF: 500 node test case The results are presented in terms of absolute LMP at each node. A base case scenario is compared to cases of increased generation limits and to a case of increased reactive power demand. The base case is shown in Figure 5.1a. One sees that AC and DC LMPs are well aligned. Both models identify 1 congested line. In the next case, the maximum active power generation of all units was increased with respect to the base case. As can be seen in Figure 5.1b, the prices dropped significantly due to the employment of more capacities of cheaper generation units. Further, the patterns of LMP differ considerably. DC-OPF identifies only 2 congested lines, which may explain the similarity in the pattern to the base case, whereas AC-OPF identifies 5 congested lines. In a third case, the minimum and maximum generation constraints are loosened for both reactive and active power generation. The

results are shown in Figure 5.1c. The overall difference in LMP patterns may be attributed to the fact that the AC-OPF identified 5 congested lines, while DC-OPF only found 4, yielding less significant spikes as observed in the previous case. The offset in prices can be explained by the difference in dispatched generation units. In order to compensate for line losses in the AC model, more generation of power is needed, which is realized through dispatching one more unit with higher marginal prices than in the DC model. For a fourth case study, the demand for reactive power was increased. The obtained LMP patterns differ quite significantly, as can be seen in Figure 5.1d. AC-OPF finds 5 lines to be congested, while DC-OPF only has 1 congested line (as in the base case), which is evidently due to the reactive flows, which are neglected in the DC approximation.

The results of the performed case study suggest that DC-OPF renders rather accurate nodal prices with little discrepancies when both models identify the same congestions and the system is not under much stress. However, this is no longer true when it comes to the border cases, i.e. just before congestion occurs; when there are large flows of reactive power; when the two models suggest a different dispatch structure of generation units; or when congested lines are not found by DC-OPF. It is, therefore, essential to bear this discrepancy in mind as one investigates such cases. However, it needs to be noted that in the application as a market-clearing tool, DC-OPF has some advantages over AC-OPF when it comes to transparency (Liu et al., 2009; Yang et al., 2018; Gross and Bompard, 2004).

B. Computational Times: 41 Cases

Figure 5.2 reports the results of the runtime experiments conducted on 41 test cases available to be used in Matpower. Shown are the computational time in seconds over the number of nodes the case's network has on a loglog scale for DC-OPF, AC-OPF, and DC unit de-commitment. For cases with less than 1,000 nodes, one sees that both DC and AC-OPF computational times lie around 1 s. As the number of nodes in the network exceeds 1,000 the trends start to deviate and AC-OPF computational times start increasing, while also DC-OPF runtimes go up, but noticeably less. The unit de-commitment calculations take longer already for several 10s of nodes in a network and start increasing significantly from around 1,000 node cases, though it has to be noticed that it is difficult to identify a clear trend as computational times vary largely for networks with 1,000s of nodes. However, consistently runtimes for cases with around 10,000 nodes are very large and

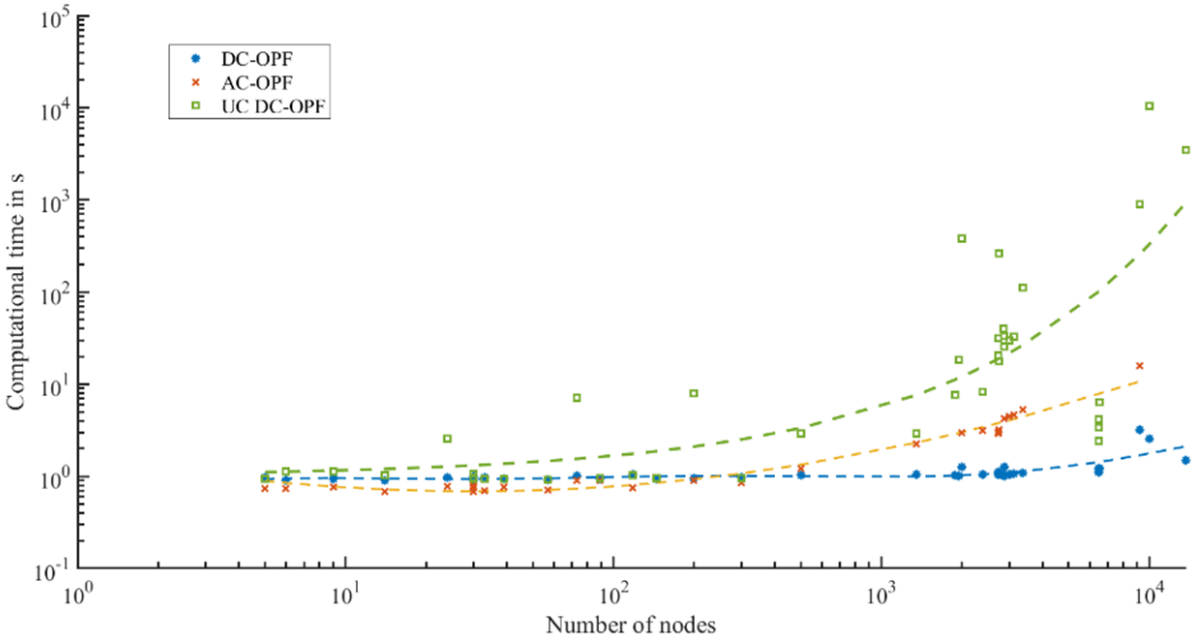

Figure 5.2: Run times in seconds (s) over the number of nodes in a network for 41 test cases. Computational times are shown for DC-OPF (stars), AC-OPF (crosses) and DC-OPF with unit de-commitment (UC DC-OPF) (open squares).

took up to 2 h and 52 min to be solved.

C. Comparison of 118 Node Case to Aggregated 12 Node Case

Figure 5.3 shows the LMPs of the IEEE118 case ordered by clusters for comparability to the approximated 12 node case. The prices fluctuate roughly between 39.5 and 40 $/MWh. Differences in LMPs originate from congested lines, 9 congested lines are found in this case. In order to make these prices more comparable to the 12-node case, the load-weighted average LMPs are shown, which is common practice in literature Zimmerman et al. (2011); Wang et al. (2007). Load-weighted average prices are reported along with the maximum and minimum prices for each cluster of the 118-node case as well as the LMPs of the 12-node case in Figure 5.4a. One sees that the prices fluctuate around the same interval, but they are mostly not well aligned. This can be understood from the fact that different lines are identified to be congested, even though the number of inter-cluster congestions is the same in both cases with 3 congested lines. In the 118-node case, lines connecting clusters 2 and 4, 2 and 8, and 7 and 8 are congested, while in the 12-node case congested lines are between clusters 2 and 5, 4 and 9, and 8 and 9. Additionally, there are congestions within clusters in the 118-node case, which are not considered in

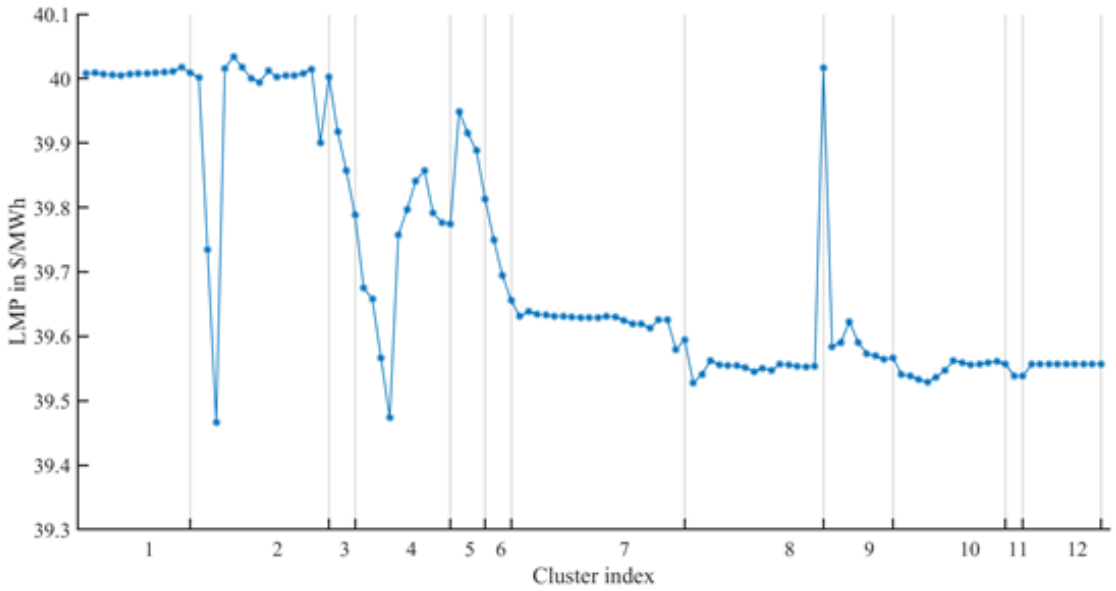

Figure 5.3: Locational Marginal Prices (LMP) in $/MWh for the IEEE 118 node case. The 118 nodes are ordered into 12 clusters for comparability to the aggregated case.

the 12-node case; those congestions occur in cluster 2, where there are 4 congested lines and one each in clusters 8 and 10. This may explain the large span between maximum and minimum LMPs reported for the 118-case in clusters 2 and 8. It also needs to be noted, that sometimes LMPs are over- and sometimes they are underestimated in the 12-node case in comparison to the 118-node average prices. This makes it difficult to make predictions on what error to expect when there is no overall trend to be detected. Figure 5.4b shows the results for several states of the 12 and the 118-node systems. The number of congestions and the maximum relative error in LMPs are compared and displayed for different load factors. It can be observed that in the base case (load factor 1), the number of detected congestions between clusters differs with 0 for the 118-node case and 3 for the 12-node case. This discrepancy remains until for higher system load more inter-cluster congestions are occurring also in the 118-node case. Interestingly, the maximum error between LMPs does not exceed 2% until a load factor of 1.014, when the error increases up until 3.4%, even though this is when both the 12 and the 118-node case have an equal amount of inter-cluster congestions of 4. What does increase significantly though are the intra-cluster congestions, which go up to 15. These type of congestions goes undetected in the aggregate 12-node network and can contribute to the increase in relative error. It needs to be noted that the optimization problems become infeasible for higher load factors, which limits this experiment to a maximum load factor of 1.018.

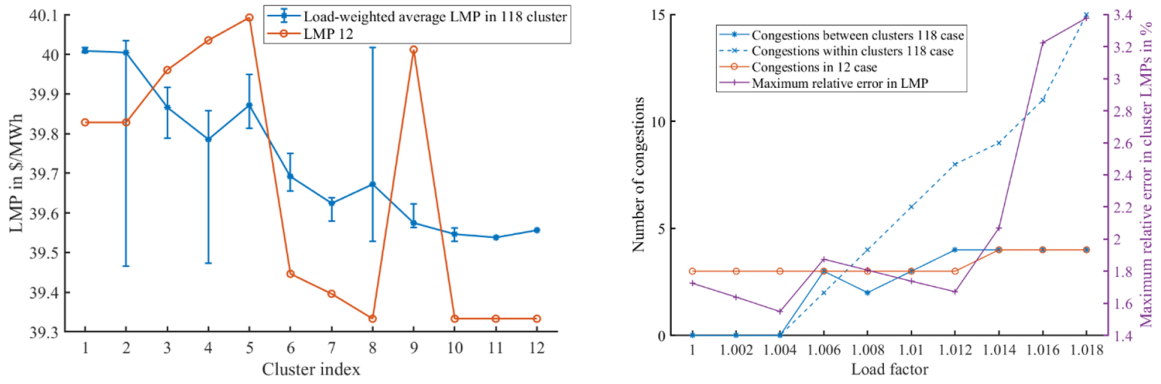

(a) **(b)**

Figure 5.4: (a) Locational marginal prices in blue the load-weighted average prices for every cluster of the 118 case, the bars indicate the span between the highest and the lowest price in every cluster. In red the LMP for each cluster in the 12-node case. (b) Number of congested lines for the 118-node case in blue (congestions between clusters: solid line; congestion within clusters: dashed line) and the 12-node case depending on the load factor applied to the base case ranging from 1 to 1.018 in ten steps of 0.002. Further reported is the maximum relative error in cluster LMPs as the difference between the LMP in a cluster for the 12-node case and the maximum or minimum price in the 118-node case within a cluster with respect to the 12-node case.

In the first part of the presented experiments, it is found that depending on the type of optimization problem solved, computational times can increase largely for a higher number of nodes, as is shown in Figure 5.2. In an electricity market context, these types of problems need to be solved several times, e.g. for the day-ahead market 24 times and when performing long-term studies a lot more, which calls to maintaining computational efforts manageable. One way to tackle this issue is by aiming to improve algorithms to solve these optimization problems. Another is to utilize different network representations, which feature a smaller number of nodes through the aggregation of the larger network. When investigating two network representations of the same systems, there are differences that occur and need to be considered. The phenomena that lead to different LMPs are congested network lines. It is thus important to notice that approximations of the same network can lead to different numbers of congestions and this is also true depending on the load present in the system as reported in Figure 5.4b. As a consequence, prices also differ and are difficult to compare, as can be drawn from Figure 5.4a. There is no single trend of over- or underestimation, which makes it difficult to assess the quality of estimation. It will depend on each individual network as well as the scope of the overall study conducted. In cases when scenarios are assessed, where there are other factors that will impact the overall outcome significantly, the estimations provided by the aggregated case may be

sufficient, while in situations when an accurate assessment of LMPs and congestions is vital, the presented approximations may not be sufficient. It is thus essential to properly chose the network models and network representations suitable for a given purpose. It needs to be borne in mind that research and practice are always facing a trade-off between higher accuracies and higher computational efforts.

5.1.5 Conclusion

The main findings of this section can be summed up as follows:

- DC-OPF and AC-OPF render similar LMPs when the same congestions are identified, and the system is not under much stress.
- LMPs differ more in border cases, i.e. just before congestion occurs; when there are large flows of reactive power; when the two models suggest a different dispatch structure of generation units; or when congested lines are not found by DC-OPF.
- AC-OPF and unit commitment formulations of the power flow problem lead to significantly higher computational times as the number of nodes in a network is increased.
- Given the advantage that DC-OPF has in terms of computational efficiency as well as transparency and the reasonably accurate performance on delivering LMP in normal operation, it is to be preferred over AC-OPF to determine nodal prices and model flows in transmission systems.
- Comparative studies between nodal and zonal pricing need to rely on different representations of the same network in order to be able to assess two pricing schemes.
- Numerical simulations on the IEEE-118 test case show the discrepancy in identified congested lines and LMPs for the full 118-nodes network and the aggregated 12-node network.

Currently, there exists wide consensus on the utilization of DC-OPF to obtain nodal prices and model electricity markets. However, there are increasing research efforts to explore improved versions of the lossless DC formulation that incorporate losses and reactive power flows to some extent.

It needs to be noted that the employed test case of 118 nodes, usually does not provide line capacity limits and the method of artificially creating them allows for questions regarding the generalization of our results. This again calls for more efforts into the investigation of network representation in the context of nodal vs. zonal pricing in order to further gauge the trade-off between accuracy and computational efforts.

5.2 The Impact of Demand Elasticity on Future Zonal Scenarios of the Italian Electricity System in a European Context

5.2.1 Introduction and Problem Description

Consumers' sensitivity to electricity prices is a subject that is increasingly receiving attention in electricity system planning. Similar to Kladnik et al. (2012), this work proposes a two-Step approach to implement demand elasticity, in which's first step renders reference price and demand for every hour of the simulation horizon. Thereby, the need to determine reference points out of estimations or averaging is abolished and reference points for every hour are used to determine hourly demand functions. In the second Step, flexible demand is simulated similarly to existing studies through a welfare maximization objective. Through analyses of the impact of demand elasticity, the current paper supports policy decision-makers and regulators in the context of demand response programs and gives indications for future design adjustments of markets. The impact of demand elasticity is presented through techno-economic modeling of the European electricity system, with a focus on Italy.

5.2.2 Model Description

In this section, the modeling methodology of incorporating demand elasticity, which follows a two-step approach, is explained. The concept of demand elasticity and linear demand functions as well as the employed European economic dispatch model is introduced.

Demand elasticity ϵ denotes consumers' sensitivity to changes in prices. It defines infinitesimal relative changes in demand to infinitesimal relative changes in prices. As discussed later, demand functions can be determined with respect to a reference price and demand. Therefore, it is necessary to determine this reference point. Thus, a two-step modeling approach is applied, where in Step one demand is a fixed input, and the corresponding reference or equilibrium prices are determined. From these and ϵ, demand functions' slopes and intercept can be calculated. These serve as input to Step two, where demand is then elastic and thus a decision variable. Demand elasticity is discussed in more detail in Appendix A.1.3.

In order to find the equilibrium points, a techno-economic power dispatch model is used. The model emulates the DAM in Europe. Scenarios are developed in a commercial power market simulation software PLEXOS (`energyexemplar.com`). The model optimizes a day-ahead generation dispatch, hydro reservoir levels, and power flows, and provides an asset performance valuation in terms of electricity prices. For every time step, power generation is optimized to minimize generation costs, subject to a list of constraints:

$$\underset{g_{ukn},F_{nm},\alpha_{ukn}}{\text{minimize}} \sum_{n\in N}\sum_{k\in K}\sum_{u\in U} c_k g_{ukn} \tag{5.5}$$

subject to

$$\sum_{k\in K}\sum_{u\in U} g_{ukn} + \sum_{m\in N(n)} F_{nm} = d_n + \sum_{m\in N(n)} \frac{1}{2}\delta_m F_{nm}, \quad \forall\ n\in N, m\in N(n) \tag{5.6}$$

$$F_{nm} = -F_{mn}, \quad \forall\ n\in N, m\in N(n) \tag{5.7}$$

$$\underline{r}_n^I \le \sum_{k\in K}\sum_{u\in U} r_{ukn}^I \quad \forall\ n\in N \tag{5.8}$$

$$\underline{r}_n^{II} \le \sum_{k\in K}\sum_{u\in U} r^I I_{ukn} \quad \forall\ n\in N \tag{5.9}$$

$$\alpha_{ukn}\underline{g}_{ukn} \le r_{ukn}^I + r_{ukn}^{II} + g_{ukn} \le \alpha_{ukn}\bar{g}_{ukn} \quad \forall\ n\in N, k\in K, u\in U \tag{5.10}$$

$$r_{ukn}^I \le \gamma_{ukn}\bar{g}_{ukn} \quad \forall\ n\in N, k\in K, u\in U \tag{5.11}$$

$$\underline{F}_{nm} \le F_{nm} \le \bar{F}_{nm} \quad \forall\ n\in N, m\in N(n). \tag{5.12}$$

c_k is the production cost for generator technology k. g_{ukn} is the generated electricity by generation unit u of generator technology k at node n. N is the set of power nodes, i.e. the modeled bidding zones in Europe. Power plants at every node n are aggregated

by technology k of set K, which are further divided into generation units u grouped in sets U. The objective of minimizing the generation costs is subject to the following constraints. The nodal power balances, which are expressed in Equation (5.6). The total power generated at every node g_{ukn} plus the net exchanges F_{mn} from the set of adjacent nodes $N(n)$ in the modeled system, must be equal to the electricity demand d_n plus transmission losses. F_{mn} is the electricity flow to node n from adjacent node m, $F_{mn} > 00$ correspond to imports to node n and $F_{mn} < 0$ correspond to exports from node n. δ is the relative loss factor. Transmission losses are shared equally between two interconnected nodes, which is expressed through the factor $\frac{1}{2}$ in Equation (5.6). Equation (5.7) ensures that imports F_{mn} to node n from node m equal exports F_{nm} from node m to node n. Emergency power reserve constraints are expressed in Equations (5.8) and (5.9). Reserves provided by generators at node n should meet the minimum reserve requirements, that is, $\underline{r}_n^I$ for the primary reserve and $\underline{r}_n^{II}$ for the secondary reserve. r_{ukn}^I and r_{ukn}^{II} are primary and secondary emergency power reserves, respectively, provided by generation unit u of technology k at node n. Only generation units being already in operation can provide reserves. Power generation constraints are expressed in Equation (5.10). Electricity generated (g_{ukn}) and provided reserves (r_{ukn}^I and r_{ukn}^{II}) of unit u of technology k at node n should be between the minimum operation power $\underline{g}_{ukn}$ and the maximum capacity $\bar{g}_{ukn}$. The formulation in Equation (5.10) includes binary decision variables α_{ukn}, which take the value 0 in case of outages and should ensure that generation units only operate within their minimum and maximum stable levels. However, due to the use of Linear Programming formulation, this binary constraint is relaxed to also allow non-binary values for α_{ukn}. Thus, the cleared price will not necessarily be equal to the marginal costs of the last dispatched generator, but rather to an average production cost. The maximum primary reserve provision is limited to a fraction γ_{ukn} of generation unit capacity $\bar{g}_{ukn}$ as expressed in Equation (5.11). Power flows F_{nm} between interconnected nodes n and m are limited to an lower $\underline{F}_{nm}$ upper $\bar{F}_{nm}$ capacity limits in Equation (5.12). The electricity wholesale prices for each node n at every time step are equal to the production cost c_k of the last generation unit dispatched. The electricity price reflects the abovementioned constraints. Under unlimited transmission capacity and no losses, all nodes have the same price for each time step, reflecting the generation cost of serving the last MW of electricity demand. However, due to limited electricity flows between the interconnected

nodes (Equation (5.12)), electricity prices can differ between nodes (the bidding zones). Prices reflect electricity transmission losses and congested lines and are found through the dual variables of the net injection constraint at every node (Equation (5.6)).

In Step two, the model is implemented to find the equilibrium point between the supply and demand curve, the parameters of which were determined in Step one, based on the selected demand elasticity value. The demand variable d_n is approximated through a step function, which, in Step two, replaces the fixed value d_n in Equation (5.5). Thus, the cost minimization objective (Equation (5.5)) becomes a welfare maximization or equivalently a negative welfare minimization problem:

$$\underset{g_{ukn},F_{ukn},\alpha_{ukn},d_{ni}}{\text{minimize}} \sum_{n\in N}\left(\sum_{k\in K}\sum_{u\in U} c_k g_{ukn} - \sum_{i=1}^{10} p_{ni} d_{ni}\right). \tag{5.13}$$

The demand is approximated through a step wise function consisting of 10 steps d_{ni}, where i is the step index. d_{ni} become decision variables, which in addition to Equations (5.10)-(5.7) add the following set of constraints to the problem:

$$0 \leq d_{ni} \leq \frac{d_n(p_n = 0)}{10}, \quad \forall\, n \in N, i = 1, \ldots, 10. \tag{5.14}$$

The length of each interval of the step function represents the upper constraint to each demand step. The prices p_{ni} in Equation (5.13) are determined in accordance with Equation (A.22) in the following way:

$$p_{ni} = b_n \cdot i \cdot \frac{1}{2} \cdot \frac{d_n(p_n = 0)}{10} + a_n, \tag{5.15}$$

where b_n is the demand slope and a_n is the demand intercept. These parameters are determined through the equilibrium price and demand quantity determined in Step one, according to Equations (A.24) and (A.25) respectively. Through implementing demand functions, the demand will react to changes in the system and new equilibrium points will be determined. The scenarios that impose these changes will be elaborated on in the following subsection. Further, details on values for the variables used in the objective function and its constraints will be provided.

5.2.3 Data Preparation

Extensive Europe-wide electricity system modeling data is available in the context of the Ten-Year Network Development Plan (TYNDP) of ENTSO-E (ENTSO-E, 2019). These data are currently available for future years up to 2040 and for different scenarios. In this paper, the year 2040 under the Sustainable Transition scenario is chosen as simulation horizon. Simulations are performed for a time step frequency of 1 hour. 36 European countries are modeled as 55 interconnected power nodes representing electricity market bidding zones. ENTSO-E provides data on the aggregated installed generation capacity per technology, key generation assumptions, demand profiles with an hourly resolution, and reference capacities for cross-zonal interconnectors (ENTSO-E, 2019). These are open-source data available for various future scenarios in Europe (ENTSO-E, 2018a). Annual hourly generation profiles from wind and solar resources are acquired from an open database: `www.renewables.ninja`. Generation from hydro energy is limited by water inflow in power plants. Maximum monthly water inflow is fixed based on historical Eurostat records (Eurostat, 2020). This is a constraint in the model, which adds seasonal behavior to hydropower plant production. Still, hydro plants can contribute to daily power balancing as a small fictitious water reservoir is added to each plant. Generation from renewable energy resources and electricity demand are based on weather conditions of 2007 – a typical year since 1990. Power plant characteristics and fuel prices are listed in Table 5.1. Minimum operation power for thermal and hydro generation technologies are obtained from ENTSO-E (ENTSO-E, 2019). Generation unit capacity is an assumption for dispatchable generators adding modeling accuracy when aggregated generation capacities are used.

Generation costs c_k depend on fuel prices P_{fuel} and CO_2 prices P_{CO_2}, power plant efficiency η (expressed through the inverse of the heat rate), the emission factor $F_{emission}$ and variable operation and maintenance (O&M) costs $C_{var_{O\&M}}$ and are calculated according to:

$$c_k = \frac{1}{\eta} \cdot P_{fuel} + \frac{1}{\eta} \cdot P_{CO_2} \cdot F_{emission} + C_{var_{O\&M}}. \tag{5.16}$$

Heat rates show the energy conversion efficiency from chemical to electrical, i.e. the fuel quantity needed (GJ) to produce one MWh of electricity (Lacal-Arantegui et al., 2014). Fossil and nuclear fuel prices are acquired from ENTSO-E Sustainable Transition scenario

(ENTSO-E, 2019). Biomass prices are obtained from Purvins et al. (2018). CO_2 prices are taken from ENTSO-E Sustainable Transition scenario ($P_{CO_2} = 45$ €$/tCO_2$) and emission factors $F_{emission}$ in fuel (t CO_2/GJ) are obtained from EIA (2016); IEA (2019), while variable O&M cost, $C_{varO\&M}$(€$/MWh$) are taken from Eurostat (2020).

Planned and unplanned outages of the power plants follow annual rates listed in Table 5.1 (World Energy Council, 2010). Outage schedules are obtained from one pre-simulation run and then kept constant for all the simulations. For this pre-simulation, planned outages are mostly scheduled during low electricity demand season. Average repair time is assumed 30 days for nuclear power plants and one day for the rest. Energy losses of 2% are assumed in the cross-zonal electricity exchange between the modeled bidding zones.

Table 5.1: Power plant characteristics and costs by source/fuel.

Source/ fuel	Min. operation power	Unit capacity, MW	Heat rate, GJ/MWh	Price, €/GJ	Variable O&M cost, €/MWh	Planned outage rate	Unplanned outage rate	Mean repair time, days
Wind	-	-	-	-	0	-	-	-
Solar	-	-	-	-	0	-	-	-
Hydro	15%	100	-	-	5	8%	6%	1
Pumped hydro	15%	100	-	-	0	8%	6%	1
Gas	35%	300	6.21	5.5	2	6%	5%	1
Gas, CHP	35%	300	6.31	5.5	4	6%	5%	1
Coal	43%	300	8	2.5	3.6	7%	8%	1
Lignite	43%	300	8.57	1.1	4.5	7%	8%	1
Nuclear	50%	1000	9.72	0.47	8	13%	5%	30
Biomass	43%	100	10.28	5.8	3.8	7%	8%	1
Oil	35%	100	9	17.1	11	3%	5%	1

Modeling is performed on a European scale, where Italy is chosen as a case study. Two scenarios for the Italian electricity system are studied: (i) a simple modeling approach where Italy is modeled as a single bidding zone and (ii) a detailed modeling approach where Italy is modeled as six bidding zones. The six-zone scenario considers the following

zones: Italy north (ITn), Italy central-north (ITcn), Italy central-south (ITcs), Italy south (ITs), Sicily (ITsic), and Sardinia (ITsar). Since Italy already consists of several zones, there are sufficient data available in order to model this under sound assumptions. Each of these two scenarios is further modeled by introducing three cases for Italy, one case where demand is assumed inelastic (zero demand elasticity) and two further cases with two different demand elasticity values: $\epsilon = -0.3$ and $\epsilon = -0.74$. Literature suggests a variety of demand elasticity values present in the current electricity system in Europe (Azevedo et al., 2011; Cialani and Mortazavi, 2018; Eskeland and Mideksa, 2010; Iimi, 2010; Krishnamurthy and Kriström, 2015; Madlener et al., 2011). An average from these studies is $\epsilon = -0.3$, which can be considered as a base case scenario. $\epsilon = -0.74$ is the average of the highest range of the reported demand elasticity values (Krishnamurthy and Kriström, 2015). Although the focus is on Italy, for which the different elasticity values and system changes are implemented, the whole European electricity system is modeled to acquire electricity trade with neighboring countries and to assess the overall effects of considering demand elasticity.

5.2.4 Numerical Experiments

Simulations are performed for every hour of the year 2040 and the interest lies on the overall outcome, the first set of results is presented for the entire European system on an annual basis in terms of (i) electricity generation cost, (ii) load-weighted average wholesale electricity price and (iii) electricity demand. For each of the three demand elasticity values, the three modeling outcomes are reported in terms of differences between the one-zone and the six-zone configuration of Italy. The results presented in Table 5.2 consider the entire modeled system of all 33 countries.

In the inelastic demand case, the total generation costs are increasing by 0.2% comparing scenarios of one and six Italian zones. With modeled demand elasticity, the total costs increase less, 0.01% for the $\epsilon = -0.3$ demand elasticity case and eventually decrease for the higher demand elasticity case of $\epsilon = -0.74$. The load-weighted price is increasing in all three scenarios in the six-zone case with respect to the one-zone case. The prices are increasing less at higher demand elasticity. The annual demand in the whole system is the same for the inelastic demand case. Elastic demand reacts to higher prices

Table 5.2: Relative changes between Scenario 1 (Italy one zone) and Scenario 2 (Italy six zones) of the three indicators total generation costs, load-weighted average wholesale electricity prices and total annual demand for the three demand elasticity values ($\epsilon = 0$ (inelastic), $\epsilon = -0.3$ and –0.74) for the entire system of 33 countries: Europe 2040.

Demand Elasticity ϵ	Δ generation cost	Δ price	Δ demand
0	0.20%	0.96%	0.00%
-0.3	0.01%	0.47%	-0.02%
-0.74	-0.05%	0.20%	-0.03%

and is decreasing. In the six-zones scenario in Italy, more constraints are introduced in the form of electricity transmission capacity limits between these new zones. Under inelastic demand, the total system costs in the whole of Europe increase slightly, by 0.2%. This is expected as an optimization algorithm tries to optimize the same objective function and under these additional constraints, the set of all feasible solutions becomes smaller. Therefore, the optimal solution cannot be improved. Introducing demand elasticity provides additional flexibility to the power dispatch and relaxes fixed demand constraint providing more room to further reduce the overall generation costs, when system changes occur, such as in this case moving from one zone to six zones in Italy. With $\epsilon = -0.3$ demand elasticity, the total generation costs in the whole system hardly change comparing one and six zones scenarios (there is only an increase of 0.01%). When implementing a demand elasticity value of $\epsilon = -0.74$ the total generation costs from one to six zones even decrease slightly by 0.04%, which means that the loosening of the load constraints becomes dominant over the tightening of constraints through the introduction of line constraints in Italy. The increase in generation costs in the inelastic demand case can be associated with higher load-weighted prices due to a more constrained system. As demand in Italy follows a linear demand curve with negative slope, the overall demand in the system decreases with higher demand elasticity values. The new equilibrium point is found through the intersection of this linear demand curve and the supply curve. This is well in line with the theory of implementing demand elasticity through linear demand functions. For a better understanding of the elastic demand impacts on electricity system modeling, changes in the Italian electricity system are depicted in Figures 5.5, since structural changes to the system and demand elasticity were only introduced in Italy. Again, displayed are the

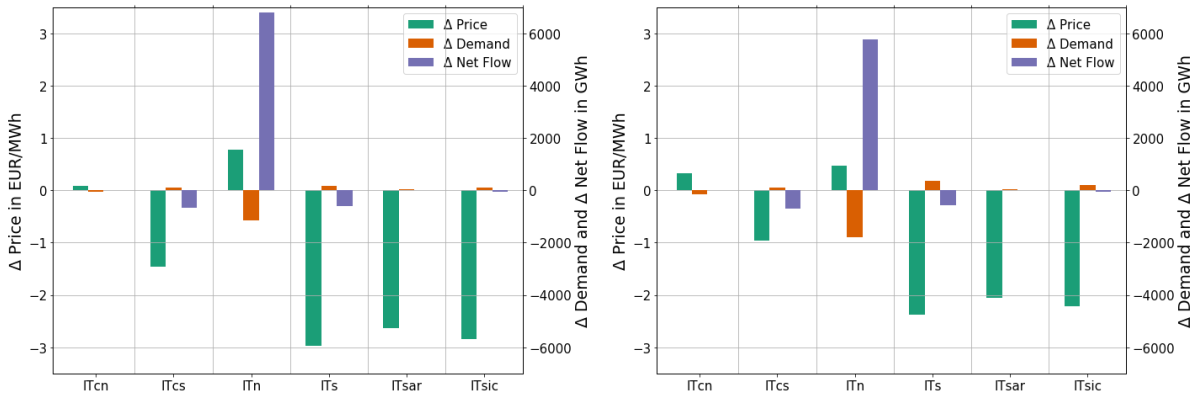

(a) **(b)**

Figure 5.5: Changes in Italy between Scenario 1 (Italy one zone) and Scenario 2 (Italy six zones) of the three indicators load-weighted average wholesale electricity prices (in EUR/MWh), annual demand (in GWh), and net flow (in GWh) from connected countries (net imports for all zones but ITsic, which is a net exporter). The indicators are shown for the six zones Italy central-north (ITcn), Italy central-south (ITs), Italy north (ITn), Italy south (ITs), Sardinia (ITsar) and Sicily (ITsic) for (a) demand elasticity of $\epsilon = -0.3$ and (b) high demand elasticity of –0.74.

relative changes between the one-zone and the six-zone scenario for the two elastic demand cases in terms of (i) annual load-weighted price (in EUR/MWh), (ii) annual demand (in GWh) and (iii) net flow from connected countries (in GWh). The latter are imports into Italy. An exception is ITsic (Sicily) as the sole net exporter among the Italian zones. The values for the six Italian zones are displayed in Figure 5.5a for the $\epsilon = -0.3$ demand elasticity scenario and in Figure5.5b for the $\epsilon = -0.74$ demand elasticity scenario.

Figure 5.5a and Figure5.5b show similar trends. An increase in load-weighted electricity price leads to a drop in electricity demand and vice versa. The net flows follow the trend of the price, i.e. both increase or decrease simultaneously. Comparing the results presented in Figure 1a and Figure 1b, the differences in load-weighted prices and flows in the $\epsilon = -0.74$ demand elasticity case are less pronounced than in the $\epsilon = -0.3$ demand elasticity case, while the opposite is true for the demand, which changes more in the higher demand elasticity case. In Figure5.5a, the load-weighted prices are reducing for all zones except for ITn and ITcn. This means that the introduction of the transmission capacity constraints within the Italian zones leads to congestions, which cause higher prices in the north of Italy. ITn is by far the zone with the highest demand, consuming more than half of the total electricity consumption in Italy. As a result, the demand is reduced in the six-zone case in accordance with this price incentive, while the flows are increased. Increasing net flows from neighboring countries in the northern part of

Italy occur when prices in those countries are lower than in ITn. This occurs more frequently in Scenario 2 - the six-zone configuration in Italy. An increase in flows to ITcn cannot be observed, as it is only interconnected with Italian zones (ITn and ITcs). In the remaining zones, demand is increasing and flows are decreasing, due to the drop in prices, as generation units dispatched in Italy are more often competitive with generators dispatched in connected zones. These considerations on the trends are also true for the higher demand elasticity case of $\epsilon = -0.74$. However, in Figure 5.5b a higher decrease in annual demand is observed. Especially in ITn, where it is most pronounced, which can be attributed to a higher demand elasticity, where demand reacts more drastically to price signals. Consequently, prices do not change so much between the one and the six-zone case, as price adopts to the lower demand. Correspondingly, flows are not increasing as much compared to the $\epsilon = -0.3$ demand elasticity case, since with higher demand elasticity of $\epsilon = -0.74$ demand decreases more and there is less need for imports. The observations in Figures 5.5 correspond with the results reported in Table 5.2. With higher demand elasticity, the overall load-weighted price is increasing less and the demand decreases more. This is the effect of introducing elastic demand, which gives the model more freedom when estimating power balance. Thus, depending on the demand elasticity value, the demand adjusts to changes in the electricity system, contributing to minimizing the total generation costs. In fact, in the $\epsilon = -0.74$ demand elasticity case this degree of freedom is becoming dominant over the constraints added to the optimization problem through the introduction of power transmission capacity limits between Italian zones. Therefore, the total generation costs are even reduced as has been reported above in Table 5.2, however, at the cost of high demand elasticity.

5.2.5 Conclusions

The main findings and contributions presented in this section can be summed up in the following points:

- A two-step modeling approach is used to incorporate demand elasticity in an economic dispatch model.
- A study on the impact of demand elasticity has been conducted on a pan-European level.

- Adding internal electricity transmission constraints in the Italian electricity system, i.e. limiting trading capacities between Italian bidding zones, electricity production costs, and consequently prices increase.
- Introducing demand elasticity affects the calculated prices due to the additional flexibility of demand and this effect can compensate for the increase in overall system costs due to additional transmission capacity constraints.
- Consumers' sensitivity to prices should be taken into account in sound electricity market modeling, in the face of the system's increasing need for flexibility to accommodate more renewable energy sources.

The costs associated with demand elasticity have not been included in the modeling. This should be considered in future work. Further case studies should be conducted, where demand elasticity is considered in entire Europe and not only in one country.

5.3 Estimating State of Charge Profiles of Hydro Storage Units for a Large-Scale Nodal Pricing Model

5.3.1 Introduction and Problem Description

In order to investigate different market designs for the whole of Europe one needs to solve large optimal power flow problems, ideally over longer time horizons (Borowski, 2020). This is a task that is computationally challenging, and it is common to subdivide a problem into smaller ones through e.g. parallelization or sequencing. One of the problems that arise in doing so is the seasonality of hydro storage facilities and the intertemporal constraints describing hydro reservoir continuity. A model that is operating under myopic foresight cannot display these aspects. Another dimension is the comparability between models with different spatial resolutions as it applies to zonal and nodal models of the European electricity system. It is necessary to ensure that models, aiming to explore the advantages or disadvantages of one design against the other, need to be run in similar conditions. Therefore, it is important to tackle the issue of limited foresight concerning

hydro storages in models with high spatial and temporal resolution.

The goal is to investigate the European electricity market under a nodal pricing regime. Nodal pricing based on so-called locational marginal prices (LMP) is opposed to the currently existing zonal pricing mechanism in Europe. In each zone z in Europe, where $z \in Z$ is the set of all zones, there will be uniform prices, while under nodal pricing, LMPs will be determined at every node n, which can be down to the resolution of individual substations, and the set of all nodes is N. Prices will differ when transmission lines are congested, and the flow $F_{n,m}$ from node n to node m reaches the capacity limit $\bar{F}_{n,m}$ or the sum of cross-zonal flows from zone z to zone $y \in Z(z)$, which border on zone z. Cross-zonal flows are found as the sum of flows in transmission lines $F_{n,m}$ from nodes n in the set of nodes $\hat{N}(z)$ belonging to zone z to nodes m that are in the set of nodes connected to node n and are also in $\hat{N}(y)$, the set of nodes connected to zone y. For comparative studies, the compatibility between the two approaches is essential; this reflects in particular on network representation. In order to calculate LMPs, one has to solve a large optimization problem. The problem is formulated as an economic dispatch model (Brown et al., 2018; Leuthold et al., 2012; Mende et al., 2018; Huang and Purvins, 2020; Goop et al., 2017; Zalzar et al., 2020), which in its full formulation reads:

$$\underset{P,P^{dis},P^{stor},soc,F,\theta}{\text{minimize}} \quad \sum_{t\in T}\left(\sum_{g\in\mathcal{G}} P_{g,t}\cdot c_g + \sum_{s\in S} P^{dis}_{s,t}\cdot c_s\right) \tag{5.17}$$

subject to

$$\sum_{d\in D(n)} P_{d,t} = \sum_{m\in N(n)} F_{m,n,t} + \sum_{g\in\mathcal{G}(n)} P_{g,t} + \sum_{s\in S(n)} \left(P^{dis}_{s,t} - P^{stor}_{s,t}\right), \quad \forall\, n\in N, t\in T \tag{5.18}$$

$$F_{n,m,t} = B_{n,m}(\Theta_{n,t} - \Theta_{m,t}), \qquad \forall\, n\in N, m\in N'(n), t\in T \tag{5.19}$$

$$F_{n,m,t} = -F_{m,n,t}, \qquad \forall\, n\in N, m\in N(n), t\in T \tag{5.20}$$

$$\beta\cdot\bar{F}_{n,m} \le F_{n,m,t} \le \beta\cdot\bar{F}_{n,m}, \qquad \forall\, n\in N, m\in N(n), t\in T \tag{5.21}$$

$$NTC_{y,z} \le \sum_{n\in\hat{N}(z)}\sum_{m\in N(n)\cap\hat{N}(y)} F_{n,m,t} \le NTC_{z,y}, \qquad \forall\, z\in Z, y\in Z(z), t\in T \tag{5.22}$$

$$0 \le P_{g,t} \le \bar{P}_g, \qquad \forall\, g\in\mathcal{G}_{conv}, t\in T \tag{5.23}$$

$$0 \le P_{g,t} \le \bar{P}_g\cdot p^{avail}_{g,t}, \qquad \forall\, g\in\mathcal{G}_{res}, t\in T \tag{5.24}$$

$$0 \le P^{dis}_{s,t} \le \bar{P}_s, \qquad \forall\, s\in S, t\in T \tag{5.25}$$

$$0 \le P^{stor}_{s,t} \le \bar{P}_s, \qquad \forall\, s\in S, t\in T \tag{5.26}$$

$$0.3\cdot\overline{SOC}_s \le soc_{s,t} \le \overline{SOC}_s, \qquad \forall\, s\in S, t\in T \tag{5.27}$$

$$soc_{s,t} = soc_{s,t-1} + \eta^{stor}\cdot P^{stor}_{s,t-1} - \frac{1}{\eta^{dis}}\cdot P^{dis}_{s,t-1} + infl_{s,t-1} - spill_{s,t-1}, \quad \forall\, s\in S, t\in T. \tag{5.28}$$

The objective Function (5.17) is minimized over all time steps t in the time horizon $T = \{t_1, t_2, \ldots, t_{end}\}$. The objective includes the costs to generate power from all generation units $\mathcal{G}$ and storage units S. Individual units' costs are calculated from c_g, the marginal costs of generator g, and the dispatched power $P_{g,t}$ of generator g at time t, and c_s the marginal costs of storage unit s and the dispatched power $P^{dis}_{s,t}$ of storage unit s at time t. The nodal power balance is defined in Equation (5.18), which ensures that at every time t the sum of demand $P_{d,t}$ of all the loads $d\in D(n)$ connected to node n equals the sum of flows $F_{m,n}$ entering from adjacent nodes $N(n)$, the generation $P_{g,t}$ from all generators $\mathcal{G}(n)$ connected to node n, and the net power dispatch of storage units $S(n)$ connected to node n, which is the difference between dispatched power $P^{dis}_{s,t}$ and stored power $P^{stor}_{s,t}$. Equation (5.19) describes the relation between power flow $F_{n,m,t}$ in AC lines and voltage angles Θ_n, where $B_{n,m}$ is the susceptance of the line connecting node n and

adjacent nodes $m \in N'(n)$ connected via an AC line. In the network, there are also high-voltage DC (HVDC) lines, in which the power flow is not determined by the physical properties of the lines but is considered controllable. Therefore, for power flows $F_{n,m,t}$ in HVDC lines, only the conservation of flow is enforced in Equation (5.20). This relation applies to both flows through AC and through HVDC lines from node n to adjacent node $m \in N(n)$. Power flow in transmission lines is limited in Equation (5.21) by the thermal capacity of lines $\bar{F}_{n,m}$, which are reduced through the factor β. Including a fixed reliability margin is a practice that is also proposed in the literature to approximate security constraints Leuthold et al. (2012). Equation (5.22) limits the cross-zonal flow from zones $z \in Z$ to adjacent zones $y \in Z(z)$ to the net-transfer capacities $NTC_{z,y}$. Power generation from conventional units $\mathcal{G}_{conv}$, renewable units $\mathcal{G}_{res}$, and storages, as well as power consumption for storage, is limited by upper capacity constraints $\bar{P}_g$ and $\bar{P}_s$, respectively, in Equations (5.23)–(5.26). The power generation constraints (5.24) from renewable energy sources solar and wind are further limited by a time-dependent reduction factor $p_{g,t}^{avail}$ of maximum power $\bar{P}_g$ output of renewable generator g at time t due to weather fluctuation. The filling of hydro storage expressed through the state of charge $soc_{su,t}$ is limited by upper and lower limits (Equation (5.27)); the lower limit is set at 30% of the total capacity $\overline{SOC}_s$. In Equation (5.28), the intertemporal continuity constraint for hydro storages is defined. It ensures that $soc_{su,t}$, the state of charge of unit s at time t, equals the state of charge at $t-1$ plus the storage power $P_{s,t-1}^{stor}$ at $t-1$ with the storage efficiency η^{stor}, minus the dispatched power $P_{s,t-1}^{dis}$ at $t-1$, where η^{dis} is the dispatch efficiency, plus $infl_{s,t-1}$ the inflow to storage unit s at time $t-1$ and minus $spill_{s,t-1}$, the spillage of storage unit s at $t-1$. The optimization variables are $P_{g,t}$, $P_{s,t}^{dis}$, $P_{s,t}^{stor}$, $soc_{s,t}$, and $\Theta_{n,t}$. LMPs will be derived as dual variables of constraints (5.18).

Given the size of the European transmission grid, solving this optimization problem is computationally highly intensive. It can be computationally tractable for short time periods, but in the case of performing simulations for an entire year with an hourly resolution, computation times can become very large, and simulations can only be conducted on high-performance computers. A previous study investigated the computational times for different formulations of the optimal power flow problem and found that while the DC approximation will be solvable in polynomial time, a large number of nodes and a long-time horizon still lead to very high computational times (Jansen

and Buzna, 2021). Therefore, it becomes necessary to perform so-called rolling horizon simulations, where the model is solved in sequences. Computations in parallel are not possible because of intertemporal constraints. These concern, in the linear program formulation of the economic dispatch problem, only hydro storage units and, in particular, the SOC of reservoirs (Equation (5.28)). Given the seasonality of inflows to hydro reservoirs and the fact that hydro units function not only as generation but also as storage units, the seasonality needs to be accounted for. However, in a rolling horizon simulation, the model has myopic foresight, and the optimization will be greedy and utilize the energy stored in hydro reservoirs within the first sequences. This is because information about future opportunities to dispatch hydropower in times of peak prices is not available for the optimization. If detailed data on hydro SOC were available for storage units in Europe, these issues would not need careful addressing. Hydro SOC profiles could then be used as input to the model. However, due to the lack of data, SOC profiles need to be determined from solving the large-scale optimization problem.

Therefore, it is necessary to develop a heuristic that passes the information about the seasonality of inflows as well as the benefits of storing energy today and utilizing it in the future. As mentioned above, the comparability of nodal outcomes to a zonal model is interesting when assessing the potential benefits of nodal pricing. While a nodal model clearly has to rely on a much higher spatial resolution than a zonal model, the two are linked through constraints (5.22). The question of comparability can be extended to the described issue of hydro storage modeling, and the utilization of zonal hydro profiles as inputs to the nodal model poses a possibility to take this into account.

5.3.2 Methodology

In this section, firstly the proposed methodology to obtain SOC profiles for the large nodal model described in Section 5.3.1 is introduced. Secondly, a method to compare nodal against zonal pricing is introduced, which incorporates redispatching into the zonal model. This is a common approach, which allows testing the applicability of the developed heuristic to obtain SOC profiles to conduct comparative zonal against nodal pricing studies.

5.3.2.1 Heuristic method to obtain SOC profiles

As the computational efforts to run the full models with an hourly resolution are large, simulations need to be performed in sequence. Therefore, the issue of hydro storage units arises, i.e., the model would utilize all the stored water in the reservoirs and empty them within the first sequences if there was no foresight included. Thus, a heuristic step-wise modeling framework is proposed, which is illustrated in Figure 5.6. Utilizing heuristic approaches in hydropower optimization is an increasingly researched topic (Azad et al., 2020). Initially, in Stage 0, data are collected and prepared to serve as inputs for the full nodal and a spatially aggregated zonal model. In Stage 1, the zonal model is run for the entire time horizon to produce initial SOC profiles. These serve as input to Stage 2, in which the nodal model is run in sequences and guided by the input profiles through soft constraints. These soft constraints are implemented through slack variables, which contribute to the objective function of the optimization problem and thus also require the setting of penalty factors that quantify this contribution; therefore, a set of penalty factors is another input to Stage 2. Finally, the produced SOC profiles are evaluated by assessing the overall system costs of generating power and storing the best-performing input parameters. The following describes Stage 1 and Stage 2 in more detail, whereas the data preparation Stage 0 is explained further in Section 5.3.3.1.

Stage 1. The target is to produce SOC profiles for an entire year from a spatially aggregated model that is referred to as zonal model. As has been mentioned in the literature review, solving aggregated models to obtain hydro profiles is a common approach. The main difference in comparison to the nodal model introduced in Equations (5.17)–(5.28) is the level of network representation. Instead of including all network constraints, the zonal model solely regards inter-zonal capacity limits. These capacities are displayed through the net-transfer capacities (NTC) Brancucci Martínez-Anido et al. (2013b); Huang and Purvins (2020); Zalzar et al. (2020). Besides the fact that the zonal model can be run in a reasonable amount of time for the whole reference year with an hourly resolution, it also emulates the European electricity day-ahead market, as it is functioning in its current design. The full mathematical description of the problem

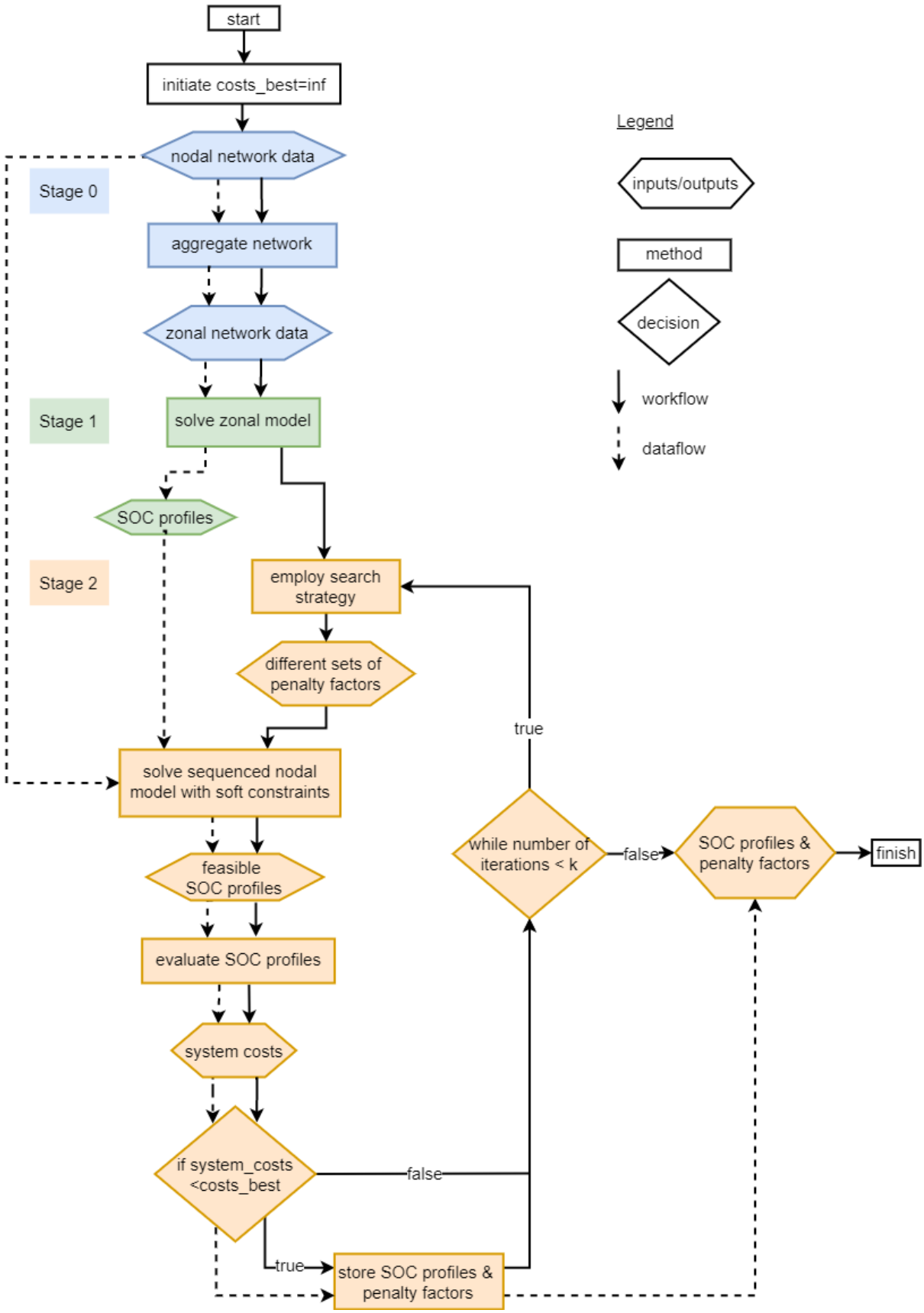

Figure 5.6: Stage-wise methodology to obtain SOC profiles for large-scale nodal models.

reads:

$$\text{minimize} \quad \sum_{t \in T} \left(\sum_{g \in \mathcal{G}} P_{g,t} \cdot c_g + \sum_{s \in S} P_{s,t}^{dis} \cdot c_s \right) \tag{5.29}$$

subject to

$$\sum_{d \in \hat{D}(z)} P_{d,t} = \sum_{y \in Z(z)} F_{z,y,t} + \sum_{g \in \hat{\mathcal{G}}(z)} P_{g,t} + \sum_{s \in \hat{S}(z)} \left(P_{s,t}^{dis} - P_{s,t}^{stor} \right), \qquad \forall\, z \in Z, t \in T \tag{5.30}$$

$$F_{z,y,t} = -F_{y,z,t}, \qquad \forall\, z \in Z, y \in Z(z), t \in T \tag{5.31}$$

$$NTC_{y,z} \leq F_{z,y,t} \leq NTC_{z,y}, \qquad \forall\, z \in Z, y \in Z(z), t \in T \tag{5.32}$$

$$(5.23) - (5.28).$$

Equation (5.29) is the objective function, where the overall costs of generating power from generators and storage units are minimized. The power balance in Equation (5.30) ensures that for all times t, all power consumed by demands $\hat{D}(z)$ at zone z equals the sum of all power generated from generators $\hat{\mathcal{G}}(z)$, the net power output of storage units $\hat{S}(z)$, and the sum of flows $F_{z,y,t}$ going into zone z from adjacent zones $y \in Z(z)$. Equation (5.31) ensures that imports $F_{z,y,t}$ to zone z from zone y equal exports $F_{y,z,t}$ from zone z to zone y. This represents a generic flow model, where flow conservation at zones is maintained. Flows in cross-zonal lines $F_{z,y,t}$ are limited by upper $NTC_{z,y}$ and lower $NTC_{y,z}$ capacity limits, the so-called net transfer capacities, expressed in Equation (5.32). The constraints for power generation and storage units were already introduced in Equations (5.23)–(5.28) and are the same as in the nodal model. Resulting from this initial run of the zonal model, hydro profiles for the hourly SOC of all the storage units present in the system are obtained. These profiles are then aggregated to a zonal level, which means that all storage units' SOCs within a zone are aggregated to obtain hourly SOC profiles for each zone. This profile, along with all the SOC profiles of individual storage units, functions as input to the next step.

Stage 2. The purpose of this stage is twofold; firstly, to produce feasible profiles for the nodal model, and second, to adjust the profiles to the more-constraint situation of the nodal network. Given the discrepancy between the zonal and nodal network representation, the outcomes of the former stage are not necessarily feasible in the nodal model. Therefore, the SOC profiles for individual storage units and zones from Stage 1 are used as target values, but they are not enforced to be met strictly. Thus, a set of soft

constraints are introduced that penalize deviations from the zonal input profiles by adding a penalty term to the objective function. The nodal optimization model will be run in sequences. These soft constraints are only introduced at the end of each sequence; thereby, complete freedom to deviate from the input profile throughout the sequence is allowed, which is a technique commonly employed in hydroelectric modeling (Philpott et al., 2000; Setz et al., 2008). Thus, the model should be able to react to short-term incentives as line overloadings or peaks in prices, while overall, the trend is followed through the soft constraint at the end of each sequence. The first step in the sequence represents an exception, as there, the constraints are also present at the beginning of the sequence time window. This is because, in the consecutive steps, the initial SOC values will be passed on from the previous step to ensure continuity, while in the first step, there is no input to be passed. Thereby, the problem is considering a trade-off between minimizing overall costs and following the target profiles, which, if not followed, increase the objective function value through penalties. There is sequence of I smaller optimization problems i, where each is solved for the set of times $T_i = \{t_{i,1}, t_{i,2}, \ldots, t_{i,end}\}$. The sets of T_i make up the whole time horizon $T = \{T_1, T_2, \ldots, T_I\}$. The formulation of problems $i \neq 1$ reads:

$$\begin{aligned} \text{minimize} \quad & \sum_{t \in T_i} \left(\sum_{g \in \mathcal{G}} P_{g,t} \cdot c_g + \sum_{s \in S} P^{dis}_{s,t} \cdot c_s \right) + \\ & + \sum_{s \in S} a_{s,t=t_{i,end}} \cdot \alpha_s + \sum_{z \in Z} a_{z,t=t_{i,end}} \cdot \alpha_z \end{aligned} \tag{5.33}$$

subject to

$$a_{s,t} \geq soc_{s,t} - SOC^{target}_{s,t}, \qquad \forall\ s \in S, t = t_{i,end} \tag{5.34}$$

$$-a_{s,t} \leq soc_{s,t} - SOC^{target}_{s,t}, \qquad \forall\ s \in S, t = t_{i,end} \tag{5.35}$$

$$a_{z,t} \geq \sum_{s \in \hat{S}(z)} soc_{s,t} - SOC^{target}_{z,t}, \qquad \forall\ z \in Z, t = t_{i,end} \tag{5.36}$$

$$-a_{z,t} \leq \sum_{s \in \hat{S}(z)} soc_{s,t} - SOC^{target}_{z,t}, \qquad \forall\ z \in Z, t = t_{i,end} \tag{5.37}$$

$$(5.18) - (5.28)$$

$$SOC^{min}_{s,t} \leq soc_{s,t}, \qquad \forall\ s \in S, t = t_{i,end}. \tag{5.38}$$

The objective function Equation (5.33) includes, next to the costs of generating power, also the penalty contributions for the SOC target values. These contributions come from the slack variables $a_{s,t}$ for the deviations from the input target values $SOC_{s,t}^{target}$ for individual storage units s (Equations (5.34) and (5.35)) and the slack variables $a_{z,t}$ for the deviations from the input target values $SOC_{z,t}^{target}$ for the sum of storage units $s \in \hat{S}(z)$ connected to zone z (Equations (5.36) and (5.37)). These deviations from the input profiles are penalized with the respective penalty factors α_s for individual storage units and α_z for the sum of SOC in a zone, to quantify the contribution to the objective function. Equations (5.18)–(5.28) have already been introduced for the full nodal model. Equation (5.38) ensures that at the end of every sequence a minimum level of $SOC_{s,t}^{min}$ is reached for each storage unit s, so that the cyclic constraint (Equation (5.28)) can also be met for the overall time horizon. To understand how these minimum target values are determined, it is necessary to differentiate between two types of hydro storages, which are pumped hydro storages (PHS) and hydro dams. The target values for each storage unit s at the end of the overall time horizon at t_{end} $SOC_{s,t=t_{end}}^{min}$ are determined from Equation (5.28). Starting from this, the target values are backcasted for storage units s belonging to the set of all PHS units S_{phs} following:

$$SOC_{s,t=t_{end}-(j+1)}^{min} = SOC_{s,t=t_{end}-j}^{min} - \eta^{stor} \cdot \bar{P}_s^{stor}, \quad \text{for } j = 0, 1, 2, \ldots, t_{end} - 1. \tag{5.39}$$

The minimum target value of SOC at every hour needs to be at least the target value of the previous hour minus the maximum storage pumping power times the corresponding efficiency, which can fill up the storage reservoir. On the other hand, storages s belonging to the set of all dam hydro storages S_{dam} can be refilled by natural inflows; therefore, their minimum SOC target values are determined from

$$SOC_{s,t=t_{end}-(j+1)}^{min} = SOC_{s,t=t_{end}-j}^{min} - infl_{s,t=t_{end}-j}, \quad \text{for } j = 0, 1, 2, \ldots, t_{end} - 1. \tag{5.40}$$

Now, as mentioned above, the formulation of the optimization problem differs only for the first step in the sequence, because there, also soft constraints for the first hour in the sequence are present. The problem for $T_1 = \{t_{1,1}, t_{1,2}, \ldots, t_{1,end}\}$, the first step in the

sequence, reads:

$$\begin{aligned}\text{minimize} \quad & \sum_{t\in T_1}\left(\sum_{g\in\mathcal{G}} P_{g,t}\cdot c_g + \sum_{s\in S} P^{dis}_{s,t}\cdot c_s\right) + \\ & + \sum_{s\in S}\left(a_{s,t=t_{1,1}}\cdot\alpha_s + a_{s,t=t_{1,end}}\cdot\alpha_s\right) + \\ & + \sum_{z\in Z}\left(a_{z,t=t_{1,1}}\cdot\alpha_z + a_{z,t=t_{1,end}}\cdot\alpha_z\right)\end{aligned} \tag{5.41}$$

subject to

$$a_{s,t} \geq soc_{s,t} - SOC^{target}_{s,t}, \qquad \forall\ s\in S, t=\{t_{1,1}, t_{1,end}\} \tag{5.42}$$

$$-a_{s,t} \leq soc_{s,t} - SOC^{target}_{s,t}, \qquad \forall\ s\in S, t=\{t_{1,1}, t_{1,end}\} \tag{5.43}$$

$$a_{z,t} \geq \sum_{s\in\hat{S}(z)} soc_{s,t} - SOC^{target}_{z,t}, \qquad \forall\ z\in Z, t=\{t_{1,1}, t_{1,end}\} \tag{5.44}$$

$$-a_{z,t} \leq \sum_{s\in\hat{S}(z)} soc_{s,t} - SOC^{target}_{z,t}, \qquad \forall\ z\in Z, t=\{t_{1,1}, t_{1,end}\} \tag{5.45}$$

(5.18) – (5.28).

Here, Equations (5.42)–(5.45) enforce the target values also at the first hour of the first sequence, as opposed to Equations (5.34)–(5.37) of the consecutive steps in the sequence, where they are only applicable to the last time step in the sequence. As discussed above, this is because the initial SOC levels are passed as inputs to consecutive steps to the intertemporal storage units constraints (Equation (5.28)).

After solving the sequence of nodal models with soft constraints, the overall system costs as the costs of generating power are assessed, and if the result outperforms the costs obtained with the previously best SOC profile, the SOC profiles, and the penalty factors that led to them are stored. Then, a search strategy is employed to generate different penalty factor combinations as inputs and perform the sequenced nodal model run again and assess the costs until the number of previously defined iterations is reached. This method is applied to benchmark cases introduced in the next section, which also briefly describes the data preparation (see Stage 0 in Figure 5.6).

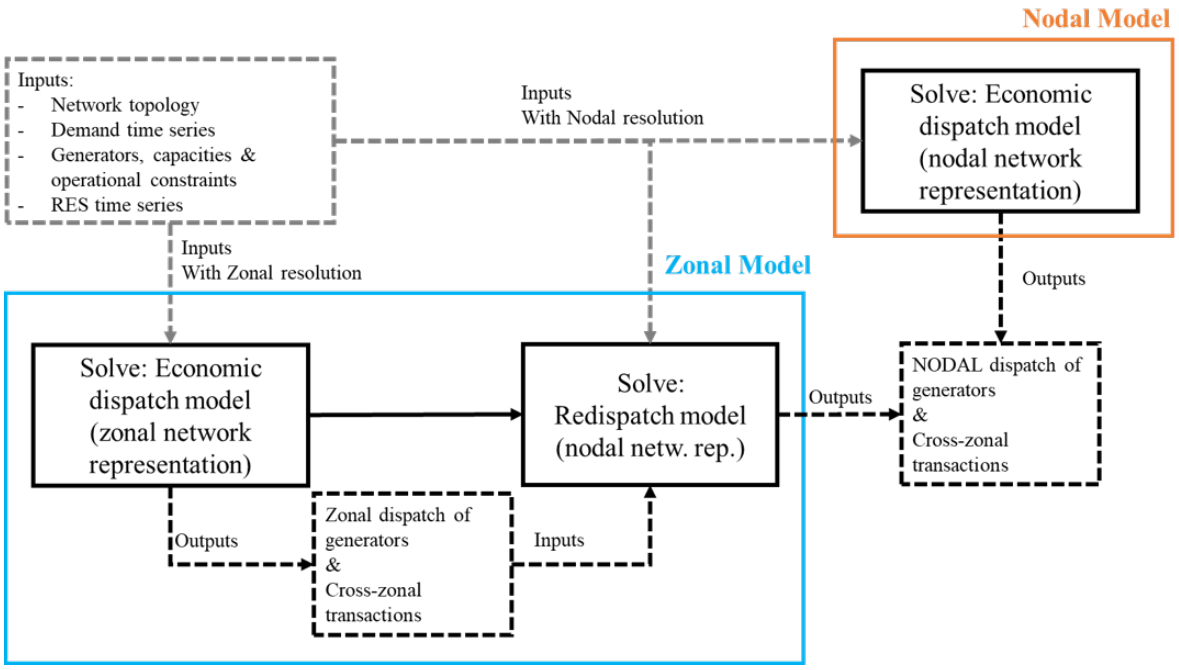

Figure 5.7: Flowchart of the zonal model, which consists of firstly an economic dispatch model with a zonal network resolution and secondly a redispatching model with nodal network representation; in comparison to the nodal model, which consists only of a single economic dispatch model with nodal network resolution.

5.3.2.2 Redispatching

The main difference between nodal and zonal models of the electricity system is the resolution of network data. In reality, this calls for remedial actions such as redispatching by TSOs, because a zonal dispatch of generators does not take the full network topology into account. Thus, a zonal model needs to consist of two parts. This difference between a nodal and zonal model is depicted in Figure 5.7. The nodal model determines a feasible nodal dispatch of generators through solving the optimization problem (5.17)-(5.28). For the zonal model, firstly, the zonal dispatch is determined by solving the optimization problem described in (5.29)-(5.32), where the data has a zonal resolution. Consecutively, this zonal dispatch needs to be corrected through redispatching to respect the physical limits of the transmission grid.

The formulation for the redispatching model is presented, which is using as input the outcomes of the zonal model in terms of power generation $P^z_{g,t}$. In general, redispatching can be formulated as cost or volume based redispatching Poplavskaya et al. (2020). The approach presented in Felling et al. (2019) is followed and the optimization problem is formulated as redispatching cost minimization:

$$\text{minimize} \quad \sum_{t \in T} \left(\sum_{g \in \mathcal{G}} u_{g,t} + \sum_{s \in S} v_{s,t} \right) \tag{5.46}$$

subject to

$$u_{g,t} \geq \left(-P^{z}_{g,t} + P_{g,t}\right) \cdot c_g, \ \forall \ g \in \mathcal{G}, t \tag{5.47}$$

$$u_{g,t} \geq \left(P^{z}_{g,t} - P_{g,t}\right) \cdot (c^{max} - c_g), \ \forall \ g \in \mathcal{G}, t \tag{5.48}$$

$$v_{g,t} \geq \left(-(P^{dis,z}_{s,t} - P^{stor,z}_{s,t}) + (P^{dis}_{s,t} - P^{stor}_{s,t})\right) \cdot c_s, \ \forall \ s \in S, t \tag{5.49}$$

$$v_{g,t} \geq \left((P^{dis,z}_{s,t} - P^{stor,z}_{s,t}) - (P^{dis}_{s,t} - P^{stor}_{s,t})\right) \cdot (c^{max} - c_s), \ \forall \ s \in S, t \tag{5.50}$$

$$(5.23) - (5.28) \tag{5.51}$$

$$(5.18) - (5.22) \tag{5.52}$$

Deviations of the power of generators $\mathcal{G}$ determined by the redispatching model $P_{g,t}$ from the input power of the zonal model $P^{z}_{g,t}$ are substituted with $u_{g,t}$ and analogously deviations of the net power dispatch from storage units S of the redispatching model $P^{dis}_{s,t} - P^{stor}_{s,t}$ from the input of the zonal model $P^{dis,z}_{s,t} - P^{stor,z}_{s,t}$ are substituted with $v_{s,t}$. In the objective function (5.46), the substitution variables are minimized. Constraints (5.47) and (5.49) ensure that upward redispatching is priced at the corresponding marginal costs c_g of generator g and c_s of storage unit s. Downward redispatching is priced through subtracting the marginal costs of corresponding generators and storage units from the marginal costs of the most expensive generator c^{max}, expressed in (5.48) and (5.50). This is ensuring that more expensive generators are primarily used for downward redispatching. Equations (5.23)-(5.28) are the generation and storage units operational constraints, (5.18) is the nodal power balance, (5.19) the relation between power flows and voltage angles and (5.21) and (5.22) the limits for flows in transmission lines, from previously defined optimization problems.

5.3.3 Data Preparation and Experimental Design

In this section, the design of the experiments is presented along with a description of the inputs and data preparation.

5.3.3.1 Nodal and Zonal Network Preparation

In this section, the workflow to build up the base dataset is laid out. This corresponds to Stage 0 of the proposed methodology (see Figure 5.6). The model is implemented in Python using the open-source tool PyPSA Brown et al. (2018). The base network is built using PyPSA-Eur Hörsch et al. (2018). PyPSA-Eur is an open-source tool that can build and solve networks of the European transmission system from various data sources. The network comprises transmission line capacities and physical properties; connected to nodes are generators and loads; for RESs, capacity availability factors are assigned to nodes that are time series indicating the maximum capacity percentage that can be dispatched for solar and wind plants connected to the respective node. As the base year, 2018 is chosen because of data availability. PyPSA-Eur is used to build the base network of 1010 nodes for Europe [1].

In a consecutive step, the nodal model is aggregated to 45 zones, which approximates the reality of the zonal market in Europe in 2018. In this aggregating step, all transmission lines are removed and replaced with inter-zonal transport lines with their NTCs. The NTCs are taken from ENTSO's ten-year net development plan (TYNDP) and are assumed constant throughout the year (ENTSO-E, 2019). Flows through these new lines will be modeled through a transport model, i.e., it is a generic flow model, where only flow conservation at a node is maintained. Therefore, only line capacities need to be provided to the model, as opposed to the DC approximation of power flow, where also physical line properties as the susceptance need to be known. All other components (generators, storage units, and loads) are reassigned to zones in accordance with the geographical location of the node they were assigned to in the nodal network. However, the level of detail for all the generation and storage units, as well as loads, is maintained. This is performed in order to maintain comparability between the zonal and the nodal network models. This becomes especially relevant when the ultimate aim of applying these models is to compare them, also including redispatching. The resulting nodal and zonal networks are illustrated in Figure 5.8.

[1] Included in the model are the following countries: Albania, Austria, Belgium, Bosnia and Herzegovina, Bulgaria, Croatia, Czech Republic, Denmark, Estonia, Finland, France, Germany, Great Britain, Greece, Hungary, Ireland, Italy, Latvia, Lithuania, Luxembourg, Montenegro, Netherlands, North Macedonia, Norway, Poland, Portugal, Romania, Serbia, Slovakia, Slovenia, Spain, Sweden, and Switzerland.

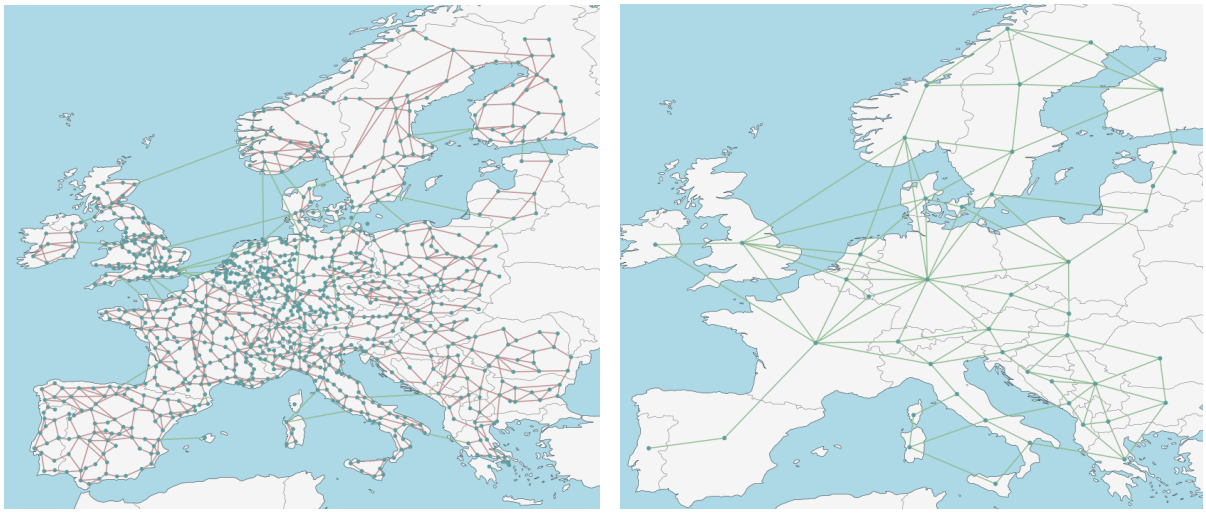

(a) (b)

Figure 5.8: Nodal network consisting of 1010 nodes (left) and zonal network consisting of 45 zones (right) obtained using PyPSA-Eur (Hörsch et al., 2018).

5.3.3.2 Experimental Design

The goal is to determine the utilization of hydro storages through the methodology described above. In particular, the state of charge time series for the different storage units should be determined. The model is implemented in Python and relies heavily on the PyPSA package (Brown et al., 2018). The optimization problems are solved using the commercial solver Gurobi. Simulations are conducted on a cluster node with two ten-core Intel Xeon processors and 750 GB RAM. The method described above in Step 2 is tested against other approaches proposed in the literature (Fosso et al., 1999; Fosso and Belsnes, 2004; Fernández-Blanco et al., 2017; Braun, 2016; Baslis et al., 2009). Concretely, the method is compared against using hydro shadow prices derived from constraint (5.28) in Stage 1 of the zonal optimization, as well as using constant bid prices for hydro, which are chosen to be higher than the marginal costs to produce electricity from hydro storages.

The different methods to obtain hydro SOC profiles are investigated under four different scenarios. Two different simulation time horizons are analyzed, four months and the whole year. Simulating an entire year is common practice in electricity market modeling. The shorter horizon is chosen as computations of the full nodal model are achievable in reasonable computational times. Then, the SOC profiles obtained from the different methods can be compared against the SOC profile determined from an optimization that simulates the entire four months in one simulation step and is therefore regarded as

the optimal profile. Further, the capacities of transmission lines are varied to simulate situations of higher congestion. In the base scenario, 70% of line capacity ($\beta = 0.7$) is used, as this value is commonly used to approximate the N-1 criterion Müller et al. (2019). Then, the available transmission line capacity is reduced to 50% of the thermal capacity. Simulations are run with an hourly resolution. For the sequenced nodal model described in Stage 2, sequences of one week are chosen. The proposed heuristic requires setting the penalty factors α_s and α_z, a grid search is performed to explore these factors (in the following, this method is referred to as $SOC\_HEUR(\alpha_z, \alpha_s)$). Concretely, the investigated penalty factor combinations are: (1000,1000); (1000,10); (1000,0); (10,1000); (10,10); (10,0); (0,1000); (0,0).

The quality of profiles is measured through different performance indicators. The objective function value or overall system costs, the level of congestion, the amount of demand not served (load shedding), and the computational times are analyzed. As a measure of congestion, the *system congestion* proposed by Göransson et al. (2014) is used. The system congestion sc_t at time t is measured through the standard deviation of the locational marginal prices (LMP):

$$sc_t = \sqrt{\frac{1}{N} \sum_{n \in N} \left(\overline{LMP}_t - LMP_{n,t}\right)^2}, \tag{5.53}$$

where $LMP_{n,t}$ is the LMP at node n at time t, and $\overline{LMP}_t$ is the average LMP over all nodes N at time t. LMPs are derived as dual variables of Equations (5.18) and (5.30) of the zonal and the nodal model, respectively Liu et al. (2009). In the following, the numerical results will be assessed using the average system costs $\overline{sc}$ over the whole time horizon.

For the redispatching case study, the SOC profile obtained with the best performing method in the long-term benchmark will be used as a basis. Then, simulations are run for a week, where high levels of congestions are identified. The results for the nodal model are compared to the zonal model and the zonal modal plus redispatching. Comparisons are done in terms of generation by technology as well as system costs.

5.3.4 Numerical Experiments

5.3.4.1 Benchmarks with Short-Time Horizon

This section presents the results for the benchmark case with the short-time horizon of four months. Reported are the overall system costs, the level of congestion, and the amount of load shedding, as well as the computation times. The results are presented for the full nodal model run with an hourly resolution (referred to as $NODAL$), which optimizes the entire four months in one simulation ((5.17)–(5.28)); the heuristic to obtain SOC profiles described in Section 5.3.2, denoted by $SOC\_HEUR(\alpha_z, \alpha_s)$ with the different penalty factor combinations for the two α; and the methods described in the literature, the one relying on shadow prices derived from Equation (5.28) of the zonal model is denoted as SH_PRICES and the one relying on constant bid prices $BIDS(bidprice)$.

An overview of outcomes for the short-time horizon benchmark with transmission capacity factor $\beta = 0.7$ is presented in Table 5.3.

The overall system costs obtained for most of the penalty factor combinations are in a similar range, while the best performing combination penalty factors are $SOC\_HEUR(1000, 1000)$, $SOC\_HEUR(1000, 10)$, $SOC\_HEUR(10, 1000)$, and $SOC\_HEUR(0, 1000)$, which differ only 0.1% from $NODAL$. Next to this, also $SOC\_HEUR(1000, 0)$ shows system costs that are close to the nodal benchmark. Notably, the combination with myopic foresight, i.e., where no guidance is provided to follow the input profile $SOC\_HEUR(0, 0)$, exhibits much larger system costs, which differ by 108.7% from $NODAL$. The average system congestion is lowest for the combinations with the lowest costs. The amount of load shed is lowest for the cases which have the lowest costs. This is in line with the high value of lost load (VoLL) of EUR $10,000$/MWh. Several penalty factor combinations reach the same amount of load shedding as the nodal benchmark case $NODAL$. The overall low level of load shedding, in combination with the observation that the lowest system costs are found among others for combination $SOC\_HEUR(1000, 1000)$, indicates that in a situation of low congestion, it is most beneficial to follow the input profile closely. The share of load shedding costs makes up around 50% of the overall costs for SH_PRICES and the three $BIDS$ cases. Thus, these costs can explain the higher system costs in comparison to $NODAL$. In terms of run times, one can observe that higher penalty factors also exhibit longer computational times.

Table 5.3: Results overview for the short-time horizon benchmark with transmission capacity factor $\beta = 0.7$. Reported are for the different methods: the total system costs, which are made up of operational costs (i.e., power generation costs) and load shedding costs, the difference between $NODAL$ and the respective method in absolute amount and relative to the total system costs of $NODAL$; the average system congestion ($\overline{sc}$); the total amount of load shed and the share of this amount with respect to the total load; and the run times.

	Costs					**Congestion**	**Load Shedding**		**Run Time**
Method	**System [B EUR]**	**Operational [B EUR]**	**Load Shedding [B EUR]**	**Difference System-NODAL [B EUR]**	**Difference System-NODAL wrt NODAL [%]**	$\overline{sc}$	**Amount [GWh]**	**Share of Tot Demand [%]**	**Run Time [h]**
ZONAL	20.07	20.07	0.00	-0.98	-4.7	7.7	0	0.000	0.6
NODAL	21.05	20.63	0.42	0.00	0.0	663.4	42	0.004	184.8
SH_PRICES	42.13	21.49	20.64	21.08	100.2	858.9	2064	0.208	1.3
BIDS(20)	42.31	21.49	20.83	21.27	101.1	861.5	2083	0.210	1.5
BIDS(40)	40.02	21.48	18.54	18.97	90.1	853.2	1854	0.187	1.2
BIDS(60)	43.34	21.53	21.81	22.30	106.0	861.2	2181	0.220	1.4
SOC_HEUR(1000,1000)	21.06	20.64	0.42	0.01	0.1	663.4	42	0.004	11.6
SOC_HEUR(1000,10)	21.06	20.64	0.42	0.01	0.1	663.4	42	0.004	4.9
SOC_HEUR(1000,0)	21.06	20.65	0.42	0.02	0.1	663.4	42	0.004	36.6
SOC_HEUR(10,1000)	21.06	20.64	0.42	0.01	0.1	663.4	42	0.004	22.5
SOC_HEUR(10,10)	21.44	20.84	0.60	0.39	1.9	675.0	60	0.006	2.0
SOC_HEUR(10,0)	21.52	20.91	0.60	0.47	2.2	675.0	60	0.006	1.6
SOC_HEUR(0,1000)	21.06	20.64	0.42	0.01	0.1	663.4	42	0.004	14.5
SOC_HEUR(0,0)	43.92	21.44	22.49	22.88	108.7	863.3	2249	0.227	1.3

The bid and shadow prices methods consistently outperform the proposed methodology in terms of run times but not so in terms of all the other performance indicators. Higher computational times for the heuristic approach can likely be attributed to the additional constraints added to the optimization problem to guide the SOC profiles. Even though computational times are always worth taking into account, for the purpose of this study, achieving low computational times is not a critical issue, as opposed to the generation of SOC profiles.

Table 5.4: Results overview for the short-time horizon benchmark with transmission capacity factor $\beta = 0.5$. Reported are for the different methods: the total system costs, which are made up of operational costs (i.e., power generation costs) and load shedding costs, the difference between $NODAL$ and the respective method in absolute amount and relative to the total system costs of $NODAL$; the average system congestion ($\overline{sc}$); the total amount of load shed and the share of this amount with respect to the total load; and the run times.

	Costs					Congestion	Load Shedding		Run Time
Method	**System [B EUR]**	**Operational [B EUR]**	**Load Shedding [B EUR]**	**Difference System-NODAL [B EUR]**	**Difference System-NODAL wrt NODAL [%]**	$\overline{sc}$	**Amount [GWh]**	**Share of Tot Demand [%]**	**Run Time [h]**
ZONAL	20.07	20.07	0.00	-5.55	-21.7	7.7	0	0.000	0.6
NODAL	25.61	21.09	4.53	0.00	0.0	763.3	453	0.046	203.2
SH_PRICES	45.92	21.99	23.93	20.31	79.3	901.2	2393	0.241	1.4
BIDS(20)	46.91	22.04	24.87	21.30	83.1	903.3	2487	0.250	1.3
BIDS(40)	45.74	21.98	23.76	20.12	78.6	900.6	2376	0.239	2.3
BIDS(60)	45.96	21.98	23.98	20.34	79.4	900.6	2398	0.242	1.3
SOC_HEUR(1000,1000)	25.63	21.10	4.53	0.01	0.1	750.9	453	0.046	17.8
SOC_HEUR(1000,10)	25.63	21.10	4.53	0.02	0.1	750.3	453	0.046	9.0
SOC_HEUR(1000,0)	26.41	21.21	5.20	0.80	3.1	771.8	520	0.052	39.5
SOC_HEUR(10,1000)	25.63	21.10	4.53	0.01	0.1	750.4	453	0.046	18.4
SOC_HEUR(10,10)	26.25	21.30	4.95	0.63	2.5	757.9	495	0.050	5.4
SOC_HEUR(10,0)	26.92	21.40	5.52	1.30	5.1	779.3	552	0.056	2.1
SOC_HEUR(0,1000)	25.63	21.10	4.53	0.01	0.1	750.4	453	0.046	17.4
SOC_HEUR(0,0)	45.79	21.95	23.84	20.17	78.8	902.8	2384	0.240	1.3

Computational experiments are performed for the short-time horizon benchmark with transmission capacity factor $\beta = 0.5$. The results are summed up in Table 5.4.

This set of results is compared against the results from the previously discussed short-time horizon benchmark with transmission capacity factor $\beta = 0.7$ (Table 5.3). The costs to generate power in the $\beta = 0.5$ scenario are consistently higher than for the $\beta = 0.7$ scenario. The best-performing penalty factor combination in terms of system costs are, again, $SOC\_HEUR(1000, 1000)$, $SOC\_HEUR(1000, 10)$, $SOC\_HEUR(10, 1000)$, and

$SOC\_HEUR(0, 1000)$. The average system congestion is higher than in the $\beta = 0.7$ case throughout the $\beta = 0.5$ scenario. The lowest system congestion is also indicating the lowest costs. The best-performing penalty factor combinations exhibit similar average system congestion to the $NODAL$ benchmark case. This can indicate that deviations from the input SOC profiles allow mitigating line overloading, while higher costs occur at another time; this will be investigated further later on. While more load shedding occurs than in the $\beta = 0.7$ scenario, when considering the percentage of load shedding with respect to the total load, one can observe that it is always less than 1%, and in the case of the penalty factor combinations, only 0.05% of the entire load. Even though this is a small amount of load, it contributes significantly to the overall system costs, as the share of load shedding costs indicates. For the lowest levels of load shedding, the associated costs make up 17.7% of the total costs, and for the SH_PRICES and three $BIDS$, the costs of load shedding make up more than half of the overall costs. Thus, load shedding explains the high costs of these methods. Regarding run times, again, the best-performing penalty factor combinations take significantly longer to compute. One can also see that it takes longer to solve the problems with penalty factors than with bidding prices or shadow prices for hydro defined.

In order to understand the above results better and, especially, shed some light on the relatively bad performance of the bidding price/shadow price methodology, some aggregated SOC profiles are shown in Figure 5.9.

Firstly, it can be observed that zonal, nodal, and penalty factor profiles exhibit the same trend. At the same time, the $NODAL$ SOC profile is shifted against the others. The penalty factor combination profile $SOC\_HEUR(1000, 10)$ follows the zonal input closely. The SH_PRICES profile differs significantly from the others, and the trend is not preserved. It also needs to be noted that, while the SOC level decreases and hydro is utilized to lower system costs, this needs to be made up for because of the end of the year constraints (see Equation (5.38)). At the end of the year, SOC levels need to align with the beginning of the year. It can be seen that the shadow price methodology is not able to reproduce the pattern of hydro production, as seen in the zonal and nodal models.

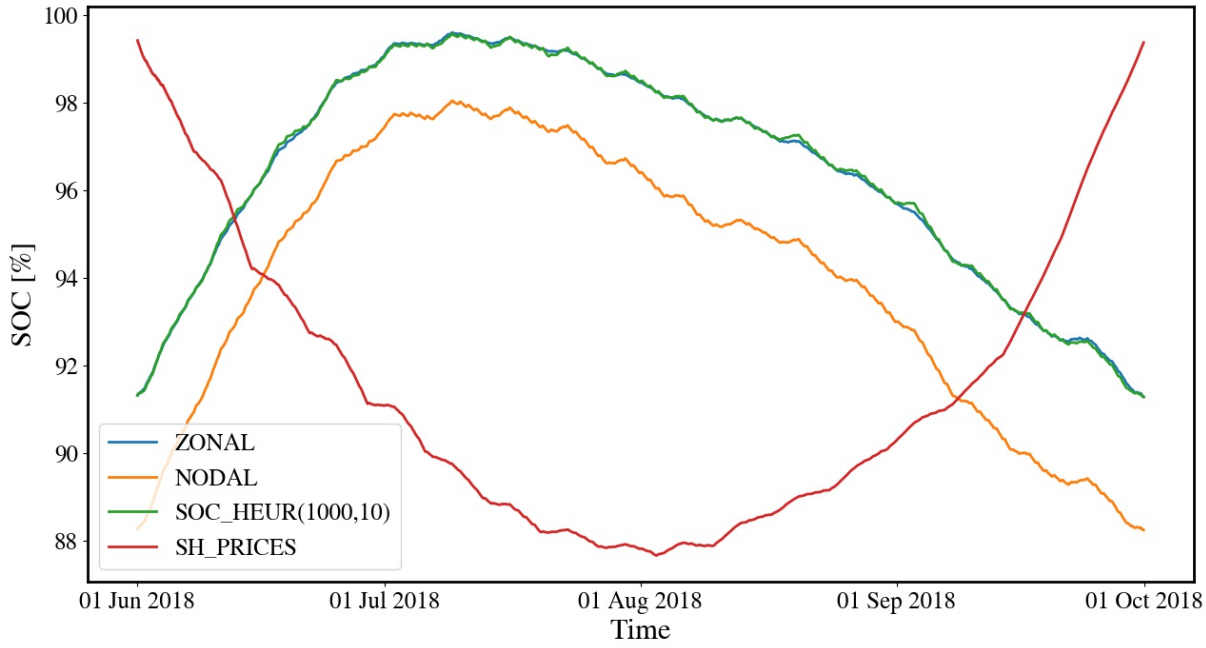

Figure 5.9: Aggregated SOC profiles in % for the short-time horizon benchmark with transmission capacity factor $\beta = 0.5$. Zonal input profile from Stage 1 (blue), full nodal benchmark case $NODAL$ (orange), and penalty factor combination $SOC\_HEUR(1000, 10)$ (green) and SH_PRICES (red).

5.3.4.2 Benchmarks with Long-Time Horizon

In this section, the results from the long-time horizon benchmark of one year are presented and discussed. In this case, the optimal SOC profile for the nodal model is unknown, which is the underlying problem addressed in this study and prevents, in the long-time horizon benchmark, from comparing to the optimal results. Therefore, as a reference case, the outcomes are compared against a zonal benchmark $ZONAL$, which provides the input SOC profiles from Stage 1 of the methodology. In Table 5.5, results for the long-time horizon benchmark with transmission capacity factor $\beta = 0.7$ are shown.

With respect to the overall system costs, the best performing SOC profiles are obtained with the proposed methodology, concretely, $SOC\_HEUR(1000, 1000)$, $SOC\_HEUR(1000, 10)$, $SOC\_HEUR(10, 1000)$, and $SOC\_HEUR(0, 1000)$. This is consistent with the short-time horizon benchmark. The costs for all $BIDS$ price parameters as well as the SH_PRICES approach are significantly higher than those of the best-performing penalty factor combinations. This is because they lack the seasonality information of hydro inflows. However, the costs are lower than in the case of providing no guidance to the optimization at all (penalty factors $SOC\_HEUR(0, 0)$). The three combinations with the lowest costs also show the lowest system congestion. The amount of load shed makes up

Table 5.5: Results overview for the long-time horizon benchmark with transmission capacity factor $\beta = 0.7$. Reported are for the different methods: the total system costs, which are made up of operational costs (i.e., power generation costs) and load shedding costs, the difference between $ZONAL$ and the respective method in absolute amount and relative to the total system costs of $ZONAL$; the average system congestion ($\overline{sc}$); the total amount of load shed and the share of this amount with respect to the total load; and the run times.

	Costs					Congestion	Load Shedding		Run Time
Method	**System [B EUR]**	**Operational [B EUR]**	**Load Shedding [B EUR]**	**Difference System-ZONAL [B EUR]**	**Difference System-ZONAL wrt ZONAL [%]**	$\overline{sc}$	**Amount [GWh]**	**Share of Tot Demand [%]**	**Run Time [h]**
ZONAL	64.74	64.74	0.00	0.00	0.0	7.0	0	0.000	2.1
SH_PRICES	216.65	68.47	148.17	151.91	234.6	957.0	14817	0.458	3.8
BIDS(20)	242.92	68.37	174.56	178.19	275.2	985.9	17456	0.539	4.1
BIDS(40)	230.50	68.75	161.74	165.76	256.0	977.6	16174	0.500	3.8
BIDS(60)	224.95	68.51	156.44	160.21	247.5	977.4	15644	0.483	4.2
SOC_HEUR(1000,1000)	68.46	66.87	1.59	3.72	5.8	664.5	159	0.005	22.9
SOC_HEUR(1000,10)	68.42	66.84	1.59	3.69	5.7	663.8	159	0.005	13.0
SOC_HEUR(1000,0)	72.98	67.35	5.63	8.24	12.7	696.0	563	0.017	34.1
SOC_HEUR(10,1000)	68.45	66.86	1.59	3.71	5.7	664.2	159	0.005	25.7
SOC_HEUR(10,10)	180.44	67.45	112.99	115.70	178.7	901.2	11299	0.349	7.7
SOC_HEUR(10,0)	220.17	67.94	152.23	155.43	240.1	973.9	15223	0.470	7.2
SOC_HEUR(0,1000)	68.45	66.86	1.59	3.71	5.7	664.2	159	0.005	24.5
SOC_HEUR(0,0)	279.17	68.96	210.22	214.43	331.2	1097.2	21022	0.650	5.8

0.005% of the annual system load for the penalty factor combinations with the lowest costs and the lowest levels of congestion. It can be seen that it is significantly higher for the bid price method, while highest for the case of no guidance $SOC\_HEUR(0,0)$. Therefore, the higher costs can be attributed to the amount of costly load shedding. This is confirmed when looking at the share of load shedding costs in the overall costs, which is as high as 75.3% for the case of myopic foresight $SOC\_HEUR(0,0)$. Run times are notably higher for the best-performing penalty factor combinations, indicating that lower costs come at a computational price.

Table 5.6: Results overview for the long-time horizon benchmark with transmission capacity factor $\beta = 0.5$. Reported are for the different methods: the total system costs, which are made up of operational costs (i.e., power generation costs) and load shedding costs, the difference between $ZONAL$ and the respective method in absolute amount and relative to the total system costs of $ZONAL$; the average system congestion ($\overline{sc}$); the total amount of load shed and the share of this amount with respect to the total load; and the run times.

	Costs					**Congestion**	**Load Shedding**		**Run Time**
Method	**System [B EUR]**	**Operational [B EUR]**	**Load Shedding [B EUR]**	**Difference System-ZONAL [B EUR]**	**Difference System-ZONAL wrt ZONAL [%]**	$\overline{sc}$	**Amount [GWh]**	**Share of Tot Demand [%]**	**Run Time [h]**
ZONAL	64.74	64.74	0.00	0.00	0	7.0	0	0.000	2.1
SH_PRICES	263.78	71.46	192.32	199.04	307.4	1122.0	19232	0.594	6.5
BIDS(20)	265.82	71.51	194.32	201.08	310.6	1133.9	19432	0.600	6.6
BIDS(40)	263.72	71.45	192.27	198.98	307.4	1121.8	19227	0.594	5.6
BIDS(60)	260.11	71.48	188.63	195.37	301.8	1119.6	18863	0.583	5.4
SOC_HEUR(1000,1000)	101.73	69.85	31.89	37.00	57.1	850.6	3189	0.099	34.8
SOC_HEUR(1000,10)	102.01	69.56	32.45	37.27	57.6	847.2	3245	0.100	17.3
SOC_HEUR(1000,0)	113.47	70.06	43.41	48.73	75.3	880.2	4341	0.134	38.3
SOC_HEUR(10,1000)	101.90	69.76	32.14	37.16	57.4	847.6	3214	0.099	36.8
SOC_HEUR(10,10)	198.37	70.06	128.31	133.63	206.4	1034.2	12831	0.396	27.8
SOC_HEUR(10,0)	273.22	70.88	202.33	208.48	322.0	1159.4	20233	0.625	10.3
SOC_HEUR(0,1000)	101.89	69.75	32.14	37.15	57.4	847.5	3214	0.099	38.1
SOC_HEUR(0,0)	335.01	71.52	263.49	270.28	417.5	1254.4	26349	0.814	6.1

To test the performance of the proposed methodology to obtain SOC profiles, it is applied to a scenario of higher congestion by reducing the available transmission capacity to 50%. An overview of the performance measures is provided in Table 5.6.

The costs in this scenario are higher as the system is more constrained. The methodologies with the lowest costs are $SOC\_HEUR(1000, 1000)$, $SOC\_HEUR(1000, 10)$, $SOC\_HEUR(10, 1000)$, and $SOC\_HEUR(0, 1000)$. The average system congestion has increased with respect to the $\beta = 0.7$ benchmark. The lowest system congestion does not correspond to the penalty factors with the lowest costs. The lowest system

congestion is reached with $SOC\_HEUR(1000, 10)$, while also $SOC\_HEUR(10, 1000)$ and $SOC\_HEUR(0, 1000)$ lead to slightly lower average system congestions than the case with the lowest costs $SOC\_HEUR(1000, 1000)$. This suggests that more freedom to adjust the SOC levels within a zone through choosing the second penalty factor to be lower can mitigate line overloading. Low system costs correlate again well with lower levels of load shedding. In this more congested benchmark case, the costs of load shedding become increasingly dominant, as they make up 78.7% of the costs in the myopic case ($SOC\_HEUR(0, 0)$). Run times are higher in almost all cases in comparison to the $\beta = 0.7$ scenario, reflecting the more constrained system. The methods relying on shadow prices and constant bid prices for hydro perform very similarly throughout the entire set of performance indicators. They only outperform the two worst penalty combinations, with low penalties $SOC\_HEUR(0, 0)$ and $SOC\_HEUR(10, 0)$.

It is especially interesting to investigate why the penalty combination with the highest factors $SOC\_HEUR(1000, 1000)$ is performing well throughout the scenario with the lower transmission capacity factor, on the one hand; and on the other hand, why more freedom to deviate from the $ZONAL$ input profile within a zone does not lead to fewer line overloadings, load shedding, and costs. Therefore, the evolution of costs differences in the $\beta = 0.5$ scenario between the $SOC\_HEUR(1000, 1000)$ and the $SOC\_HEUR(1000, 0)$ is investigated and displayed in Figures 5.10 and 5.11.

When regarding the costs to generate power (Figure 5.10), from January to April, the costs for $SOC\_HEUR(1000, 0)$ are lower than in the case of $SOC\_HEUR(1000, 1000)$. Throughout the following months, the costs fluctuate rather evenly, before the costs increase in the last two months. This can be explained by the fact that minimum targets are enforced for the end of the simulation horizon. Small gains in cost reduction at the beginning of the year are lost at the end of the year when the optimization in $SOC\_HEUR(1000, 0)$ needs to fulfill the annual water balance and the generation costs increase. When analyzing the difference in costs for load shedding (Figure 5.11), it can be concluded that these constraints also contribute to higher load shedding costs towards the end of the year.

In this context, it is also informative to examine the aggregated SOC profiles. In Figure 5.12, one can see the deviation of SOC profiles from the input profile obtained from Stage 1 ($ZONAL$). Concretely, the profiles for $SOC\_HEUR(1000, 1000)$ and

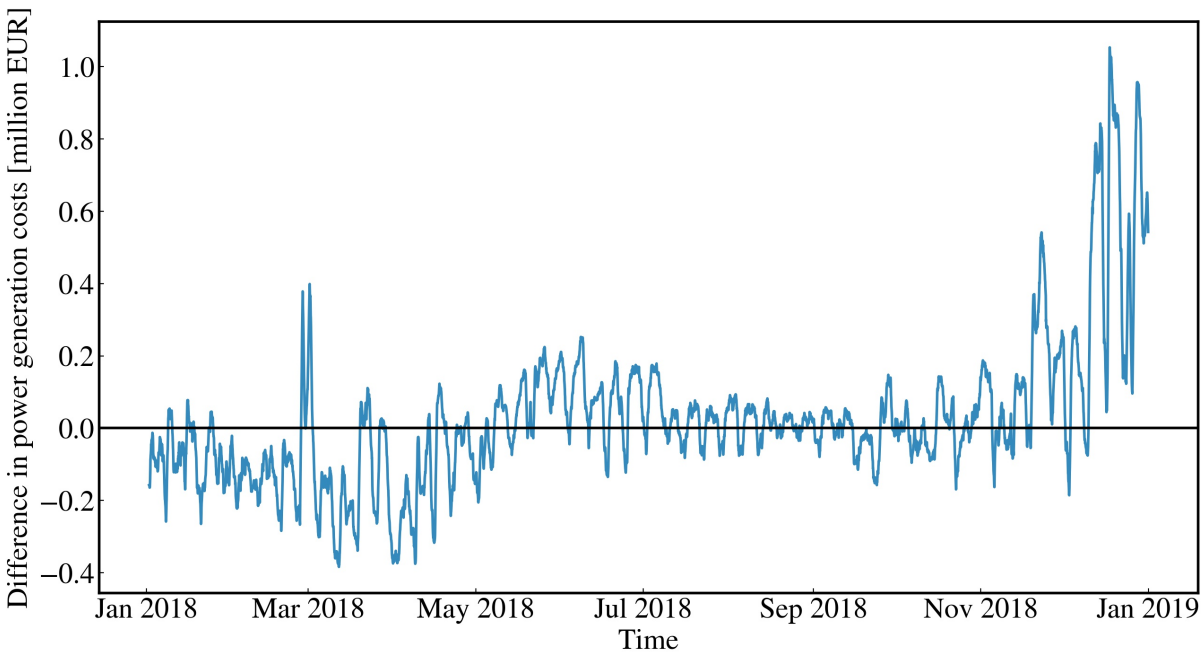

Figure 5.10: Difference in power generation costs between $SOC\_HEUR(1000, 0)$ and $SOC\_HEUR(1000, 1000)$. Displayed is the differences in power generation costs in million EUR. Displayed is the daily rolling average of the cost time series.

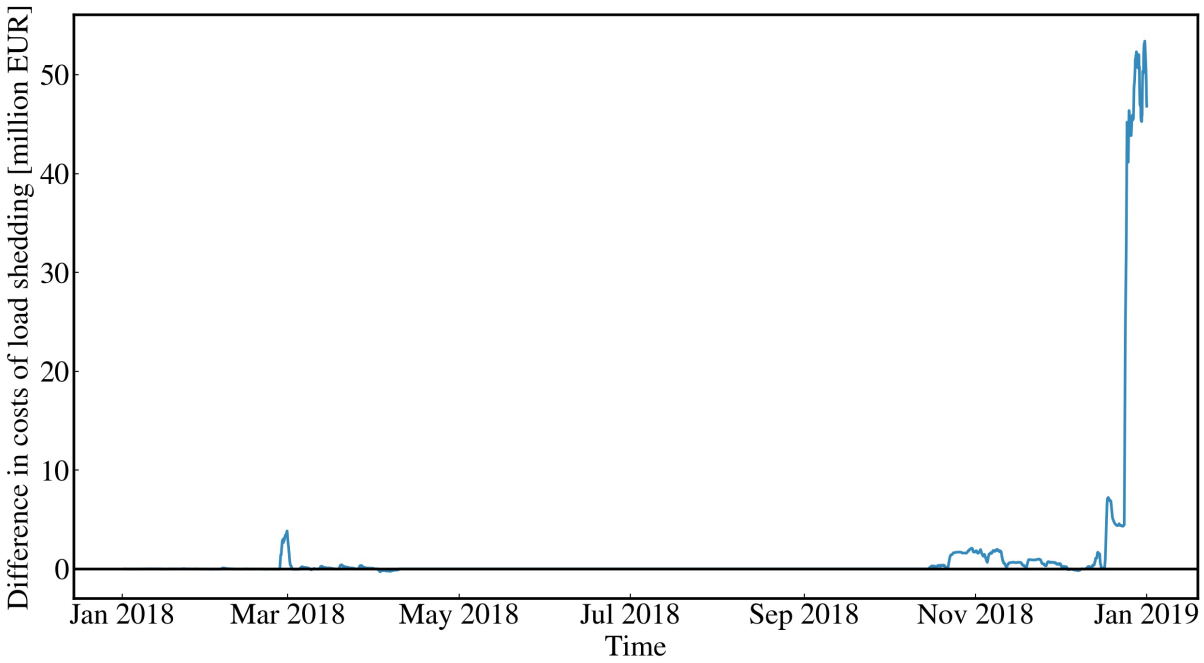

Figure 5.11: Difference in load shedding costs between $SOC\_HEUR(1000, 0)$ and $SOC\_HEUR(1000, 1000)$. Displayed is the difference in costs of load shedding in million EUR. Displayed is the daily rolling average of the cost time series.

$SOC\_HEUR(1000, 0)$ under the two scenarios of transmission capacity of $\beta = 0.7$ and $\beta = 0.5$ are compared. One can observe that, in general, higher penalty factors lead to smaller differences with respect to the input profile. Inspecting the SOC profiles of

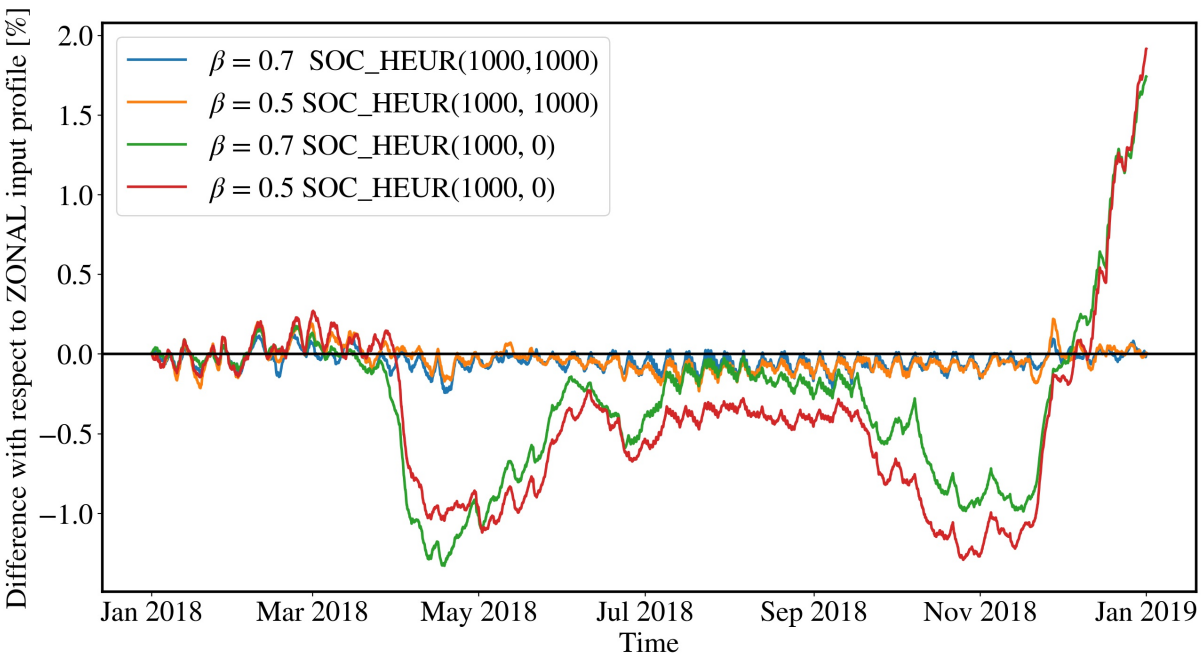

Figure 5.12: Aggregated SOC profile difference between the $ZONAL$ input profile of Stage 1 and $SOC\_HEUR(1000, 1000)$ and $SOC\_HEUR(1000, 0)$, respectively, in % with respect to the $ZONAL$ profile.

$SOC\_HEUR(1000, 1000)$, one can see that within a sequence (i.e., a week), the profiles can deviate; thus, the optimization has the freedom to adjust to line overloadings on a short timescale. This is because target values are only enforced through soft constraints at the end of each sequence. $SOC\_HEUR(1000, 0)$, on the other hand, may also deviate on a longer timescale from the target profiles because of the penalty factor for individual storage unit deviations $\alpha_s = 0$. For this case, the graph shows that under the higher congested case ($\beta = 0.5$), the profiles will deviate even more from the zonal input profile. Under more congestions, the optimization tries to reduce costs by deviating more from the input profile. Considering again in this context Figures 5.10 and 5.11, this leads to gains in the system costs. However, because of the final year targets, the SOC profiles ultimately need to align again, and this leads to higher costs, both in power generation and load shedding. Therefore, it is beneficial to follow the input profiles on a longer timescale and only deviate on a shorter timescale.

5.3.4.3 Redispatching Case Study

The best-performing method obtained from the heuristic for the $\beta = 0.7$ benchmark, i.e. $SOC\_HEUR(1000, 10)$ is used for a redispatching case study. The results are compared in

terms of generation by technology and system costs for the zonal model, the zonal model plus redispatching, broken down in positive and negative redispatching, and the full nodal model. Simulations are performed for one week, in which high levels of congestion are detected. The results are summed up in Tables 5.7 & 5.8.

Table 5.7: Results on system costs from the redispatching case study of one week for the nodal model, the zonal model and zonal + redispatching model (zonal+RD).

	System costs [bn EUR]		
Model	Total	Operational	Load shedding
Nodal	1.783	1.575	0.208
Zonal	1.512	1.512	0
Zonal+RD	1.829	1.617	0.213

Table 5.8: Results on generation by technology from the redispatching case study of one week for the nodal model, the zonal model and zonal + redispatching model (zonal+RD), for which generation is broken down in upward and downward redispatching with respect to the zonal model. Shown is generation by technologies in GWh for gas, coal and lignite, oil, nuclear, wind (on- and off-shore), solar, other RES (biomass, geothermal and run-of-river), hydro storage (hydro dams and PHS) and load shedding.

	Generation by technology [GWh]								
Model	Gas	Coal & lignite	Oil	Nuclear	Wind	Solar	Other RES	Hydro storage	Load shedding
Nodal	6682.6	20414.9	177.4	21460.1	11504.1	1774.2	3877.4	9556.9	20.8
Zonal	3835.6	22752.1	0.0	21911.8	11539.5	1774.3	4019.2	9635.8	0.0
Zonal+RD	6285.5	21198.1	416.9	21088.0	11337.7	1754.4	3846.8	9519.6	21.3
Upward RD	2449.9	16.6	416.9	0.0	0.0	0.0	0.0	25.7	21.3
Downward RD	0.0	-1570.6	0.0	-823.8	-201.8	-19.9	-172.4	-141.9	0.0

Considering the overall system costs in Table 5.7, the zonal model has the lowest costs, but if the redispatching is included the costs are higher than the ones of the nodal model. This trend is also seen when only considering the operational costs. The change in costs can be understood when considering the generation by technology (Table 5.8). One can observe that net positive redispatching occurs for gas and oil-fired generators, and also load shedding is increasing in the redispatching model. These are the technologies

with the highest marginal costs. Consequently, negative redispatching affects coal and lignite, nuclear, wind, solar, other RES, and hydro storages. In comparison to the full nodal model, renewable resources are dispatched less in the redispatching model, which is not favorable, as they are the cleaner and cheaper alternative to conventional generation technologies.

5.3.5 Conclusions

The main outcomes and contributions of the work presented in this section is summed up in the following points:

- A heuristic to obtain state of charge profiles for large-scale nodal and zonal models of the European electricity market is proposed.
- The method helps to overcome the following issues related to modeling hydro storage SOC: data availability, myopic foresight of a sequenced model, maintaining seasonality pattern of SOC profiles, and respecting intertemporal constraints.
- From the results on system costs, system congestion, and load shedding, it is found that the introduced methodology renders better results than a model with myopic foresight, and the methodology also outperforms the shadow price and bid price approaches when penalty factor combinations are chosen beneficially.
- The method gives freedom to the optimization to adjust profiles on a short timescale, even for high penalty factors.
- In general, it seems reasonable to choose high penalty factors, which perform well under different scenarios of transmission capacity availability.
- A case study on redispatching is performed that demonstrates the applicability of the proposed heuristic framework.
- Results of the numerical experiments show that the nodal model renders lower overall system costs than the zonal model, which includes redispatching.
- More expensive generators are affected by upward redispatching, and predominantly renewable technologies are affected by downward redispatching. In comparison to the full nodal model, overall less renewable generators are dispatched.

Given that the need to develop the proposed method in the first place arose from a lack of data, in general, it would be ideal to pursue an open data policy that would allow for sound energy system modeling.

Improving the method in future work can be achieved by exploring dynamic penalty factors. Through this, more long-term deviations from the initial profiles of Stage 1 could be allowed in times of line overloadings, while in times of few congestions, following the zonal profiles more closely could be enforced. This would require predictions of congestions and would allow the methodology to behave in a more proactive way. Another indication for future research regards the application of the proposed methodology to perform comparative studies for nodal vs. zonal pricing through solving large-scale optimization problems. Therefore, also further research should be put into analyzing the outcomes from the redispatching model.

Chapter 6

Summary & Conclusions

6.1 Summary & Contributions

This section summarizes the main findings and contributions of the conducted studies presented in Section 5. The outcomes will be contextualized with the initially formulated research questions in Section 2. Therefore, the following focuses on how the different modeling aspects of a nodal model were investigated within the studies performed in the context of this Ph.D.

Technical aspects: power flow model and network representation

In Section 5.1, the technical modeling aspect of the formulation of the optimal power flow problem has been examined. Further, a study was presented that investigates the role of network aggregation. The DC-OPF and AC-OPF formulation of the power flow problem have been compared in the context of obtaining nodal prices under different scenarios that stress the system. It was found that DC-OPF renders relatively accurate estimates of nodal prices when the optimization is able to identify congestions in the system. However, under scenarios of increased stress, when reactive power flows become more dominant, there is merit in utilizing AC-OPF to determine nodal prices. Further, the impact of the formulation of the optimization problem on run times was analyzed by solving several test cases with increasing numbers of nodes in their networks. It was found that run times for networks with less than 1,000 nodes were comparable for DC-OPF and AC-OPF . As the number of nodes increased, the computational times for AC-OPF increased significantly. This can be attributed to the formulation as a quadratically

constrained non-convex optimization problem. Run times were also compared for unit commitment DC-OPF, which already exhibited longer computational times for a few 10s of nodes in the network. Furthermore, as node numbers increased, the run times increased significantly more than for the two other OPF formulations. Various research has already been conducted on different approximations of reactive power flows that improve the DC formulation without adding all the additional computational difficulty to the problem, and this can be an interesting path to explore further. However, for large-scale electricity market models, DC-OPF is the preferred approach given its transparency, computational efficiency, and reasonable accuracy.

For comparative studies between nodal and zonal systems, the comparability of networks is essential. To perform such analyses, networks need to be spatially aggregated. On a 118-node test case, the impact of network aggregation was tested concerning the effects on identified congestions and locational marginal prices. In a higher-resolution network, congestions can be identified, and LMPs reflect these congestions, which is the case for nodal pricing in general. The discrepancy between the aggregated and the full network points toward the relevance of network representation in large-scale nodal models and their comparability to zonal models. The question of network representation and OPF formulation are interconnected as both will affect run times. Often, it is necessary to consider a trade-off between accuracy and computational tractability. Especially the aggregation of networks in comparative studies of zonal and nodal models is a topic that should be investigated further in future research.

Economic aspect: demand elasticity

The study presented in Section 5.2 addresses an economic aspect of modeling electricity markets, i.e. demand elasticity. A two-step modeling approach is introduced. Firstly, demand function parameters are determined from equilibrium prices of a cost minimization problem. These are then implemented through a step-wise function in the second step of the modeling process, where a welfare maximization problem is solved. Included in the formulation of the economic dispatch problem are the provision of reserves and unit commitment through binary variables, which render the optimization problem a MILP. For the first time, a pan-European study was performed that includes demand elasticity consideration in the investigation of future scenarios of the European electricity system.

A study conducted on the future Italian system under different zonal constellations demonstrates the impact of demand elasticity on prices and welfare. More bidding zones and thus more transmission constraints lead to higher overall costs. However, considering demand to be elastic contributes to lowering these additional costs. Under a scenario of high demand elasticity, the costs from additional transmission capacity constraints can be fully compensated by elastic demand. This indicates that modeling the demand elasticity in models that consider the full physical transmission network is an essential task, especially given the increasing interest in demand response technologies and the potential it is expected to have in the future. An aspect that has not been explored is the costs associated with demand elasticity, which should be included in future studies.

Technical aspect: intertemporal dependencies and hydro modeling

In Section 5.3, a novel heuristic algorithm is introduced to determine hydro SOC profiles for large-scale nodal models. Simulating large-scale nodal models with a high spatial and temporal resolution over horizons of one year is computationally expensive. Performing such computations in a reasonable amount of time and using fewer computational resources calls for parallelization or sequentialization of the problem. Due to the lack of data, the seasonality of hydro inflows to storage reservoirs, and the intertemporal nature of hydro storage constraints, it is necessary to pre-determine hydro profiles that render a cost-optimal solution to the large-scale problem. Thus, a stage-wise methodology to accurately model these technical and economic aspects of hydro storages was proposed and tested on different case studies. A heuristic approach allows adjusting SOC profiles obtained from a first stage optimization of a spatially aggregated zonal model. The adjustment occurs in a second stage, where the zonal SOC profiles are used as guidance for a sequential nodal model. By using soft-constraints, deviations from the input profile are penalized with different weights, allowing freedom to adjust the input profile to the more constrained reality of the nodal model. The proposed methodology is tested using different input parameters against other methods applied in the literature on four benchmarks of different time horizons and levels of congestion. It is found that the introduced methodology outperforms the case of myopic foresight and approaches presented in the literature. Under scenarios of increased congestions in the network, it can be beneficial to explore the usage of dynamic parameters that allow adjusting to time-varying constraints and congestion.

Especially the discrepancy between the obtained results and the sequenced model with myopic foresight underlines the relevance of accurately modeling the seasonality and intertemporal dependence of hydro storages.

To demonstrate the applicability of the proposed heuristic, the obtained SOC profiles are used to perform a case study on redispatching to compare nodal against zonal plus redispatching. It is found that the system costs of the nodal model are lower than those of the zonal model, which includes redispatching. This is because more expensive generators are affected by upward redispatching, and predominantly renewable technologies are affected by downward redispatching. Compared to the full nodal model, overall, fewer renewable generators are dispatched. This study shows that the heuristic enables conducting comparative studies between zonal and nodal models. Further research should examine the employed redispatching methodology more carefully and also explore solely price-based redispatching or market-based redispatching to estimate the costs associated with redispatching more accurately.

6.2 Conclusions & Outlook

This work has explored various modeling aspects relevant to assessing nodal pricing in large-scale European electricity market models. Concretely, technical aspects of optimization problem formulation as DC-OPF, AC-OPF , and unit commitment have been explored. Further, network capacity representation and intertemporal constraints of unit commitment and hydro storages have been assessed. As to the economic aspects, the role of demand elasticity in compensating costs of increased network resolution has been considered, as well as the welfare effects of myopic foresight in hydro storage modeling.

Further, a redispatching step was implemented as part of a zonal model that allows for a sound comparison between nodal and zonal pricing. This proved the applicability of the developed methodology to estimate hydro SOC profiles and showed the path to finalize the model. It should be further explored how to implement and conduct redispatching modeling by comparing different approaches in the literature. In the effort to combine the lessons learned from this Ph.D. thesis, a joint model that combines especially the elements of demand elasticity with sound hydro modeling and redispatching should be developed.

There are various modeling choices one has to make when designing electricity market

models, and thus this work is by no means exhaustive in assessing all of them. Future work could focus on environmental aspects by including the costs of externalities or greenhouse gas emission reduction targets into the objective. This will surely become more relevant given the transformation of the power sector that lays ahead of us. In this context, the distribution of welfare is also an interesting topic to consider, as a switch from zonal to nodal pricing would entail distributional effects that need to be accounted for when assessing the benefits and drawbacks of a switch in pricing schemes.

Building up on the work already conducted, it will be interesting to explore nodal against zonal pricing in a pan-European context through exploring future scenarios of the evolution of the power system. While various country-specific studies have already been conducted, a broader perspective on the costs and benefits of nodal pricing is needed and should be explored in future applications of the developed model.

Appendix A

Theory, Literature & Code

A.1 Theoretical Background

This section will give an overview of relevant concepts from optimization, power flow and economics that are essential to understand electricity markets.

A.1.1 Lagrangian Duality and the Karush-Kuhn-Tucker Conditions

Consider this optimization problem in standard form[1]:

$$\begin{aligned} \underset{x}{\text{minimize}} \quad & f_0(x) \\ \text{subject to} \quad & f_i(x) \leq 0, \qquad i = 1, \ldots, m \\ & h_i(x) = 0, \qquad i = 1, \ldots, p, \end{aligned} \tag{A.1}$$

where $x \in \mathbb{R}^{\mathrm{n}}$ is the variable, domain $\mathcal{D} = \bigcap_{i=0}^{m} \mathbf{dom}\ f_i \ \cap \ \bigcap_{i=1}^{p} \mathbf{dom}\ h_i$, which is nonempty and the optimal value p^*. The problem does not need to be assumed to be convex. For this problem, one can formulate the Lagrangian $L : \mathbb{R}^{\mathrm{n}} \times \mathbb{R}^{\mathrm{m}} \times \mathbb{R}^{\mathrm{p}} \to \mathbb{R}$, which can be interpreted as the weighted sum of the objective function and the constraints:

$$L(x, \nu, \lambda) = f_0(x) + \sum_{i=1}^{m} \nu_i f_i(x) + \sum_{i=1}^{p} \lambda_i h_i(x), \tag{A.2}$$

[1]Much of this subsection drawn from Boyd and Vandenberghe (2004) and Buzna (2019).

with **dom** $L = \mathcal{D} \times \mathbb{R}^{\mathrm{m}} \times \mathbb{R}^{\mathrm{p}}$. ν_i and λ_i are the Lagrangian multipliers or dual variables associated with the constraints $f_i(x)$ and $h_i(x)$ respectively. One can then write the Lagrange dual function $g : \mathbb{R}^{\mathrm{m}} \times \mathbb{R}^{\mathrm{p}} \to \mathbb{R}$ as:

$$g(\nu, \lambda) = \inf_{x \in D} L(x, \nu, \lambda) \tag{A.3}$$

$$= \inf_{x \in D} \left(f_0(x) + \sum_{i=1}^{m} \nu_i f_i(x) + \sum_{i=1}^{p} \lambda_i h_i(x) \right). \tag{A.4}$$

L is affine in (ν, λ) and g is the infimum of an affine functions, thus g is concave, even if (A.1) was not convex. The dual function takes the value $-\infty$, if the Lagrangian is unbounded below in x.

If $\nu \succeq 0$ [2] then the dual function represents a lower bound to the optimization problem $g(\nu, \lambda) \leq p^*$. Thus one can formulate the so-called dual problem:

$$\underset{\nu,\lambda}{\text{maximize}} \quad g(\nu, \lambda) \tag{A.5}$$

$$\text{subject to} \quad \nu \succeq 0. \tag{A.6}$$

It will yield the optimal value d^*, which is the best lower bound on p^*. Thus, $d^* \leq p^*$ holds, even for non-convex optimization problems (A.1), and is referred to as weak duality. For convex problems usually strong duality holds and the optimal duality gap is zero, i.e. $d^* = p^*$, where the optimal value of the dual function delivers the optimal value of the original problem. There are a number of constraint qualifications, which are conditions under which strong duality holds. A sufficient condition is Slater's constraint qualification, which states that if the problem (A.1) is convex and there exists an x so that all (affine) equality constraints are respected and all non-linear inequality constraints hold strictly, i.e. $f_i(x) < 0$, then strong duality holds.

[2] $\succeq$ represents a vector inequality.

If strong duality holds and x^* is primal and ν^* and λ^* are dual optimal respectively, then:

$$\begin{aligned} f_0(x^*) &= g(\nu^*, \lambda^*) \\ &= \inf_{x \in D} \left(f_0(x) + \sum_{i=1}^{m} \nu_i^* f_i(x) + \sum_{i=1}^{p} \lambda_i^* h_i(x) \right) \\ &\leq f_0(x^*) + \sum_{i=1}^{m} \nu_i^* f_i(x^*) + \sum_{i=1}^{p} \lambda_i^* h_i(x^*) \\ &\leq f_0(x^*). \end{aligned} \tag{A.7}$$

These two inequalities hold with equality. Therefore, it follows that x^* minimizes $L(x, \nu^*, \lambda^*)$. Further, $\sum_{i=1}^{m} \nu_i^* f_i(x^*) = 0$ and since all terms in this sum are non positive it follows that $\nu^* f_i(x^*) = 0, i = 1, \ldots, m$. This is referred to as complementary slackness and often formulated in the following two equivalent ways:

$$\nu_i^* > 0 \implies f_i(x^*) = 0, \qquad f_i(x^*) < 0 \implies \nu_i^* = 0. \tag{A.8}$$

If there are x^*, ν^* and λ^*, which are any primal and dual optimal points and strong duality holds then x^*, ν^* and λ^* satisfy the Karush-Kuhn-Tucker (KKT) conditions. The KKT conditions for a problem (A.1) with differentiable f_i and h_i are:

1. for primal constraints: $f_i(x^*) \leq 0, i = 1, \ldots, m, \quad h_i(x^*) = 0, i = 1, \ldots, p,$
2. for dual constraints: $\nu^* \succeq 0,$
3. complementary slackness: $\nu_i f_i(x^*) = 0, i = 1, \ldots, m,$
4. the gradient of the Lagrangian with respect to x^* vanishes: $\nabla f_0(x^*) + \sum_{i=1}^{m} \nu_i^* \nabla f_i(x^*) + \sum_{i=1}^{p} \lambda_i^* \nabla h_i(x^*) = 0.$

For a convex optimization problem that satisfies Slater's condition and has differentiable f_0, f_i and h_i, the KKT conditions are necessary and sufficient criteria for optimality.
When strong duality holds, dual variable yield important information, which can be

understood through considering the perturbed optimization problem:

$$\begin{aligned} \underset{x}{\text{minimize}} \quad & f_0(x) \\ \text{subject to} \quad & f_i(x) \leq u_i, \qquad i = 1, \ldots, m \\ & h_i(x) = v_i, \qquad i = 1, \ldots, p, \end{aligned} \tag{A.9}$$

where x is the primal variable, u and v are parameters and $f_0^*(u, v)$ is the optimal value. The perturbed problem is similar to (A.1) where the inequality constraints have been tightened or loosened by u_i and an additional term v_i is introduced in the equality constraints. The dual variables ν_i and λ_i can be interpreted as the sentsitivities of the objective function value to small changes in the parameters given that f^* is differentiable at $u = 0$ and $v = 0$:

$$\nu_i^* = \frac{\partial f_0^*}{\partial u_i}\bigg|_{u=0,v=0}, \qquad \lambda_i^* = \frac{\partial f_0^*}{\partial v_i}\bigg|_{u=0,v=0}. \tag{A.10}$$

This means when a constraint is modified by an infinitesimal amount, the respective dual variable reflects the rate at which the objective function value changes.

A.1.2 Basic Formulation of the Power Flow Problem

In power flow analysis the electricity grid is considered as a network of nodes or buses connected through lines or edges[3]. With each node i a number of variables are associated: voltage amplitude v_i, voltage angle θ_i, net active power P_i and net reactive power Q_i. There are different node types defined according to the variables known at that particular node: PQ nodes, P_i and Q_i are known and v_i and θ_i need to be calculated; and PV nodes, where P_i and v_i are known and Q_i and θ_i need to be determined. The former ones are usually associated with loads without voltage control, while the latter represent generating nodes that do have a voltage control. Additionally, there are so-called slack nodes or reference nodes $V\theta$, where v_i and θ_i are known and P_i and Q_i need to be calculated. As the name suggests a reference node serves as a point of reference for the voltage angle, for this variable is determined with respect to a reference angle. Furthermore, $V\theta$ nodes are needed to balance generation, loads and losses, due to the initially unknown active power

[3]Much of this Chapter is drawn from Andersson (2012).

losses.

The equations describing the network flow can be derived from Kirchhoff's Law. Kirchhoff's current law states specifically that the current injected into one node i needs to flow out again into the adjacent nodes $k \in N(i)$:

$$I_i = \sum_{k \in N(i)} I_{ik}, \tag{A.11}$$

where I_i is the current injected or extracted at node i and I_{ik} is the current flowing from node i to the adjacent node j. Applying Ohm's law, which describes the relation between current, voltage and admittance (the inverse of the impedance), yields:

$$I_i = \sum_{k \in N(i)} Y_{ik} V_k, \tag{A.12}$$

where Y_{ik} is the corresponding element of the admittance matrix and V_j the voltage at node j. The admittance matrix elements are comprised of the conductance G_{ik} and the susceptance B_{ik}, which are a property of the line or edge connecting node i with node k:

$$Y_{ik} = G_{ik} + jB_{ik}, \tag{A.13}$$

where j is the imaginary unit. According to Euler's formula one can express an alternating sinusoidal voltage in polar form:

$$V_i = v_i(cos\theta_i + jsin\theta_i) = v_i e^{j\theta_i}, \tag{A.14}$$

where v_i is the voltage amplitude and θ_i is the voltage angle. Using this relation and (A.13), we can write (A.12) as:

$$I_i = \sum_{k \in N(i)} \left(G_{ik} + jB_{ik}\right) v_k e^{j\theta_k}. \tag{A.15}$$

Further, we utilize the relationship between current and voltage and complex power at node i:

$$S_i = P_i + jQ_i = V_i I^*, \tag{A.16}$$

where S_i is the complex or apparent power, P_i is the real or active power, Q_i is the reactive power, V_i is the complex voltage and I^* is the complex conjugate of the complex current. Plugging in (A.15) and using (A.14), (A.16) becomes:

$$S_i = P_i + jQ_i = v_i e^{j\theta_i} \sum_{k \in N(i)} (G_{ik} - jB_{ik})\, v_k e^{-j\theta_k}. \tag{A.17}$$

Now, one can identify the real and the imaginary parts, using Euler's Equation (A.14) in order to obtain the equations for the active and reactive power injected at node i:

$$P_i = v_i \sum_{k \in N(i)} v_k (G_{ik} cos(\theta_i - \theta_k) + B_{ik} sin(\theta_i - \theta_k)), \tag{A.18}$$

$$Q_i = v_i \sum_{k \in N(i)} v_k (G_{ik} sin(\theta_i - \theta_k) - B_{ik} cos(\theta_i - \theta_k)). \tag{A.19}$$

These nodal power equations describe the main power flow problem, which is represented by a set of nonlinear equations. Depending on the node type either P_i and Q_i or P_i and v_i are known and the other variables need to be determined. This problem is usually formulated as a root problem and solved using for example Newton-Raphson method.

A.1.3 Economic concepts

A market is in general a place where buyers and sellers meet to exchange goods [4]. A particularity of electricity markets in comparison to markets of other commodities lies in the non-storability of electricity. Though there are increasingly storage technologies under development, there is no large-scale solution that would allow to trade electricity similarly to easily storable commodities. Resulting from this electricity generation and consumption need to be in almost perfect balance at all time. Firstly, the economic consideration of suppliers and consumers of electricity will be introduced.

A.1.3.1 Fundamentals of Markets: Demand, Supply and Welfare

It has been a custom for entities supplying electricity to consumers to supply load forecasts to system operators, which would result in a single defined demand quantity. In electricity

[4] This Chapter largely draws from Kirschen and Strbac (2019) and Ranci and Cervigni (2013).

markets however, consumers or energy supplying utilities submit demand bids to the market (Kirschen, 2003). A demand bid i is defined by a price p_i and a demand quantity q_i. This leads to a step-wise demand function comprised of all the bids I_d:

$$d(p) = \sum_{i \in I_d} d_i(p), \tag{A.20}$$

where

$$d_i(p) = \begin{cases} q_i, & \text{if } p \leq p_i \\ 0, & \text{otherwise.} \end{cases} \tag{A.21}$$

In case of a large number of bids, (A.20) becomes a continuous function. Though, a more commonly used version is the (inverse) linear demand function $p_d(q)$[5], which is displayed in Figure A.1:

$$p_d(q) = bq + a, \tag{A.22}$$

where b is the demand slope and a is the demand intercept. Displayed by a demand function is a consumer's willingness to pay for a certain quantity of electricity.

The concept of demand elasticity refers to the sensitivity of consumers to changes in electricity prices and a consequential change in demand. Demand elasticity is usually denoted with ϵ and defined as the infinitesimal relative change in demand to the infinitesimal relative change in electricity price

$$\epsilon = \frac{\frac{\delta q}{q}}{\frac{\delta p}{p}} = \frac{\delta q}{\delta p}\frac{p}{q}, \tag{A.23}$$

where q is the quantity of demand and p is electricity price. For a given reference price p_{ref} and demand quantity q_{ref} and a price demand elasticity ϵ, one can determine the demand slope according to

$$b = \frac{\delta p}{\delta q} = \frac{p_{ref}}{q_{ref}\epsilon} \tag{A.24}$$

and the demand intercept according to

$$a = p_{ref} - \frac{p_{ref}}{\epsilon}. \tag{A.25}$$

[5]Even though inverse demand function would be the correct term, we will refer to the function $p_d(q)$ as simply demand function as it is common practice.

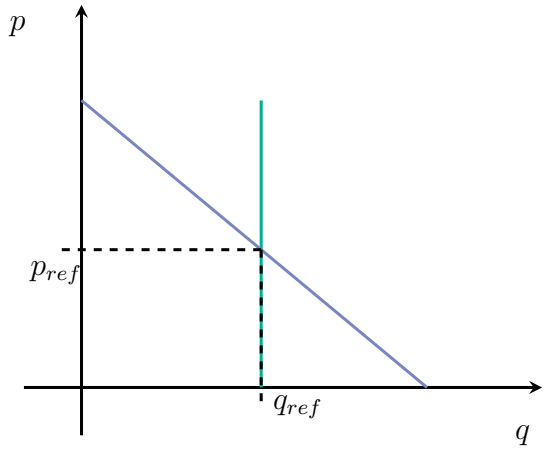

Figure A.1: Demand functions, in green inelastic and in blue elastic demand, determined around the reference equilibrium point with p_{ref} and q_{ref} and a given demand elasticity ϵ.

Similarly to the consumers, producers will make supply bids defined by a generated electricity quantity q_i and price p_i to a market to offer their electricity. They will do so in accordance with their costs to produce the next MWh of electricity. Again, the supply function can be displayed as a step-wise function consisting of all the generation bids I_g:

$$g(p) = \sum_{i \in I_g} g_i(p), \tag{A.26}$$

where

$$g_i(p) = \begin{cases} q_i, & \text{if } p \geq p_i \\ 0, & \text{otherwise.} \end{cases} \tag{A.27}$$

If the numbers of bids is large enough, (A.26) becomes a continuous fashion. In accordance with Equation (A.22) $p_g(q)$ is the inverse supply function. As a connected concept we introduce the cost function $c(g)$, which displays the costs to generate electricity, in its discrete form:

$$c(g) = \sum_{i \in I_g} g_i(p) \cdot p_i. \tag{A.28}$$

In a perfect competitive market all market participants are price takers and cannot affect the price by their individual actions. Under this assumptions the market clearing price or equilibrium price p^* is determined through the intercept of supply and demand function. This is where the quantity of electricity that consumers would like to purchase at that price is equal to the quantity that producers are willing to provide at that price,

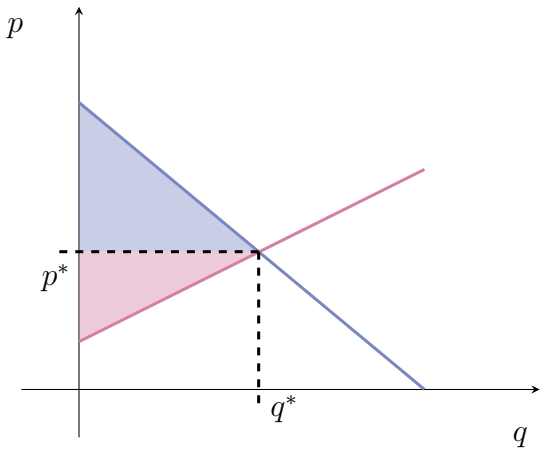

Figure A.2: Inverse supply and demand curve, displaying price as a function of quantity q. Indicated at p^* and q^* are equilibrium price and quantity. The shaded are is the total social welfare, consisting of consumer surplus (blue area) and producer surplus (red area).

which is the equilibrium quantity q^* thus:

$$g(p^*) = d(p^*) = q^*. \tag{A.29}$$

The equilibrium price constitutes the price at which *all* electricity is traded. From Figure A.2 one can see that the market clearing price is lower than the price some consumers are willing to pay. The area under the inverse demand curve, minus the costs to purchase the equilibrium quantity q^*, is defined as the consumer surplus. Correspondingly, producers, who receive a higher price than they would be willing to sell their electricity for, lead to the so-called producer surplus as also indicated in Figure A.2. The sum of consumer and producer surplus is referred to as social or economic welfare W and can be determined through:

$$W = \int_0^{q^*} p_d(q)\,\mathrm{d}q - \int_0^{q^*} p_g(q)\,\mathrm{d}q \tag{A.30}$$

We can identify the second integral of (A.30) to be the cost associated with generating the amount of electricity q^*. When designing electricity markets, the maximization of social welfare is often the objective.

A.2 Literature Review: Overview of Case Studies

Table A.1 summarizes several case studies presented in Section 4.

Table A.1: Case studies and applications of nodal and zonal models.

Reference	Geographic coverage	Purpose	Findings	Recommendations & Shortcomings
ENTSO-e. (2018)	Pan-European	Assessment of bidding zone configuration	Inconclusive with regard to bidding zone configuration	Lack of simulation tool to optimize market and topology measures (congestion management) simultaneously
Leuthold, et al. (2012)	Germany in European context	Integration of large-scale wind power and impact on congestion management when switching zonal to nodal	Savings in cost for congestion management in nodal system	Need for extension of grid representation
Bjørndal, et al. (2018)	Poland & 3 neighbors	Impact of Poland switching to nodal pricing (under large extension of wind capacity in Germany)	Poland benefits from less redispatching; Germany from maintaining relatively low uniform price	Impact of extension of nodal system; pan-European context
Breuer, et al. (2013)	Pan-European	Determine optimal bidding zone configuration	Inconclusive for bidding zone configuration	Improve accounting for redispatching and generation costs
Quelhas, et al. (2007)	USA	Global perspective of the energy system, include environmental aspects and investment planning	LMP support economic interdependencies between fuel networks and efficient investment in networks	Focus on electricity; many simplifications due to lack of data
Kunz et al. (2016)	Germany	Zonal vs. nodal pricing and allocation of financial transmission rights (FTR)	Nodal can increase surplus under their allocation methodology of allocating FTR	FTR for intermittent RES do not mitigate distributional effects, other schemes
Egerer, et al. (2016)	Germany	Split Germany into 2 (4) pricing zones; impact of wind in the North on pricing and distribution effects	Reduced need fro redispatching under 2 and 4 zones; redistribution effects significant	Impact of increased wind (& other RES) on exchanges esp. with Southern Europe
Felling, et al. (2019)	7 European countries	Assessment of improved bidding zone configurations using FBMC model and RD model	Welfare gain for switch in cluster through decreased costs for redispatching; unequal distribution of welfare gains	Extension to full nodal system; pan-European context
Bjørndal, et al. (2013)	Sweden (27 nodes), Norway (178), Denmark & Finland (1)	Effects of different congestion management methods on market outcomes under zonal and nodal pricing and different zonal configurations	NTCs that are too tight may lead to higher prices in zonal than nodal; prices in nodal slightly higher than average zonal; optimal zonal configuration is case dependent	Many assumptions nodal disaggregation and nodal bid curves; establish better datasets, include counter trading
Bjørndal, et al. (2014)	13 node Norway & Sweden (& Finland)	Hybrid zonal nodal system benchmarked against full nodal and full zonal	Hybrid works well unless cross-zonal capacities are bottlenecks then wrong incentives are sent and more congestions triggered	Simplified and aggregated network model; cross-border capacity definition
Grimm et al. (2018)	Germany	Employ multi-level equilibrium model to investigate impact of policy proposals on electricity markets	Split Germany into 2 zones, moderate welfare gains, while reducing need for network extensions	Extend their model to put into European context
Riegler (2017)	Germany (+AT), Belgium, France & Netherlands	ABM to assess IEM; how cross-border congestion management & capacity mechanism affect welfare	Trade-off between adequacy and welfare optimum as consequence of capacity mechanisms and network investments	Different price zone configurations and FBMC and other capacity mechanisms impact on market results and policy targets
Hu et al. (2018)	N/A	Literature review of market designs favoring increased RES in system	Barriers in the way of RES integration, 2 aspects to be tackled through e.g. reduction of integration costs and business case for RES	Model based CBA of suggested LMP market; capacity-based support schemes should be explored

A.3 Model Code

The code developed in the context of this Ph.D. will be made available on the author's github page `https://github.com/LucaLJ`.

Bibliography

Abdel-Karim, N. and Abdel-Ghaffar, H. Operational sensitivities of Northeastern US grid to wind power integration scenarios. *IEEE PES General Meeting, PES 2010*, pages 1–8, 2010. doi: 10.1109/PES.2010.5589306.

Agora Energiewende and Sandbag. The European Power Sector in 2017. State of Affairs and Review of Current Developments. 2018. URL `www.sandbag.org.uk{%}0Awww.agora-energiewende.de`.

Andersson, G. Power System Analysis: Power Flow Analysis, Fault Analysis, Power System Dynamics and Stability. Technical Report September, ETH Zürich, Zürich, 2012.

Antonopoulos, G., Vitiello, S., Fulli, G., and Masera, M. Nodal pricing in the European internal electricity market. Technical Report EUR 30155 EN, Publications Office of the European Union, Luxembourg, 2020.

Azad, A. S., Md, M. S., Watada, J., Vasant, P., and Vintaned, J. A. G. Optimization of the hydropower energy generation using Meta-Heuristic approaches: A review. *Energy Reports*, 6:2230–2248, 2020. ISSN 23524847. doi: 10.1016/j.egyr.2020.08.009. URL `https://doi.org/10.1016/j.egyr.2020.08.009`.

Azevedo, I. M., Morgan, M. G., and Lave, L. Residential and Regional Electricity Consumption in the U.S. and EU: How Much Will Higher Prices Reduce CO2 Emissions? *Electricity Journal*, 24(1):21–29, 2011. ISSN 10406190. doi: 10.1016/j.tej.2010.12.004.

Baghayipour, M. R. and Foroud, A. A. Modification of DC optimal power flow, based on nodal approximation of transmission losses. *Iranian Journal of Electrical and Electronic Engineering*, 8(1):76–90, 2012. ISSN 17352827.

Bakirtzis, A., Biskas, P., Ilias, M., and Ntomaris, A. DR Model for Adequacy Procedure: Final Report (D5). Technical report, Aristotle University of Thessaloniki, Thessaloniki, 2018.

Baslis, C. G., Papadakis, S. E., and Bakirtzis, A. G. Simulation of optimal medium-term hydro-thermal system operation by grid computing. *IEEE Transactions on Power Systems*, 24(3):1208–1217, 2009. ISSN 08858950. doi: 10.1109/TPWRS.2009.2023261.

Bernstein, R. and Madlener, R. Short- and long-run electricity demand elasticities at the subsectoral level: A cointegration analysis for German manufacturing industries. *Energy Economics*, 48:178–187, 2015. ISSN 01409883. doi: 10.1016/j.eneco.2014.12.019. URL `http://dx.doi.org/10.1016/j.eneco.2014.12.019`.

Bjørndal, E., Bjørndal, M., and Gribkovskaia, V. Congestion Management in the Nordic Power Market – Nodal Pricing versus Zonal Pricing. Technical report, Institute for Research in Economics and Business Administration, Bergen, 2013.

Bjørndal, E., Bjørndal, M., and Cai, H. Nodal pricing in a coupled electricity market. In *11th International Conference on the European Energy Market (EEM14)*, Cracow, may 2014. ISBN 9781479960958. doi: 10.1109/EEM.2014.6861222.

Bjørndal, E., Bjørndal, M., Cai, H., and Panos, E. Hybrid pricing in a coupled European power market with more wind power. *European Journal of Operational Research*, 264 (3):919–931, feb 2018. ISSN 03772217. doi: 10.1016/j.ejor.2017.06.048.

Blázquez, L., Boogen, N., and Filippini, M. Residential electricity demand in Spain: New empirical evidence using aggregate data. *Energy Economics*, 36:648–657, 2013. ISSN 01409883. doi: 10.1016/j.eneco.2012.11.010. URL `http://dx.doi.org/10.1016/j.eneco.2012.11.010`.

Bo, R. and Li, F. Comparison of LMP simulation using two DCOPF algorithms and the ACOPF algorithm. *3rd International Conference on Deregulation and Restructuring and Power Technologies, DRPT 2008*, (April):30–35, 2008. doi: 10.1109/DRPT.2008.4523375.

Borowski, P. F. Zonal and Nodal Models of Energy Market in European Union. *Energies*, 16(13), 2020. doi: 10.3390/en13164182.

Boyd, S. P. and Vandenberghe, L. *Convex optimization*. Cambridge University Press, 2004. ISBN 9780521833783.

Brancucci Martínez-Anido, C., L'Abbate, A., Migliavacca, G., Calisti, R., Soranno, M., Fulli, G., Alecu, C., and De Vries, L. J. Effects of North-African electricity import on the European and the Italian power systems: A techno-economic analysis. *Electric Power Systems Research*, 96:119–132, 2013a. ISSN 03787796. doi: 10.1016/j.epsr.2012.11.001. URL http://dx.doi.org/10.1016/j.epsr.2012.11.001.

Brancucci Martínez-Anido, C., Vandenbergh, M., de Vries, L., Alecu, C., Purvins, A., Fulli, G., and Huld, T. Medium-term demand for European cross-border electricity transmission capacity. *Energy Policy*, 61:207–222, 2013b. ISSN 03014215. doi: 10.1016/j.enpol.2013.05.073. URL http://dx.doi.org/10.1016/j.enpol.2013.05.073.

Braun, S. Hydropower Storage Optimization Considering Spot and Intraday Auction Market. *Energy Procedia*, 87:36–44, 2016. ISSN 18766102. doi: 10.1016/j.egypro.2015.12.355. URL http://dx.doi.org/10.1016/j.egypro.2015.12.355.

Brown, T., Hörsch, J., and Schlachtberger, D. PyPSA: Python for power system analysis. *Journal of Open Research Software*, 6(1), 2018. ISSN 20499647. doi: 10.5334/jors.188.

Buzna, L. Applications of Optimization in Machine Learning: Lecture Notes. Technical report, University of Zilina, Zilina, 2019.

Chychykina, I. *Comparison of Different Redispatch Optimization Strategies*. Phd thesis, Otto-von- Guericke-Universität Magdeburg, 2019.

Cialani, C. and Mortazavi, R. Household and industrial electricity demand in Europe. *Energy Policy*, 122(July):592–600, 2018. ISSN 03014215. doi: 10.1016/j.enpol.2018.07.060. URL https://doi.org/10.1016/j.enpol.2018.07.060.

Dietrich, K., Hennemeier, U., Hetzel, S., Jeske, T., Leuthold, F., Rumiantseva, I., Rummel, H., Sommer, S., Sternberg, C., and Vith, C. Nodal Pricing in the German Electricity Sector - A Welfare Economics Analysis, with Particular Reference to Implementing Offshore Wind Capacities. 2005.

Egerer, J., Weibezahn, J., and Hermann, H. Two price zones for the German electricity market — Market implications and distributional effects. *Energy Economics*, 59:365–381, 2016. ISSN 01409883. doi: 10.1016/j.eneco.2016.08.002. URL http://dx.doi.org/10.1016/j.eneco.2016.08.002.

EIA. Carbon Dioxide Emissions Coefficients, 2016. URL https://www.eia.gov/environment/emissions/co2{_}vol{_}mass.php.

ENTSO-E. Maps & Data: TYNDPs, 2018a. URL https://tyndp.entsoe.eu/maps-data/.

ENTSO-E. First Edition of the Bidding Zone Review: Final Report. Technical report, ENTSO-E, Brussels, 2018b.

ENTSO-E. TYNDP 2018: Data and expertise as key ingredients. Technical Report October, ENTSO-E, Brussels, 2019. URL https://tyndp.entsoe.eu/tyndp2018/tyndp2018.

ENTSO-E. ENTSO-E Grid Map, 2022. URL https://www.entsoe.eu/data/map/.

Eskeland, G. S. and Mideksa, T. K. Electricity demand in a changing climate. *Mitigation and Adaptation Strategies for Global Change*, 15(8):877–897, 2010. ISSN 13812386. doi: 10.1007/s11027-010-9246-x.

European Commission. CACM: Comission Regulation (EU) 2015/1222 establishing a guideline on capacity allocation and congestion management. Technical Report July, Brussels, 2015.

European Commission. Clean Energy For All Europeans COM/2016/0860 final. Technical report, Brussels, 2016a. URL http://eur-lex.europa.eu/legal-content/EN/TXT/?qid=1512481277484{&}uri=CELEX:52016DC0860.

European Commission. FCA: Commission Regulation (EU) 2016/1719 establishing a guideline on forward capacity allocation, 2016b. ISSN 1098-6596. URL http://data.europa.eu/eli/reg/2016/1719/oj.

European Commission. Impact Assessment of the Market Design Initiative SWD(2016) 410 final. Technical report, European Commission, Brussels, 2016c.

European Commission. SO GL: Comission Regulation (EU) 2017/1485 establishing a guideline on electricity transmission system operation. Technical Report August, Brussels, 2017a.

European Commission. Commission Regulation (EU) 2017/2195 of 23 November 2017 establishing a guideline on electricity balancing, 2017b. URL https://eur-lex.europa.eu/legal-content/EN/TXT/?uri=uriserv:OJ.L{_}.2017.312.01.0006.01.ENG{&}toc=OJ:L:2017:312:TOC{#}d1e2376-6-1.

European Union. Directive 96/92/EC: Common Rules for the Internal Market in Electricity. *Official Journal of the European Communities*, 1993(L27):20–29, 1996. ISSN 0308597X. doi: 10.1016/j.biocon.2008.10.006.

European Union. Directive of 2009/72/EC: Common Rules for the Internal Market in Electricity. *Official Journal of the European Union*, L211(August):L 211/55 – L 211/93, 2009. ISSN 0036-8075. doi: 10.1126/science.202.4366.409.

Eurostat. European Water Statistics, 2020. URL https://ec.europa.eu/eurostat/web/environment/water.

Felling, T. and Weber, C. Consistent and robust delimitation of price zones under uncertainty with an application to Central Western Europe. *Energy Economics*, 75: 583–601, 2018. ISSN 01409883. doi: 10.1016/j.eneco.2018.09.012. URL https://doi.org/10.1016/j.eneco.2018.09.012.

Felling, T., Felten, B., Osinski, P., and Weber, C. Flow-Based Market Coupling Revised - Part II: Assessing Improved Price Zones in Central Western Europe. *SSRN Electronic Journal*, (07), 2019. doi: 10.2139/ssrn.3404046.

Felten, B., Felling, T., Jahns, C., Osinski, P., Podewski, C., and Weber, C. KoNeMaSim – Kopplung von Netz- und Marktsimulationen für die Netzplanung. (April), 2019a.

Felten, B., Felling, T., Osinski, P., and Weber, C. Flow-Based Market Coupling Revised - Part I: Analyses of Small- and Large-Scale Systems. *SSRN Electronic Journal*, (06), 2019b. doi: 10.2139/ssrn.3404044.

Fernández-Blanco, R., Kavvadias, K., and Hidalgo González, I. Quantifying the water-power linkage on hydrothermal power systems: A Greek case study. *Applied Energy*, 203:240–253, 2017. ISSN 03062619. doi: 10.1016/j.apenergy.2017.06.013.

Ford, A. Boom and Bust in Power Plant Construction: Lessons from the California Electricity Crisis. Technical Report 2, 2002.

Fosso, O. B. and Belsnes, M. M. Short-term Hydro Scheduling in a Liberalized Power System. In *2004 International Conference on Power System Technology-POWERCON*, number November, Singapore, 2004. IEEE. ISBN 0780386108.

Fosso, O. B., Gjelsvik, A., Haugstad, A., Mo, B., and Wangensteen, I. Generation scheduling in a deregulated system. the norwegian case. *IEEE Transactions on Power Systems*, 14(1):75–80, 1999. ISSN 08858950. doi: 10.1109/59.744487.

Goop, J., Odenberger, M., and Johnsson, F. The effect of high levels of solar generation on congestion in the European electricity transmission grid. *Applied Energy*, 205(July): 1128–1140, 2017. ISSN 03062619. doi: 10.1016/j.apenergy.2017.08.143. URL `http://dx.doi.org/10.1016/j.apenergy.2017.08.143`.

Göransson, L., Goop, J., Unger, T., Odenberger, M., and Johnsson, F. Linkages between demand-side management and congestion in the European electricity transmission system. *Energy*, 69:860–872, 2014. ISSN 03605442. doi: 10.1016/j.energy.2014.03.083. URL `http://dx.doi.org/10.1016/j.energy.2014.03.083`.

Grijalva, S., Sauer, P. W., and Weber, J. D. Enhancement of linear ATC calculations by the incorporation of reactive power flows. *IEEE Transactions on Power Systems*, 18 (2):619–624, 2003. ISSN 08858950. doi: 10.1109/TPWRS.2003.810902.

Grimm, V., Martin, A., SSlch, C., Weibelzahl, M., and ZZttl, G. Market-Based Redispatch May Result in Inefficient Dispatch. *SSRN Electronic Journal*, 2018. ISSN 1556-5068. doi: 10.2139/ssrn.3120403.

Gross, G. and Bompard, E. Optimal power flow application issues in the Pool paradigm. *International Journal of Electrical Power and Energy System*, 26(10):787–796, 2004. ISSN 01420615. doi: 10.1016/j.ijepes.2004.08.004.

Gupta, A. P., Member, S., Mohapatra, A., and Singh, S. N. Power System Network Equivalents : Key Issues and Challenges. *TENCON 2018 - 2018 IEEE Region 10 Conference*, (October):2291–2296, 2018.

Harvey, S. M. and Hogan, W. W. Nodal and Zonal Congestion Management and the Exercise of Market Power. Technical report, 2000. URL `http://ksgwww.harvard.edu/people/whogan`.

Heitkoetter, W., Medjroubi, W., and Vogt, T. Comparison of Open Source Power Grid Models — Combining a Mathematical , Visual and Electrical Analysis in an Open Source Tool. 2019. doi: 10.3390/en12244728.

Hogan, W. Contract Networks for Electric Power Transmission. *Journal of Regulatory Economics*, 4(3):211–242, 1992.

Hogan, W. Transmission Congestion: The Nodal-Zonal Debate Revisited. Technical report, Harvard University, Cambridge, 1999.

Holmberg, P. and Lazarczyk, E. Comparison of congestion management techniques: Nodal, zonal and discriminatory pricing. *The Energy Journal*, 36(2):145–166, 2015. doi: 10.5547/01956574.36.2.7.

Horsch, J. and Brown, T. The role of spatial scale in joint optimisations of generation and transmission for European highly renewable scenarios. *International Conference on the European Energy Market, EEM*, pages 1–8, 2017. ISSN 21654093. doi: 10.1109/EEM.2017.7982024.

Hörsch, J., Hofmann, F., Schlachtberger, D., and Brown, T. PyPSA-Eur: An open optimisation model of the European transmission system. *Energy Strategy Reviews*, 22(September):207–215, 2018. ISSN 2211467X. doi: 10.1016/j.esr.2018.08.012. URL `https://doi.org/10.1016/j.esr.2018.08.012`.

Hu, J., Harmsen, R., Crijns-Graus, W., Worrell, E., and van den Broek, M. Identifying barriers to large-scale integration of variable renewable electricity into the electricity market: A literature review of market design. *Renewable and Sustainable Energy Reviews*, 81(September 2016):2181–2195, 2018. ISSN 18790690. doi: 10.1016/j.rser.2017.06.028. URL `https://doi.org/10.1016/j.rser.2017.06.028`.

Huang, J. and Purvins, A. Validation of a Europe-wide electricity system model for techno-economic analysis. *International Journal of Electrical Power and Energy Systems*, 123(March):106292, 2020. ISSN 01420615. doi: 10.1016/j.ijepes.2020.106292. URL https://doi.org/10.1016/j.ijepes.2020.106292.

Hutcheon, N. and Bialek, J. W. Updated and validated power flow model of the main continental European transmission network. *2013 IEEE Grenoble Conference PowerTech, POWERTECH 2013*, pages 1–5, 2013. doi: 10.1109/PTC.2013.6652178.

IEA. CO2 Emissions Database (2019 Edition). *International Energy Agency*, page 92, 2019. ISSN 15509613. doi: 10.1670/96-03N. URL http://wds.iea.org/wds/pdf/Worldco2{_}Documentation.pdf.

Iimi, A. Price Elasticity of Nonresidential Demand for Energy in South Eastern Europe. *Policy Research Working Paper Finance,Economics and Urban Development(FEU)The World Bank*, WPS5167(January):1–29, 2010. URL http://econ.worldbank.org/external/default/main?pagePK=64165259{&}piPK=64165421{&}theSitePK=469382{&}menuPK=64166093{&}entityID=000158349{_}2010010710180.

Janda, K., Málek, J., and Rečka, L. Influence of renewable energy sources on transmission networks in Central Europe. *Energy Policy*, 108(February 2017):524–537, 2017. ISSN 03014215. doi: 10.1016/j.enpol.2017.06.021.

Jansen, L. L. and Buzna, L. Evaluation of Modeling Differences of Nodal vs . Zonal Pricing Based Electricity Markets : Optimization Models and Network Representation. In *18th International Conference on Emerging eLearning Technologies and Applications (ICETA) 2020*, Kosice, 2021. IEEE. doi: 10.1109/ICETA51985.2020.9379255.

Kirschen, D. S. Demand-Side View of Electricity Markets - Invited Paper. *Ieee Transactions on Power Systems*, 18(2):520–527, 2003.

Kirschen, D. S. and Strbac, G. *Fundamentals of power system economics*. John Wiley & Sons, Inc., 2019.

Kladnik, B., Artac, G., and Gubina, A. An assessment of the effects of demand response in electricity markets. *International transactions on electrical energy systems*, (23):380–

391, 2012. ISSN 03787796. doi: 10.1002/etep.666. URL http://ieeexplore.ieee.org/lpdocs/epic03/wrapper.htm?arnumber=4137655{%}5Cn.

Klein, D., Spieker, C., Ruberg, S., Liebenau, V., and Rehtanz, C. Aggregation of large-scale electrical energy transmission networks. *2016 IEEE International Energy Conference, ENERGYCON 2016*, 2016. doi: 10.1109/ENERGYCON.2016.7513897.

Krishnamurthy, C. K. B. and Kriström, B. A cross-country analysis of residential electricity demand in 11 OECD-countries. *Resource and Energy Economics*, 39: 68–88, 2015. ISSN 09287655. doi: 10.1016/j.reseneeco.2014.12.002. URL http://dx.doi.org/10.1016/j.reseneeco.2014.12.002.

Kunz, F., Neuhoff, K., and Rosellón, J. FTR allocations to ease transition to nodal pricing: An application to the German power system. *Energy Economics*, 60:176–185, nov 2016. ISSN 01409883. doi: 10.1016/j.eneco.2016.09.018.

Lacal-Arantegui, R., Jäger-Waldau, A., Vellei, M., Sigfusson, B., Magagna, D., Jakubcionis, M., del Mar Perez Fortes, M., Moles, C., Lazarou, S., Giuntoli, J., Weidner, E., de Marco Amanda, G., and Spisto, A. *ETRI 2014 - Energy Technology Reference Indicator projections for 2010-2050*, volume 57. Luxembourg, 2014. ISBN 9789279444036. doi: 10.2790/057687.

Leuthold, F. U., Weigt, H., and von Hirschhausen, C. A Large-Scale Spatial Optimization Model of the European Electricity Market. *Networks and Spatial Economics*, 12(1):75–107, 2012. ISSN 1566113X. doi: 10.1007/s11067-010-9148-1.

Li, F. and Bo, R. DCOPF-based LMP simulation: Algorithm, comparison with ACOPF, and sensitivity. *IEEE Transactions on Power Systems*, 22(4):1475–1485, 2007. ISSN 08858950. doi: 10.1109/TPWRS.2007.907924.

Li, F., Bo, R., and Zhang, W. Comparison of different LMP calculations in power market simulation. *2006 International Conference on Power System Technology, POWERCON2006*, pages 1–6, 2006. doi: 10.1109/ICPST.2006.321838.

Liu, H., Tesfatsion, L., and Chowdhury, A. A. Locational marginal pricing basics for restructured wholesale power markets. *2009 IEEE Power and Energy Society General Meeting, PES '09*, pages 1–8, 2009. doi: 10.1109/PES.2009.5275503.

Madlener, R., Bernstein, R., and Gonzalez, M. Econometric Estimation of Energy Demand Elasticities. *E.ON Energy Research Center Series*, 3(8):59, 2011.

Medjroubi, W. and Vogt, T. Open Source Data and Models for a Sustainable power Grid Modelling and Analysis. (October), 2017.

Medjroubi, W., Müller, U. P., Scharf, M., Matke, C., and Kleinhans, D. Open Data in Power Grid Modelling: New Approaches Towards Transparent Grid Models. *Energy Reports*, 3:14–21, 2017. ISSN 23524847. doi: 10.1016/j.egyr.2016.12.001. URL `http://dx.doi.org/10.1016/j.egyr.2016.12.001`.

Meibom, P., Barth, R., Hasche, B., Brand, H., Weber, C., and O'Malley, M. Stochastic optimization model to study the operational impacts of high wind penetrations in Ireland. *IEEE Transactions on Power Systems*, 26(3):1367–1379, 2011. ISSN 08858950. doi: 10.1109/TPWRS.2010.2070848.

Mende, D., Stock, D. S., Hennig, T., Lower, L., and Hofmann, L. Multiobjective optimization in congestion management considering technical and economic aspects. *Asia-Pacific Power and Energy Engineering Conference, APPEEC*, 2016-Decem:1061–1066, 2016. ISSN 21574847. doi: 10.1109/APPEEC.2016.7779711.

Mende, D., Böttger, D., Löwer, L., Becker, H., Akbulut, A., and Stock, S. About the Need of Combining Power Market and Power Grid Model Results for Future Energy System Scenarios. *Journal of Physics: Conference Series*, 977(1), 2018. ISSN 17426596. doi: 10.1088/1742-6596/977/1/012009.

Müller, U. P., Schachler, B., Scharf, M., Bunke, W. D., Günther, S., Bartels, J., and Pleßmann, G. Integrated techno-economic power system planning of transmission and distribution grids. *Energies*, 12(11):1–30, 2019. ISSN 19961073. doi: 10.3390/en12112091.

Neuhoff, K. and Boyd, R. Technical Aspects of Nodal Pricing. Technical report, CPI Workshop Report, Climate Policy Initiative, Climate Policy Initiative,, Berlin, 2011. URL `http://hdl.handle.net/10419/65877www.econstor.eu`.

Newbery, D., Strbac, G., and Viehoff, I. The benefits of integrating European electricity

markets. *Energy Policy*, 94:253–263, jul 2016. ISSN 03014215. doi: 10.1016/j.enpol.2016.03.047.

Open Energy Modeling Initiative. openmod, 2022. URL https://www.openmod-initiative.org/index.html{#}.

Overbye, T. J., Cheng, X., and Sun, Y. A comparison of the AC and DC power flow models for LMP calculations. *Proceedings of the Hawaii International Conference on System Sciences*, 37(C):725–734, 2004. ISSN 10603425. doi: 10.1109/hicss.2004.1265164.

Philpott, A. B., Craddock, M., and Waterer, H. Hydro-electric unit commitment subject to uncertain demand. *European Journal of Operational Research*, 125(2):410–424, 2000. ISSN 03772217. doi: 10.1016/S0377-2217(99)00172-1.

Poplavskaya, K., Totschnig, G., Leimgruber, F., Doorman, G., Etienne, G., and de Vries, L. Integration of day-ahead market and redispatch to increase cross-border exchanges in the European electricity market. *Applied Energy*, 278:115669, 2020. ISSN 03062619. doi: 10.1016/j.apenergy.2020.115669. URL https://doi.org/10.1016/j.apenergy.2020.115669.

Purvins, A., Sereno, L., Ardelean, M., Covrig, C. F., Efthimiadis, T., and Minnebo, P. Submarine power cable between Europe and North America: A techno-economic analysis. *Journal of Cleaner Production*, 186:131–145, 2018. ISSN 09596526. doi: 10.1016/j.jclepro.2018.03.095. URL https://doi.org/10.1016/j.jclepro.2018.03.095.

Quelhas, A., Gil, E., McCalley, J. D., and Ryan, S. M. A multiperiod generalized network flow model of the U.S. integrated energy system: Part I - Model description. *IEEE Transactions on Power Systems*, 22(2):829–836, may 2007. ISSN 08858950. doi: 10.1109/TPWRS.2007.894844.

Ranci, P. and Cervigni, G. *The Economics of Electricity Markets*. 2013. ISBN 9781118775752. doi: 10.4337/9780857933966.

Ringler, P., Keles, D., and Fichtner, W. How to benefit from a common European electricity market design. *Energy Policy*, 101(May 2016):629–643, 2017. ISSN

03014215. doi: 10.1016/j.enpol.2016.11.011. URL http://dx.doi.org/10.1016/j.enpol.2016.11.011.

Sahraoui, Y., Bendotti, P., and D'Ambrosio, C. Real-world hydro-power unit-commitment: Dealing with numerical errors and feasibility issues. *Energy*, 184: 91–104, 2019. ISSN 03605442. doi: 10.1016/j.energy.2017.11.064. URL https://doi.org/10.1016/j.energy.2017.11.064.

Schittekatte, T., Reif, V., and Meeus, L. The EU Electricity Network Codes (2019ed.). Technical Report February, European University Institute,, Florence, 2019.

Schubert, E. S., Hurlbut, D., Adib, P., and Oren, S. The Texas Energy-Only Resource Adequacy Mechanism. *Electricity Journal*, 19(10):39–49, dec 2006. ISSN 10406190. doi: 10.1016/j.tej.2006.11.003.

Schweppe, F. C., Caramanis, M. C., Tabors, R. D., and Bohn, R. E. *Spot Pricing of Electricity*. Kluwer Academic Publisher, Boston, 4 edition, 1988. ISBN 9781461289500.

Setz, C., Heinrich, A., Rostalski, P., Papafotiou, G., and Morari, M. *Application of Model Predictive Control to a Cascade of River Power Plants*, volume 41. IFAC, 2008. ISBN 9783902661005. doi: 10.3182/20080706-5-kr-1001.02027. URL http://dx.doi.org/10.3182/20080706-5-KR-1001.02027.

Sharma, D., Yadav, N. K., Bhargava, G., and Bala, A. Comparative analysis of ACOPF and DCOPF based LMP simulation with distributed loss model. *ICCCCM 2016 - 2nd IEEE International Conference on Control Computing Communication and Materials*, (Iccccm):1–6, 2017. doi: 10.1109/ICCCCM.2016.7918260.

Shi, D. and Tylavsky, D. J. A Novel Bus-Aggregation-Based Structure-Preserving Power System Equivalent. *IEEE Transactions on Power Systems*, 30(4):1977–1986, 2015. ISSN 08858950. doi: 10.1109/TPWRS.2014.2359447.

Spieker, C., Schwippe, J., Klein, D., and Rehtanz, C. Transmission system congestion analysis based on a European electricity market and network simulation framework. *19th Power Systems Computation Conference, PSCC 2016*, 2016. doi: 10.1109/PSCC.2016.7540967.

Stoll, B., Andrade, J., Cohen, S., Brinkman, G., and Brancucci Martinez-anido, C. Hydropower Modeling Challenges. Technical Report April, No. NREL/TP-5D00-68231. National Renewable Energy Lab.(NREL), Golden, CO, United States, 2017.

Syranidou, C., Koch, M., Matthes, B., Winger, C., Linßen, J., Rehtanz, C., and Stolten, D. Development of an open framework for a qualitative and quantitative comparison of power system and electricity grid models for Europe. *Renewable and Sustainable Energy Reviews*, 159(November 2021), 2022. ISSN 18790690. doi: 10.1016/j.rser.2021.112055.

Taylor, J. A. *Convex Optimization of Power Systems*. Cambridge University Press, Toronto, 2015. ISBN 978-1-107-07687-7.

Thimmapuram, P. R. and Kim, J. Consumers' price elasticity of demand modeling with economic effects on electricity markets using an agent-based model. *IEEE Transactions on Smart Grid*, 4(1):390–397, 2013. ISSN 19493053. doi: 10.1109/TSG.2012.2234487.

Tuohy, A., Member, S., Meibom, P., Denny, E., and Malley, M. O. Unit Commitment for Systems With Significant Wind Penetration. 24(2):592–601, 2009.

UNFCCC. Paris Climate Change Conference-November 2015, COP 21. *Adoption of the Paris Agreement. Proposal by the President.*, 21932(December):32, 2015. ISSN 1098-6596. doi: FCCC/CP/2015/L.9/Rev.1. URL `http://unfccc.int/resource/docs/2015/cop21/eng/l09r01.pdf`.

Van Den Bergh, K., Couckuyt, D., Delarue, E., and D'Haeseleer, W. Redispatching in an interconnected electricity system with high renewables penetration. *Electric Power Systems Research*, 127:64–72, 2015. ISSN 03787796. doi: 10.1016/j.epsr.2015.05.022. URL `http://dx.doi.org/10.1016/j.epsr.2015.05.022`.

Wang, H., Murillo-Sanchez, C. E., Zimmerman, R. D., and Thomas, R. J. On Computational Issues of Market-Based Optimal Power Flow. *IEEE Transactions on Power Systems*, 22(3):1185–1193, aug 2007. ISSN 1558-0679. doi: 10.1109/TPWRS.2007.901301.

Weibelzahl, M. Nodal, zonal, or uniform electricity pricing: how to deal with network congestion. *Frontiers in Energy*, 11(2):210–232, 2017. ISSN 20951698. doi: 10.1007/s11708-017-0460-z.

Weibelzahl, M. and Märtz, A. On the effects of storage facilities on optimal zonal pricing in electricity markets. *Energy Policy*, 113(January 2017):778–794, 2018. ISSN 03014215. doi: 10.1016/j.enpol.2017.11.018. URL https://doi.org/10.1016/j.enpol.2017.11.018.

Wiese, F., Bökenkamp, G., Wingenbach, C., and Hohmeyer, O. An open source energy system simulation model as an instrument for public participation in the development of strategies for a sustainable future. *Wiley Interdisciplinary Reviews: Energy and Environment*, 3(5):490–504, 2014. ISSN 2041840X. doi: 10.1002/wene.109.

Wiese, F., Schlecht, I., Bunke, W. D., Gerbaulet, C., Hirth, L., Jahn, M., Kunz, F., Lorenz, C., Mühlenpfordt, J., Reimann, J., and Schill, W. P. Open Power System Data – Frictionless data for electricity system modelling. *Applied Energy*, 236(November 2018): 401–409, 2019. ISSN 03062619. doi: 10.1016/j.apenergy.2018.11.097. URL https://doi.org/10.1016/j.apenergy.2018.11.097.

World Energy Council. Performance of Generating Plant : New Metrics for Industry in Transition. pages 1–119, 2010. URL https://www.worldenergy.org/assets/downloads/PUB{_}Performance{_}of{_}Generating{_}Plant{_}2010{_}WEC.pdf.

Yang, Z., Zhong, H., Bose, A., Zheng, T., Xia, Q., and Kang, C. A Linearized OPF Model with Reactive Power and Voltage Magnitude: A Pathway to Improve the MW-Only DC OPF. *IEEE Transactions on Power Systems*, 33(2):1734–1745, 2018. ISSN 08858950. doi: 10.1109/TPWRS.2017.2718551.

Zalzar, S., Bompard, E., Purvins, A., and Masera, M. The impacts of an integrated European adjustment market for electricity under high share of renewables. *Energy Policy*, 136(May 2018):111055, 2020. ISSN 03014215. doi: 10.1016/j.enpol.2019.111055. URL https://doi.org/10.1016/j.enpol.2019.111055.

Zhou, Q. and Bialek, J. W. Approximate model of European Interconnected system as a benchmark system to study effects of cross-border trades. *IEEE Transactions on Power Systems*, 20(3):1663, 2005. ISSN 08858950. doi: 10.1109/TPWRS.2005.854741.

Zimmerman, R. D., Murillo-Sánchez, C. E., and Thomas, R. J. MATPOWER: Steady-state operations, planning, and analysis tools for power systems research and education.

IEEE Transactions on Power Systems, 26(1):12–19, 2011. ISSN 08858950. doi: 10.1109/TPWRS.2010.2051168.

List of Author's Publications

International Impacted Journals

Jansen, L. L., Thomaßen, G., Antonopoulos, G., & Buzna, Ľ. (2022). **An Efficient Framework to Estimate the State of Charge Profiles of Hydro Units for Large-Scale Zonal and Nodal Pricing Models.** Energies, 15(12), 1–23. https://doi.org/10.3390/en15124233

Conferences

Jansen, L. L., & Buzna, Ľ. (2020). **Comparison of AC-OPF and DC-OPF in the Context of Nodal Pricing.** Proceedings of the 2020 Conference on Mathematics in Science and Technologies (MiST).

Jansen, L. L., & Buzna, Ľ. (2020). **Evaluation of Modeling Differences of Nodal vs . Zonal Pricing Based Electricity Markets : Optimization Models and Network Representation.** 18th International Conference on Emerging ELearning Technologies and Applications (ICETA) 2020. https://doi.org/10.1109/ICETA51985.2020.9379255

Jansen, L. L., Purvins, A., Buzna, Ľ., Antonopoulos, G., & Zani, A. (2020). **Modeling Methodology to Assess the Impact of Demand Elasticity on the Italian Electricity System in a European Context.** 2020 17th International Conference on the European Energy Market (EEM), 1–6. https://doi.org/10.1109/EEM49802.2020.9221900

Jansen, L. L., Thomaßen, G., Antonopoulos, G., & Buzna, Ľ. (2022). **An Efficient Framework to Estimate the State of Charge Profiles of Hydro Units for Large-Scale Zonal and Nodal Pricing Models.** [Unpublished manuscript]. International Conference on Electrical, Computer and Energy Technologies (ICECET 2022).